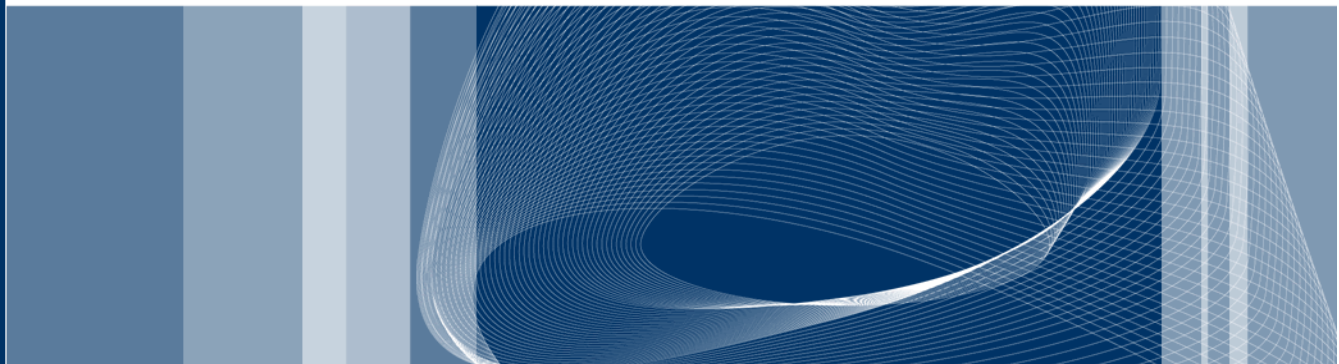




Dipartimento di Chimica, Materiali e Ingegneria Chimica "G. Natta"
Politecnico di Milano



Lumping Procedures in the Detailed Kinetics of Pyrolysis, Gasification and Combustion of Solid Fuels



Eliseo Ranzi



Abstract

Detailed chemistry of thermal treatments of solid fuels (large numbers of species and reactions) requires careful simplifications.

This multi-component and multi-phase problem requires to apply

chemical lumping procedures at four different levels:

- 1- Characterization of the Solid Fuel in terms of Reference Components
- 2- Multistep Kinetic Models of Devolatilization of Reference Components
- 3- Heterogeneous Gas-Solid Reactions of Char with O₂/H₂O/CO₂
- 4- Secondary Gas-Phase Reactions of Tars and Volatile Components

The comprehensive description of coupled transport and kinetic processes, both at particle and reactor scale, increases the mathematical complexity of solid fuel gasification and combustion.

Two application examples at the reactor scale:

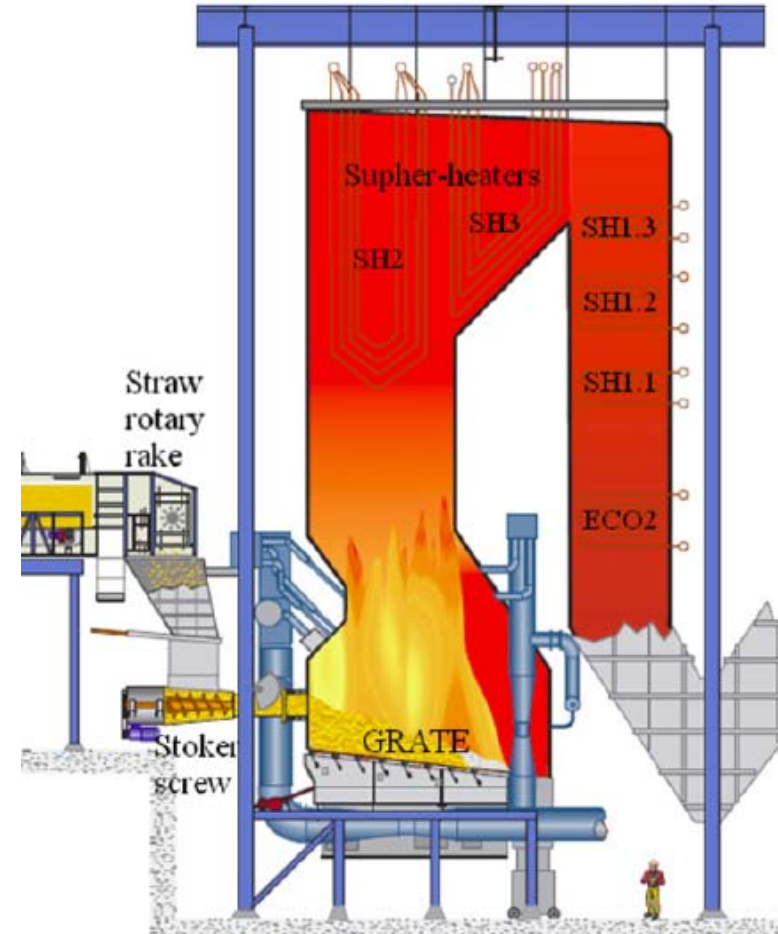
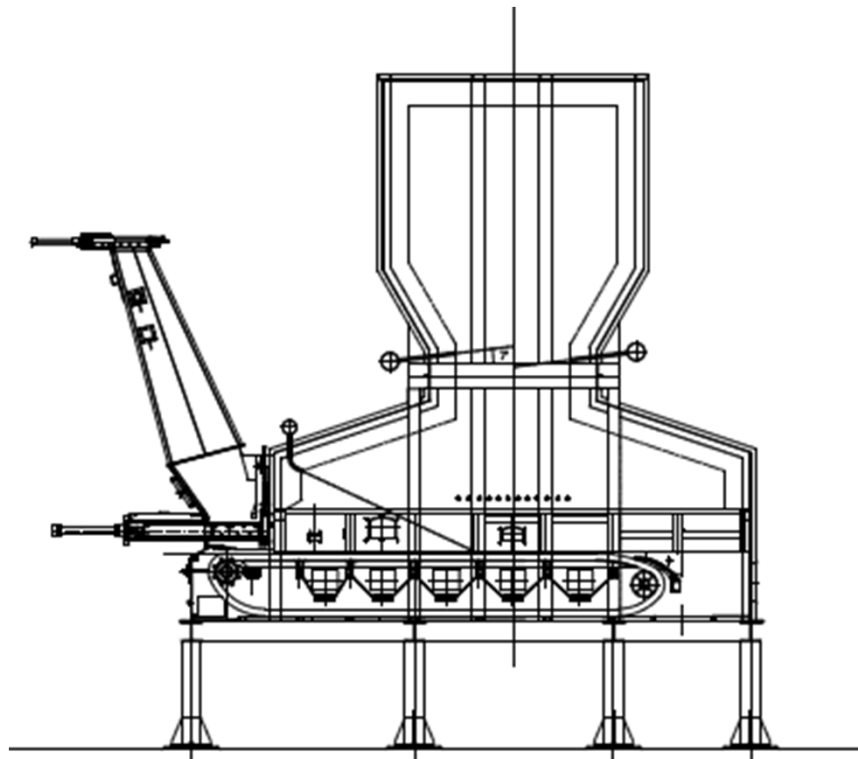
Countercurrent Coal or Biomass Gasifier

Biomass Combustor on a Travelling Grate

illustrate the viability of this approach.

A compromise needs to be found between computation efforts and prediction accuracy.

A complex
multi-component
multi-phase
and multi-scale problem.



Biomass Travelling Grate Combustor

Yin, C , Rosendahl , LA , Kaer , SK Prog. Energy Comb. Science 34 (2008) 725

Mathematical Modeling of a Travelling Grate Combustor

4

Requires at least to analyse the three following features:

- Solid Fuel Characterization
- Kinetics

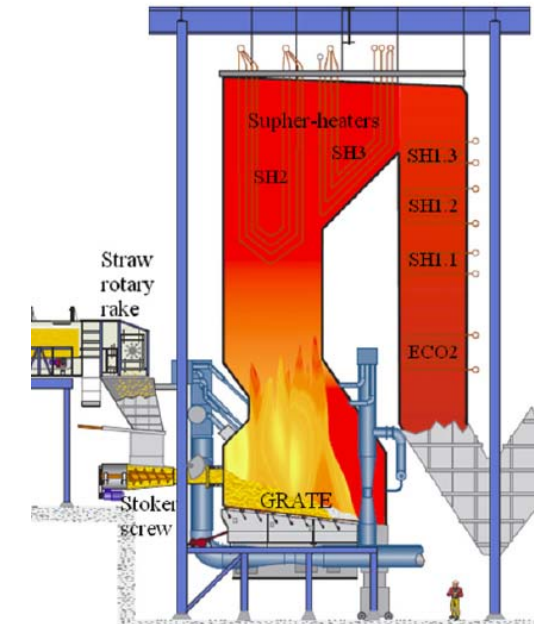
Pyrolysis of Solid Fuel (release of volatile components)

Heterogeneous Reactions (char gasification and combustion)

Homogeneous Reactions of gases and tars

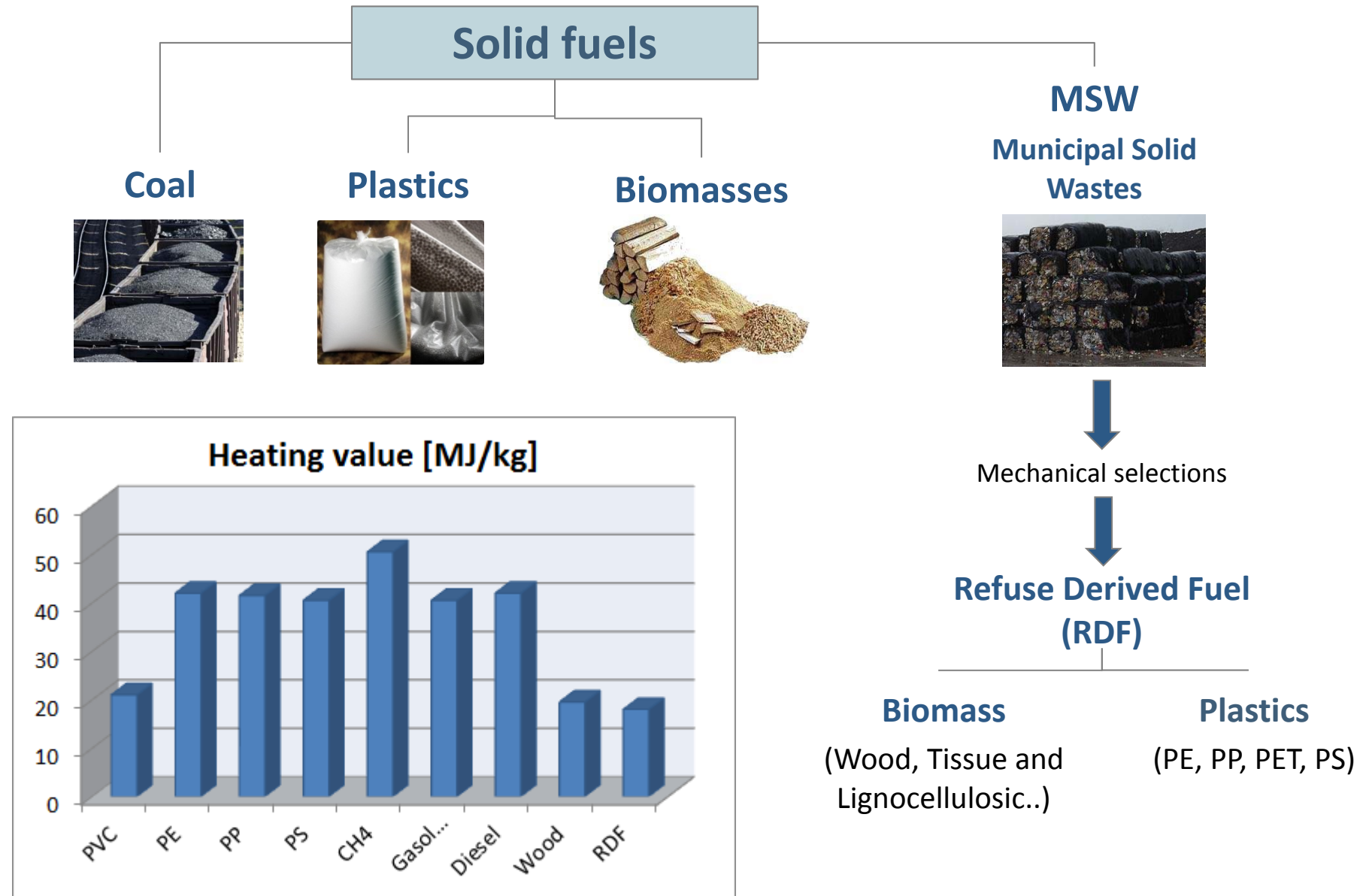
- Mathematical Model → Balance Equations

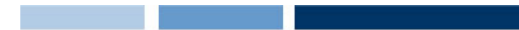
Particle and Reactor Scale



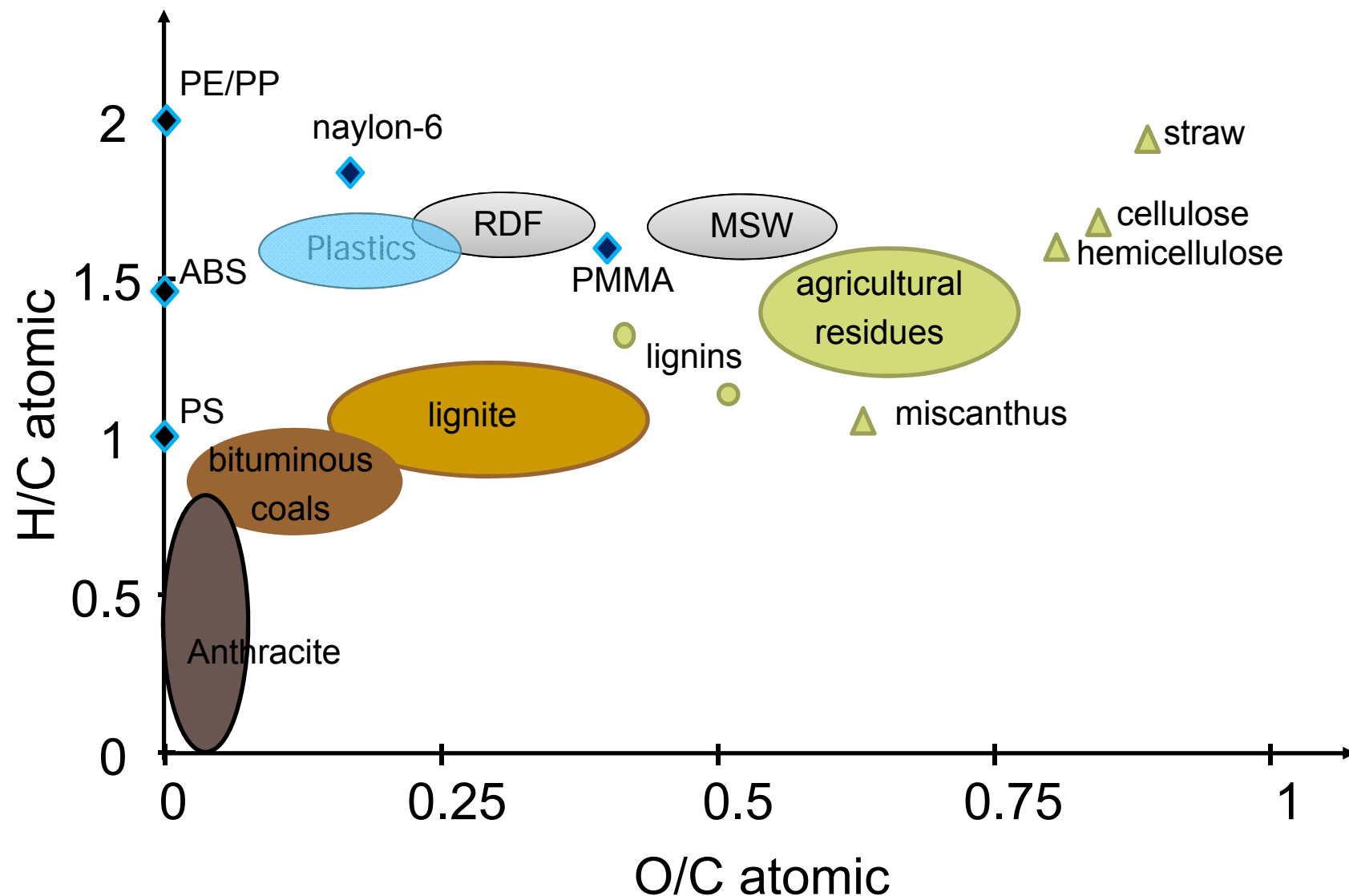
- **Solid Fuels Characterization**
 - Biomass (Cellulose, Hemicellulose, Lignins)
 - Coal, Plastic and Refuse Derived Fuels
- **Kinetic Models and Lumping Approach**
 - Solid Fuel Pyrolysis and Devolatilization
 - Char Gasification and Combustion
 - Secondary Gas-Phase Reactions
- **Comprehensive Multi-Scale and Multi-Phase Model**
(Balance Equations)
 - Particle and Reactor Scale
- **Application Examples**
 - Countercurrent Coal or Biomass Gasifier
 - Biomass Combustor on a Travelling Grate

SOLID FUELS





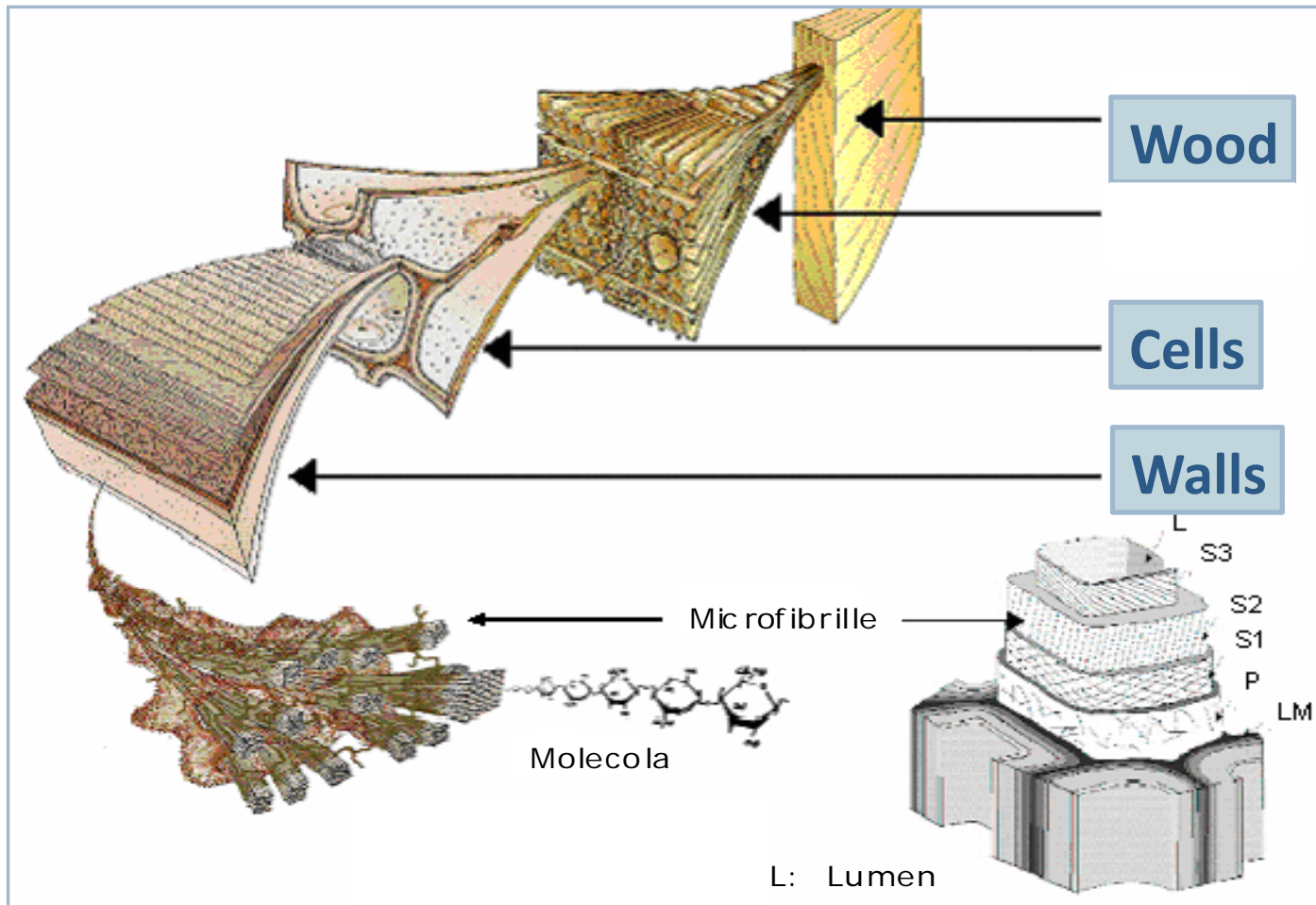
Solid Fuels in Van Krevelen Diagram.



After: R.H. Hurt (1998) "Structure, properties, and reactivity of solid fuels." 27th Symposium on Combustion. 2887-2904

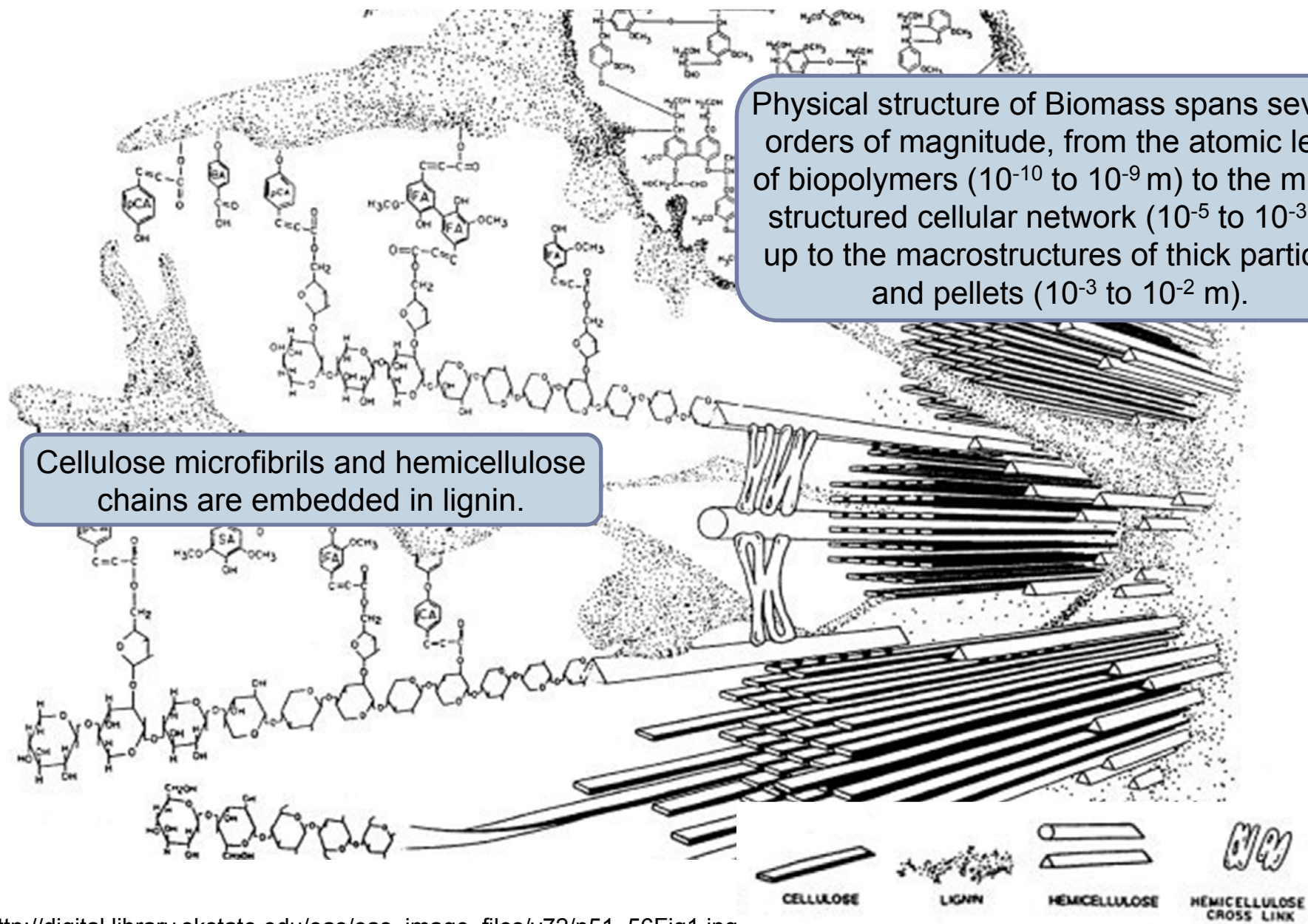
Biomass Characterization

Morphology and Composition of Biomass



Molecular Composition of Biomass

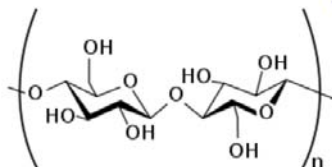
9



http://digital.library.okstate.edu/oas/oas_image_files/v72/p51_56Fig1.jpg

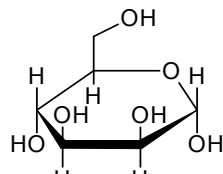
Biomass composition: Cellulose, Hemicellulose and Lignin

Cellulose ($-C_6H_{10}O_5-$)

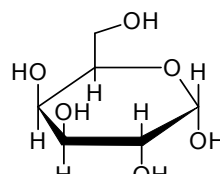


Cellulose is the structural component of the primary cell wall of green plants. Cellulose is a linear polymer of up to 10,000 D-glucose molecules $(C_6H_{10}O_5)_n$

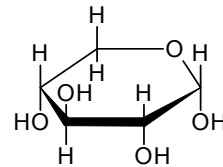
Hemicellulose ($-C_5H_8O_4-$)



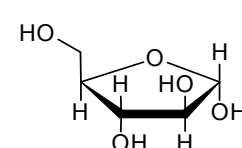
mannose



galactose



xylose



arabinose

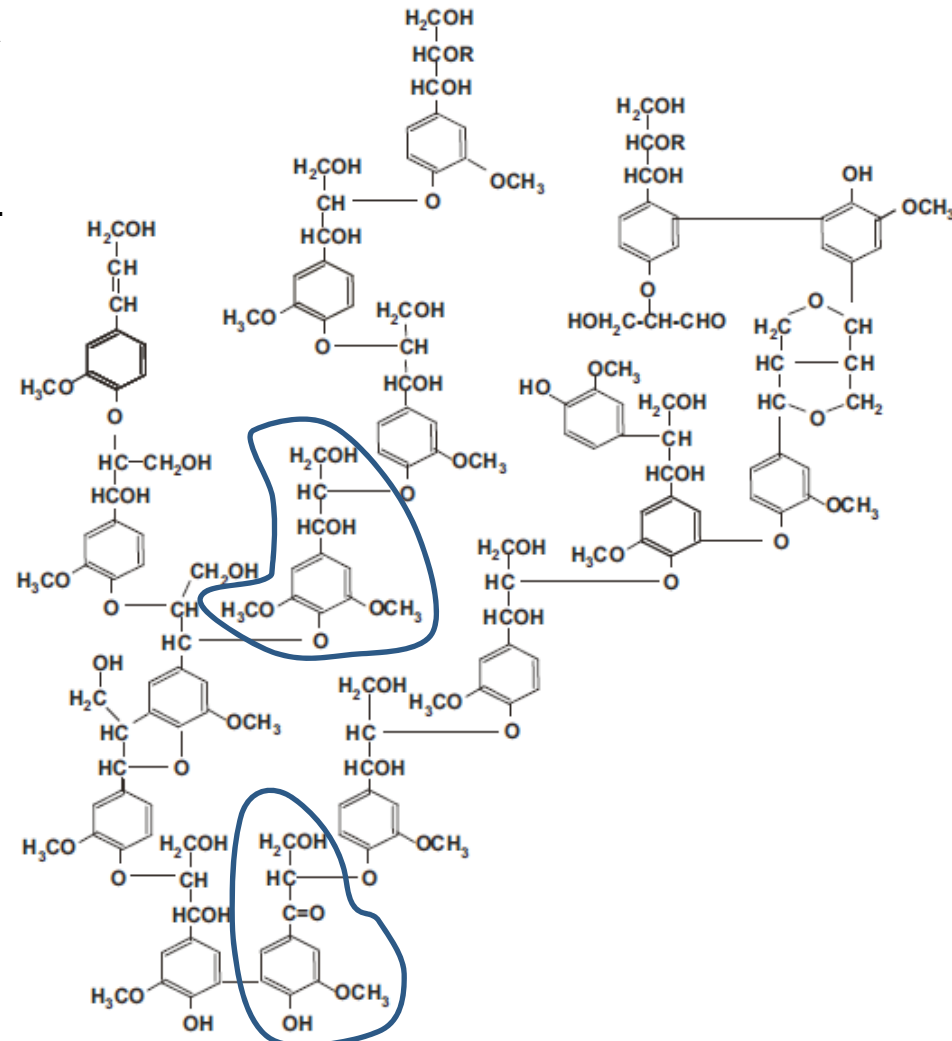
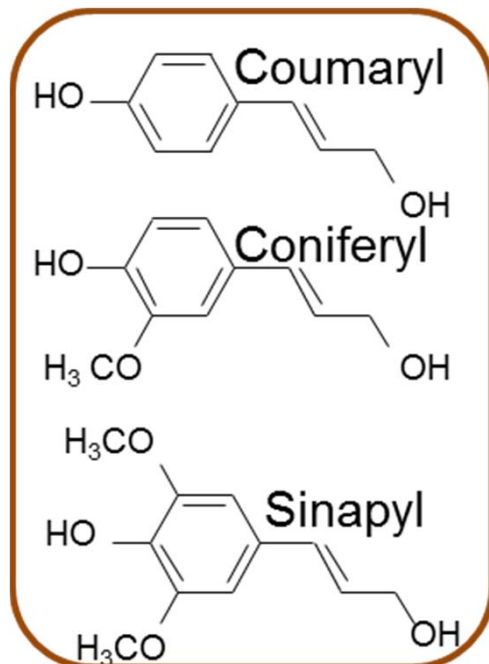
Hemicellulose is a complex mixture of different sugar monomers (xylose, mannose, galactose, arabinose,...) generally being xylose the most abundant. It is the biomass component with a high char formation tendency

Lignin

Lignin is a complex macromolecule with a high molecular mass (>10,000 um)

It confers mechanical strength to the plant.

There are three main alcohol monomers, with different methylation degree.



Adapted from: Adler E.. Wood Sci Technol 1977;11:169–218.

Biochemical Analysis of Biomasses

Wood species		Cellulose	Hemicellulose	Lignin
Softwoods				
Picea	glauca	41	31	27
Abies	balsamea	42	27	29
Pinus	strobes	41	27	29
Tsuga	canadensis	41	23	33
Norway	spruce	46	25	28
Loblolly	pine	39	25	31
Thuja	occidentalis	41	26	31
Hardwoods				
Eucalyptus	globulus	45	35	19
Acer	rubrum	45	29	24
Ulmus	americana	51	23	24
Populus	tremuloides	48	27	21
Betula	papyrifera	42	38	19
Fagus	grandifolia	45	29	22
Agricultural residues				
Corn	stover	40	17	25
Wheat	straw	30	20	50
Switchgrass		45	12	30

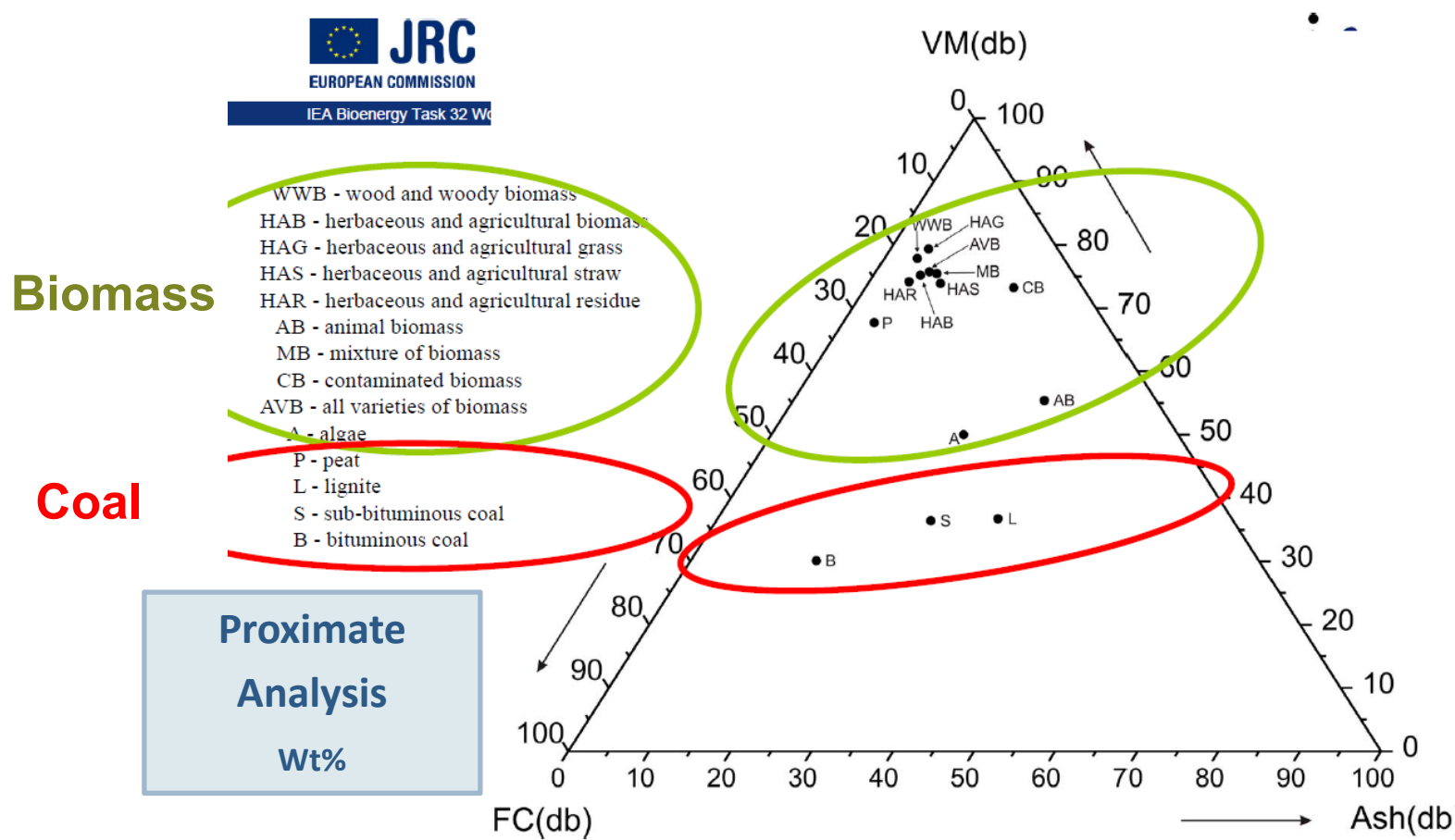
Extractives:

The biomass material that is soluble in either water or ethanol during exhaustive extraction.

Fengel D, Wegener G. Wood. Chemistry, ultrastructure, reactions. Walter de Gruyter: Berlin, 613 pp (1984).

Zhang YP. Reviving the carbohydrate economy via multi-product lignocellulose biorefineries. J Ind Microbiol Biot 35:367-375 (2008).

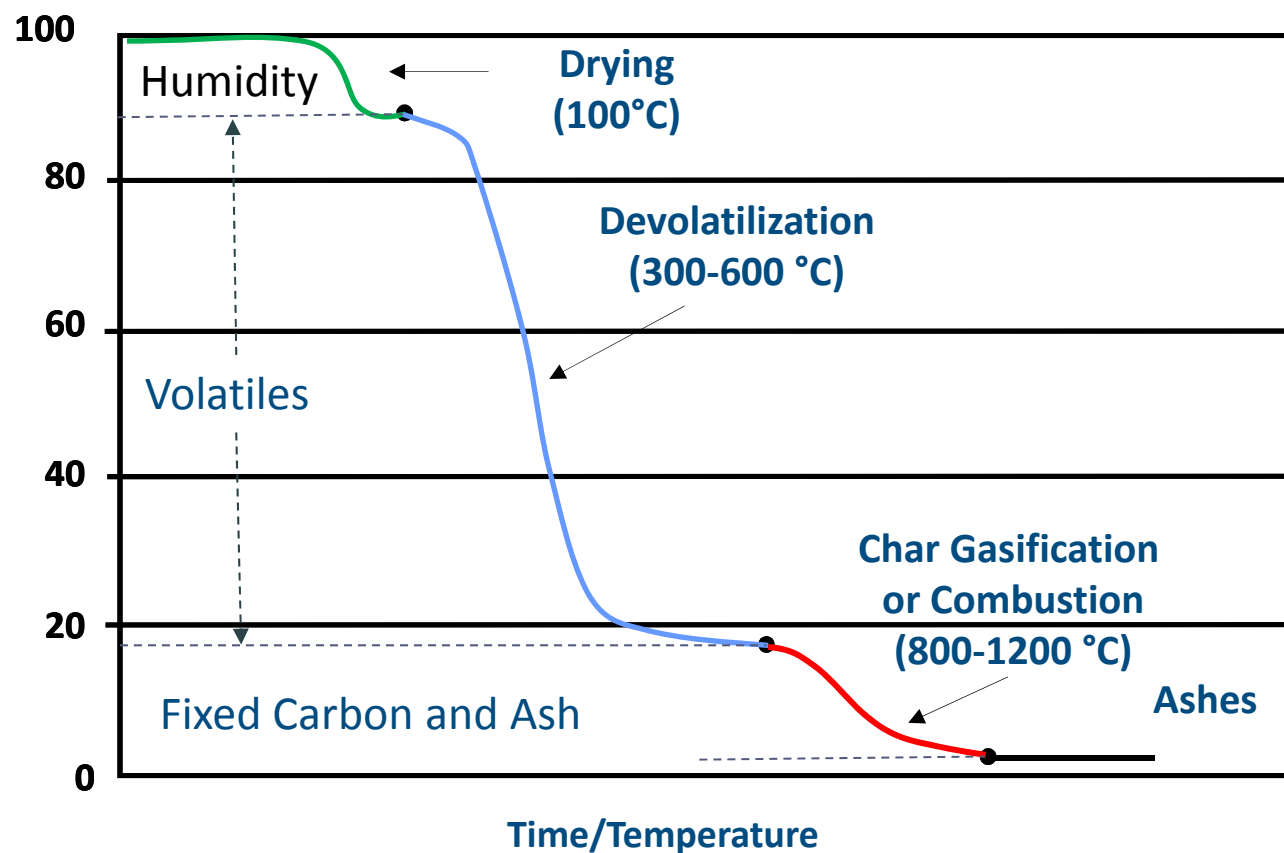
Biomass Composition



The **proximate analysis** gives moisture, volatile content **VM** (when heated to 950 C), the fixed carbon **FC** remaining at that point, the **Ash** (mineral) together with the high heating value (HHV).

http://www.ieabcc.nl/workshops/task32_Lyon/full%20page/04%20David%20Baxter.pdf

Proximate Analysis (Moisture, Volatiles, Fixed Carbon, Ash) is derived from Thermo Gravimetric Analysis (TGA)



TGA is a recording of mass changes, as a function of a combination of temperature with time.

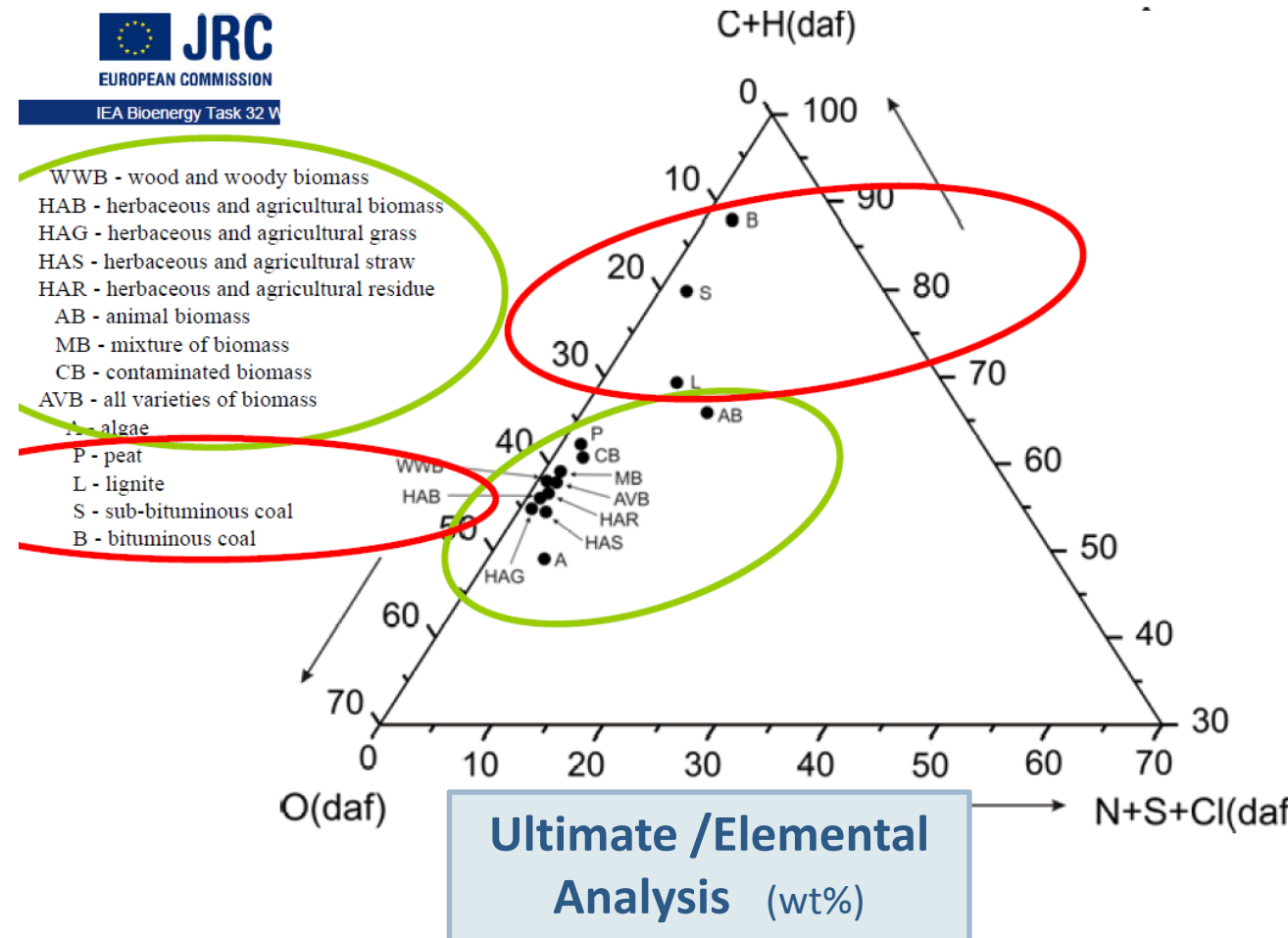
Proximate Analysis of typical Biomasses

Fuel (Oven dried)	Proximate analysis, ar				HHV MJ/kg (dry)
	Moisture	VM	FC	Ash	
Wood pine chips	4.0	81.3	14.6	0.1	20.23
Willow, SRC	6.96	75.70	16.31	1.03	18.68
Miscanthus giganteus	14.2	70.4	14.1	1.3	19.88
Switch Grass	7.17	73.05	15.16	4.62	17.82
Straw-wheat straw	7.78	68.83	17.09	6.30	17.42
Rice husks	9.4	74	13.2	12.8	16.3
Palm PKE	7.60	72.12	16.18	4.10	20.00
Sugar cane bagasse	10.4	76.7	14.7	2.2	19.47
Olive residue	6.40	65.13	19.27	9.20	19.67
Cow dung	13.9	60.5	11.9	13.7	17.36
Lignin	9.0	73.5	1.5	16	25
Cellulose	4.1	94.0	0.2	1.7	18.6

A. Williams, J.M. Jones, L. Ma, M. Pourkashanian 'Pollutants from the combustion of solid biomass fuels' Progress in Energy and Combustion Science 38 (2012) 113-137

Biomass Composition

Biomass
Coal



The **ultimate analysis** gives the composition of the biomass in weight percentage of **Carbon, Hydrogen and Oxygen** as well as **Sulfur and Nitrogen**.

http://www.ieabcc.nl/workshops/task32_Lyon/full%20page/04%20David%20Baxter.pdf

Proximate and Ultimate (Elemental) Analysis of typical Biomasses

Typical proximate (ar, %) and ultimate analyses %(non-aqueous, daf) and (higher heating) calorific values for a range of biomass types.

Fuel (Oven dried)	Proximate analysis, ar				Ultimate analysis, daf				S	Cl
	Moisture	VM	FC	Ash	C	H	O	N		
Wood pine chips	4.0	81.3	14.6	0.1	52.0	6.2	41.59	0.12	0.08	0.01
Willow, SRC	6.96	75.70	16.31	1.03	51.62	5.54	42.42	0.38	0.03	0.01
Miscanthus giganteus	14.2	70.4	14.1	1.3	49.1	6.4	43.98	0.26	0.13	0.13
Switch Grass	7.17	73.05	15.16	4.62	49.40	5.70	44.25	0.45	0.1	0.1
Straw-wheat straw	7.78	68.83	17.09	6.30	49.23	5.78	43.99	0.64	0.1	0.26
Rice husks	9.4	74	13.2	12.8	42.3	6.1	50.56	1.1	0.1	0.04
Palm PKE	7.60	72.12	16.18	4.10	51.12	7.37	38.21	2.80	0.3	0.2
Sugar cane bagasse	10.4	76.7	14.7	2.2	49.9	6	43.15	0.4	0.04	0.51
Olive residue	6.40	65.13	19.27	9.20	54.42	6.82	37.29	1.40	0.05	0.04
Cow dung	13.9	60.5	11.9	13.7	54.00	6.4	36.7	0.83	0.03	1.0
Lignin	9.0	73.5	1.5	16	72.0	6.6	21.34	0	0	0
Cellulose	4.1	94.0	0.2	1.7	44.4	6.17	49.3	0	0	0

C/H/O atomic balances allow to define biomass composition in terms of three Reference Components

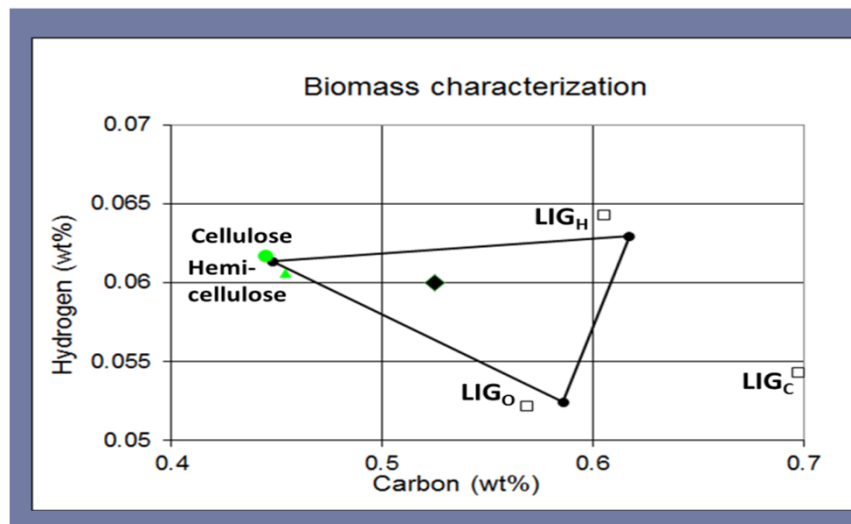
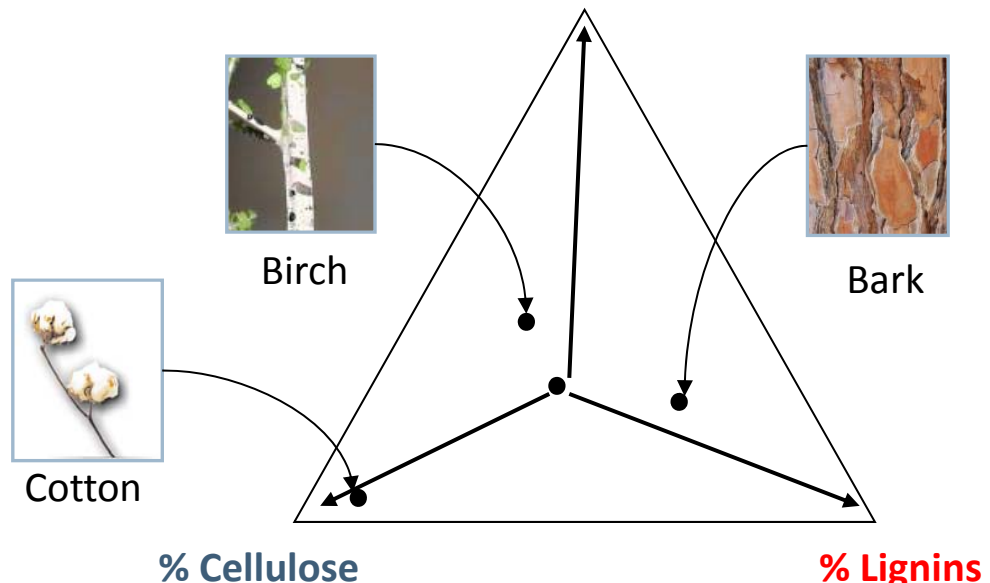
A. Williams, J.M. Jones, L. Ma, M. Pourkashanian 'Pollutants from the combustion of solid biomass fuels' Progress in Energy and Combustion Science 38 (2012) 113-137

Biomass Characterization

Biomass is considered as a linear combination of Cellulose, Hemicellulose and Lignins

Ultimate Analysis allows to derive
Biomass composition in terms of
Cellulose, Hemicellulose and Lignins

18
% Hemicellulose



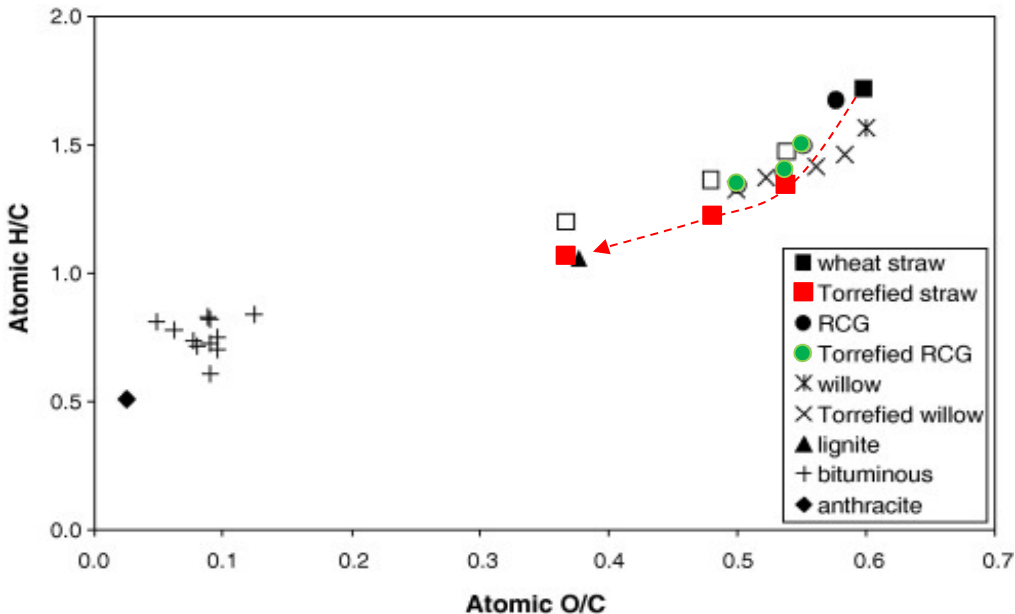
Weight fraction of reference components:
(daf basis)

Cellulose	$-C_6H_{10}O_5^-$	0.329
Hemicellulose	$-C_5H_8O_4^-$	0.179
LIG_H	$-C_{22}H_{28}O_9^-$	0.253
LIG_O	$-C_{20}H_{22}O_{10}^-$	0.175
LIG_C	$-C_{15}H_{14}O_4^-$	0.064

Ranzi, E., Cuoci, A., Faravelli, T., Frassoldati, A., Migliavacca, G., Pierucci, S., & Sommariva, S. (2008). Chemical kinetics of biomass pyrolysis. Energy & Fuels, 22(6), 4292-4300. Energy & Fuels, 2008, 4292-4300

Pyrolysis and Devolatilization

Biomass and Cellulose



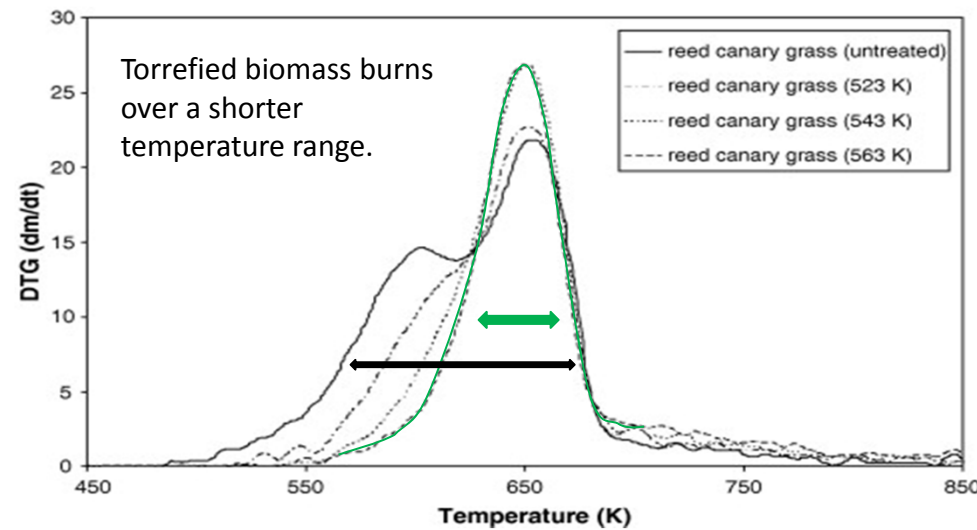
Van Krevelen diagram for coals, biomass and **torrefied biomass**.

The advantages are more pronounced at higher torrefaction temperatures.

Biomass Torrefaction is a first step in the Pyrolysis Process

Torrefied biomass devolatilises and burns over a shorter temperature range.

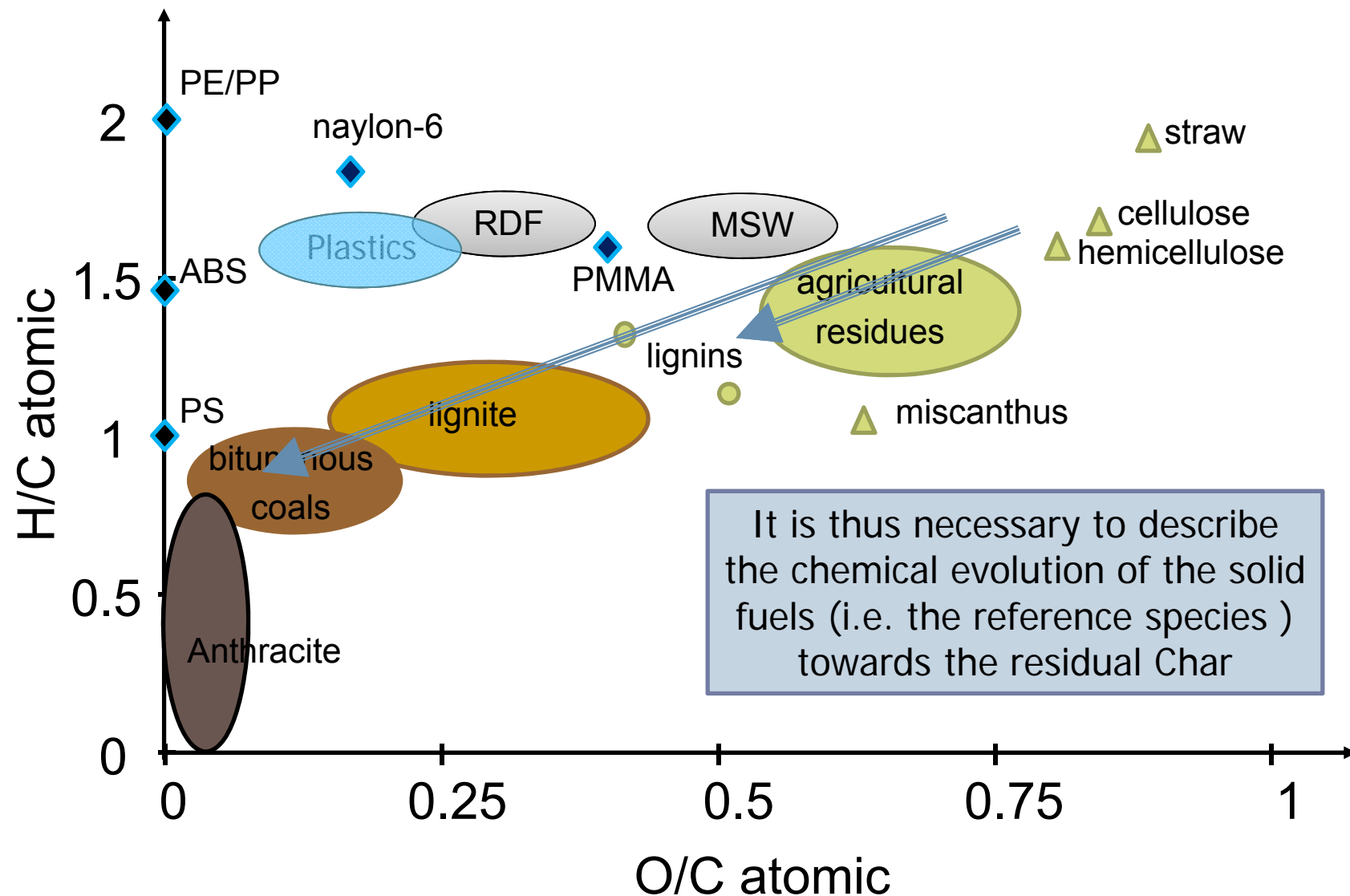
The higher fixed carbon content means that torrefied biomass has a greater combustion heat.



Devolatilisation profiles of untreated and treated reed canary grass (RCG).

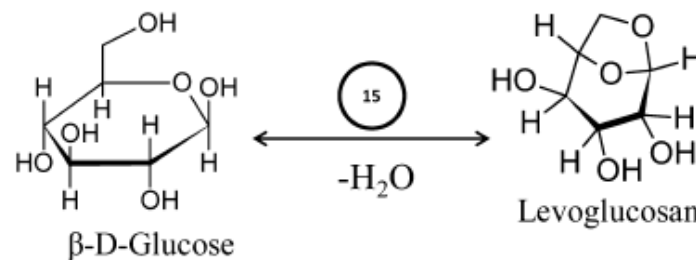
T.G. Bridgeman , J.M. Jones , I. Shield , P.T. Williams (2008) 'Torrefaction of reed canary grass, wheat straw and willow to enhance solid fuel qualities and combustion properties' *Fuel* 87(6) 844 - 856

Torrefaction and Pyrolysis are the first steps in Thermal Treatments of Solid Fuels.

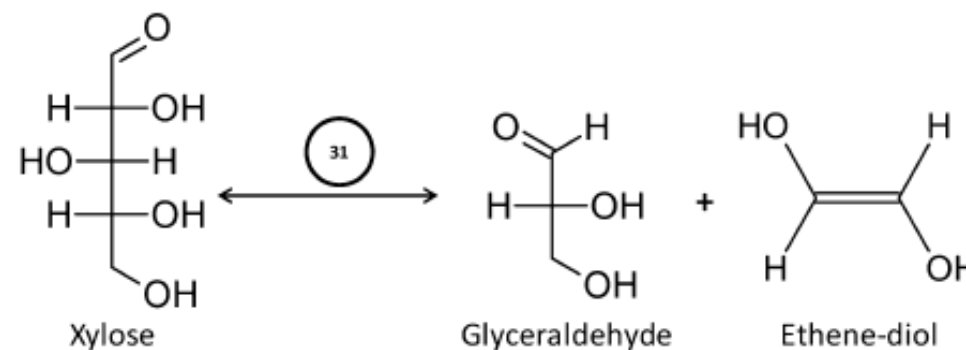


Cellulose Pyrolysis.

Concerted Reactions and Mechanism of Glucose Pyrolysis and Implications for Cellulose Kinetics



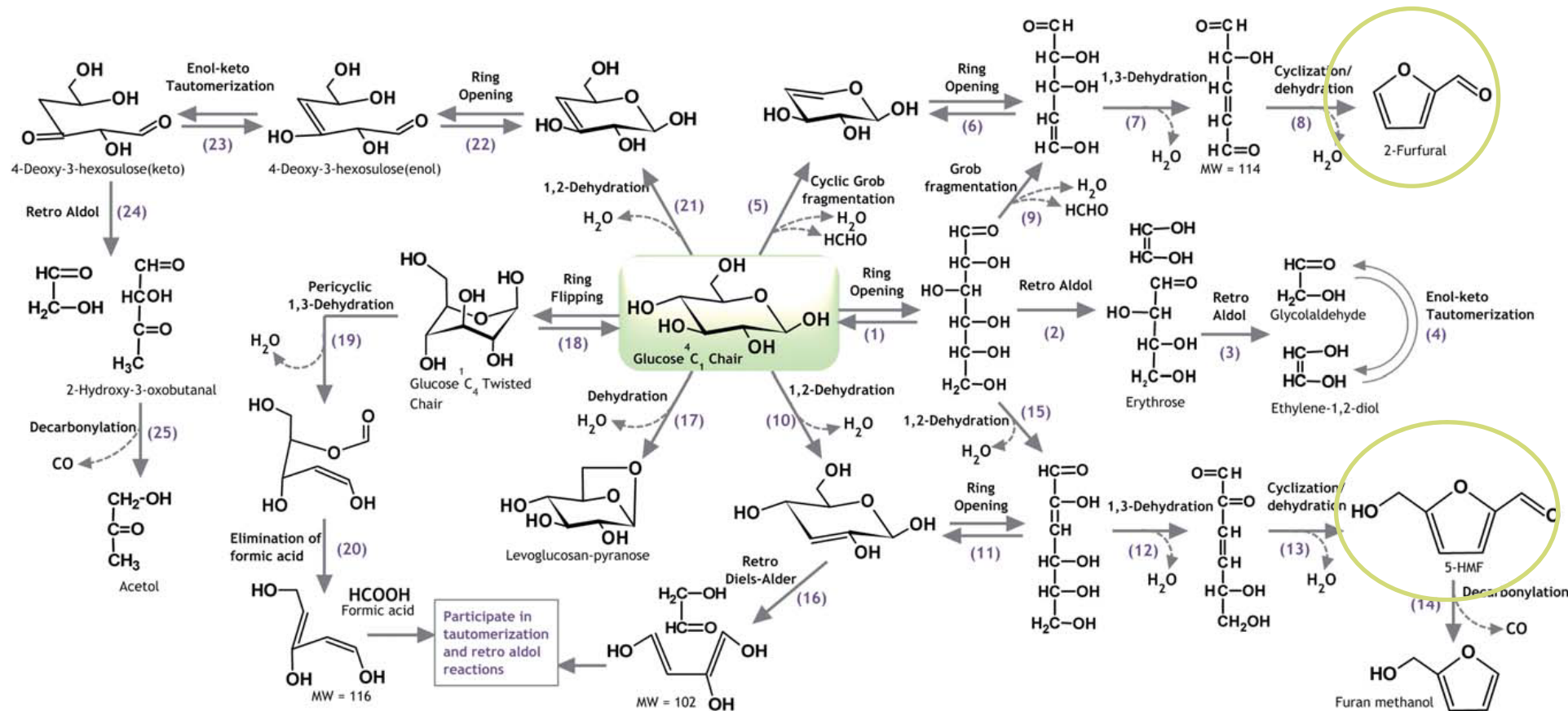
Formation of levoglucosan from β-D-glucose by dehydration.



Retro-aldol condensation of xylose

V. Seshadri and P. R. Westmoreland 'Concerted Reactions and Mechanism of Glucose Pyrolysis and Implications for Cellulose Kinetics' J. Phys. Chem. A 2012, 116, 11997–12013

Mechanism of formation of C1–C6 organic compounds from glucose



Intermediates produced from glucose via concerted reactions in the condensed phase.

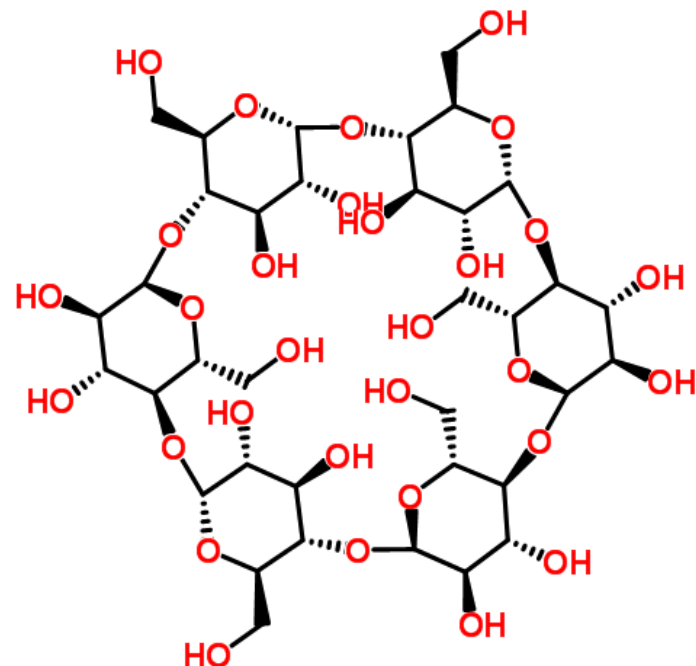
Glucose is short-lived and rapidly transforms to various melt phase and vapor phase species.

R. Vinu and L. J. Broadbelt (2012) 'A mechanistic model of fast pyrolysis of glucose-based carbohydrates to predict bio-oil composition'
Energy Environ. Sci., 2012

Conversion of cellulose to furans and small oxygenates

Ab initio molecular dynamics simulations are performed with α -cyclodextrin to reveal the pathways of cellulose pyrolysis.

Homolytic cleavage of glycosidic linkages and furan formation directly from cellulose without any small-molecule (e.g., glucose) intermediates are obtained.



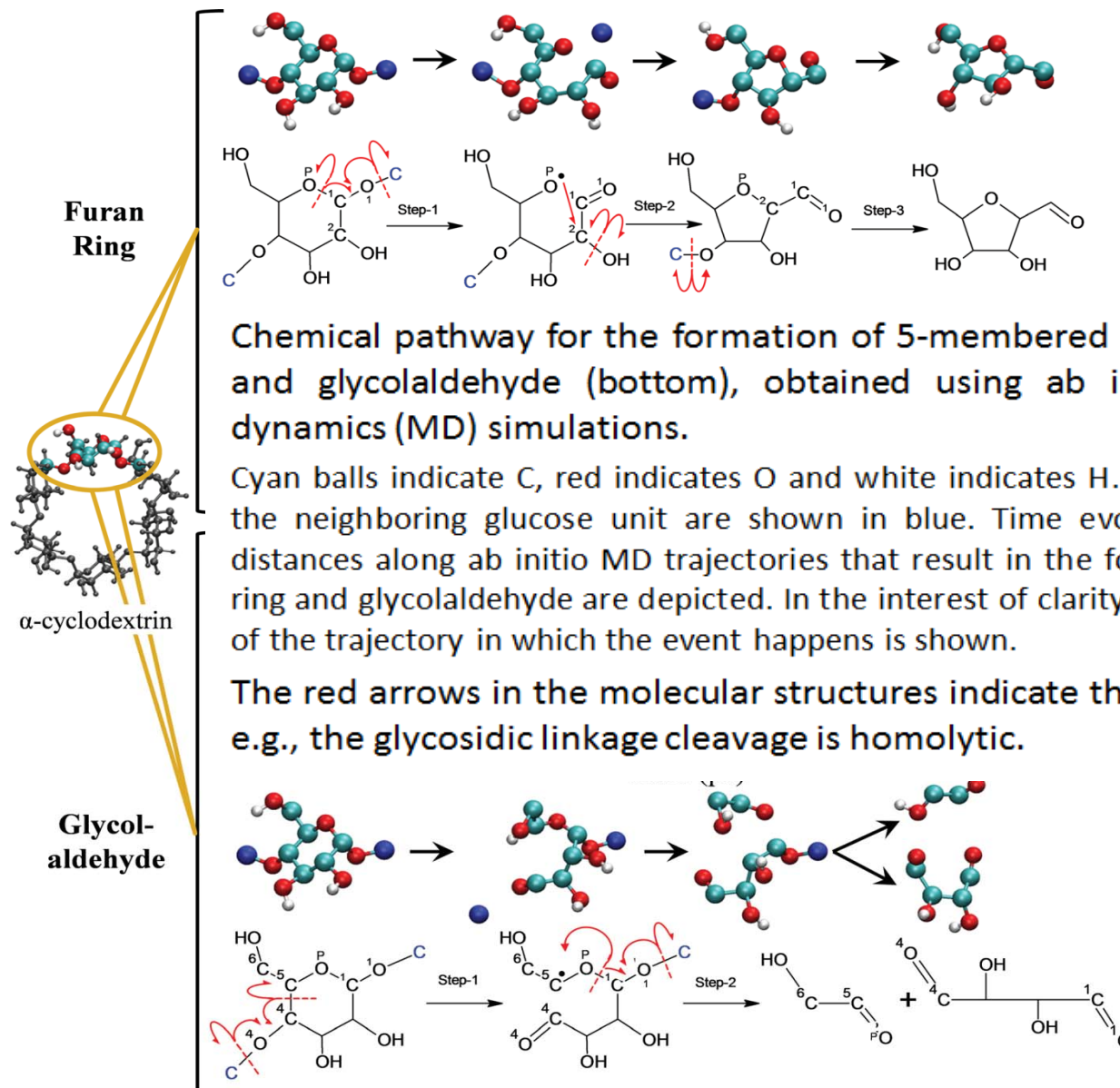
α -cyclodextrin is an appropriate surrogate of cellulose.

Contrary to previous pyrolysis work using mm-scale cellulose samples, thin-film pyrolysis enables the study of condensed-phase pyrolysis chemistry under isothermal conditions and minimizes the breakdown of volatile products.

This work combines thin-film technology with first-principles computations to elucidate major condensed-phase pyrolysis paths.

M. S. Mettler, S. H. Mushrif, A. D. Paulsen, A. D. Javadekar, D. G. Vlachos and P. J. Dauenhauer 'Revealing pyrolysis chemistry for biofuels production: Conversion of cellulose to furans and small oxygenates' *Energy Environ. Sci.*, 2012, 5, 5414-5424

Reaction Pathways of α -cyclodextrin Pyrolysis.



Chemical pathway for the formation of 5-membered furan ring (top) and glycolaldehyde (bottom), obtained using ab initio molecular dynamics (MD) simulations.

Cyan balls indicate C, red indicates O and white indicates H. Carbon atoms of the neighboring glucose unit are shown in blue. Time evolution of atomic distances along ab initio MD trajectories that result in the formation of furan ring and glycolaldehyde are depicted. In the interest of clarity, only the portion of the trajectory in which the event happens is shown.

The red arrows in the molecular structures indicate the electron flow, e.g., the glycosidic linkage cleavage is homolytic.

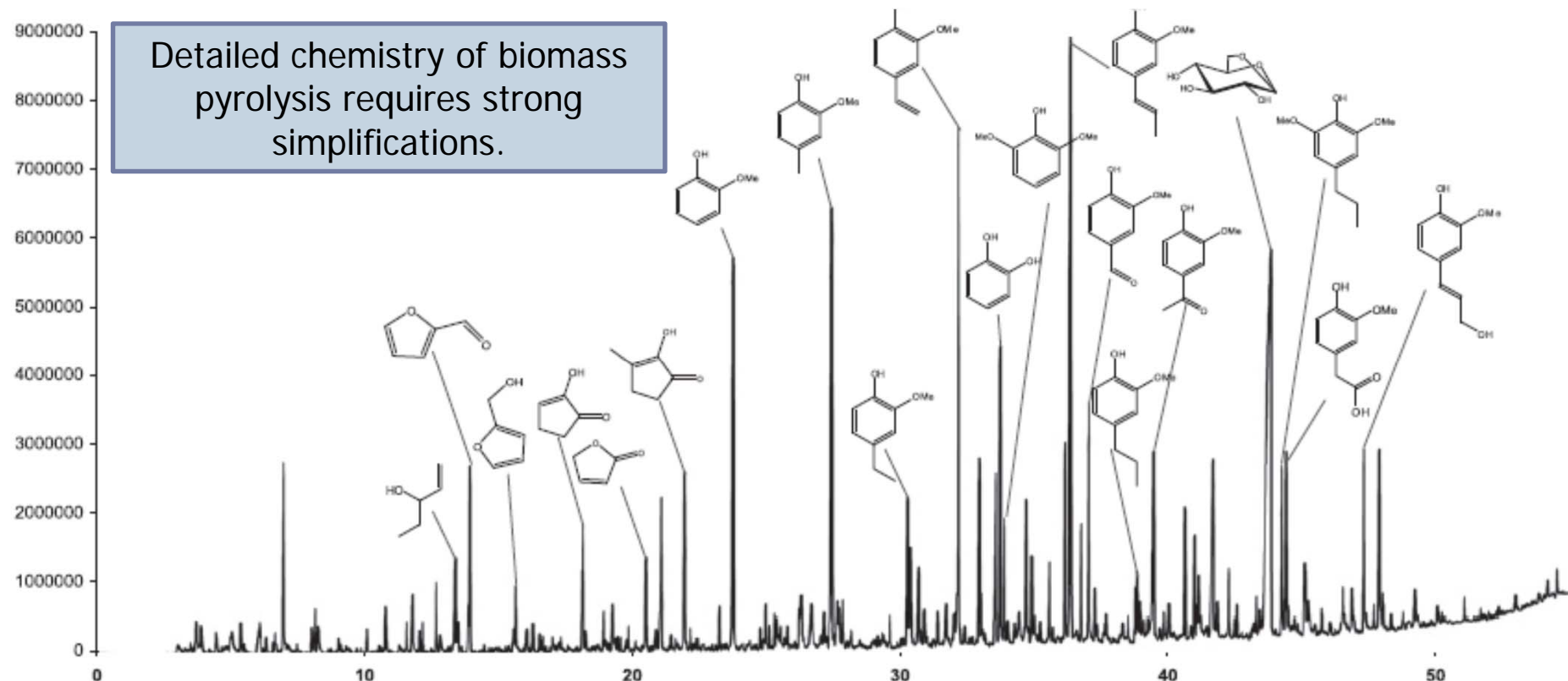
M. S. Mettler et al., *Energy Environ. Sci.*, 2012, 5, 5414-5424

Compounds from thin-film pyrolysis experiments

Compound	Cellulose powder yield [%C]	Cellulose thin film yield [%C]	α -Cyclodextrin thin film yield [%C]
Char ^{b,c}	9 ± -	12 ± -	14 ± -
Levoglucosan ^{b,c,d}	48 ± 4	27 ± 2	24 ± 1
Hydroxymethylfurfural ^{b,c,d}	3.9 ± 0.5	3.7 ± 0.1	3.6 ± 0.2
Glycoaldehyde ^{b,c}	1.9 ± 0.6	7.9 ± 0.4	8.3 ± 0.6
Methylglyoxal ^{b,g}	2.0 ± 0.7	6.7 ± 0.3	6.9 ± 0.5
Formic acid ^{b,f}	2 ± 1	10 ± 2	2.1 ± 0.2
ADGH ^{a,d}	3.8 ± 0.6	3.2 ± 0.1	5.2 ± 0.3
1,6 Anhydroglucofuranose ^{a,c,d}	4.0 ± 0.3	1.4 ± 0.4	1.5 ± 0.03
Carbon dioxide ^{b,c,f}	2.0 ± 0.6	3.4 ± 0.2	2.9 ± 0.4
Furfural ^{b,c,e}	1.6 ± 0.1	1.6 ± 0.2	1.2 ± 0.1
Carbon monoxide ^{b,g}	1.4 ± 0.1	3.1 ± 0.2	2.4 ± 0.2
2-Furanmethanol ^{b,c}	0.4 ± 0.4	0.6 ± 0.06	0.7 ± 0.1
Formaldehyde ^{b,f,g}	4.4 ± 0.9	2.6 ± 0.2	2.1 ± 0.1
Glyoxal ^{b,f,g}	0.3 ± 0.1	1.2 ± 0.04	0.9 ± 0.1
Acetic acid ^{b,c,e,f,g}	0.27 ± 0.04	0.6 ± 0.06	0.5 ± 0.2
Hydroxyacetone ^{b,c,f,g}	0.54 ± 0.08	2.6 ± 0.3	2.4 ± 0.1
2,5 Dimethyl furan ^{b,e}	0.34 ± 0.09	0.8 ± 0.1	0.5 ± 0.1
2,3 Butanedione ^{b,f}	0.37 ± 0.02	0.8 ± 0.06	0.8 ± 0.1
5-Methyl furfural ^{b,c}	0.48 ± 0.4	0.7 ± 0.2	0.6 ± 0.2
DHGP ^{a,c,d}	0.98 ± 0.09	2.2 ± 0.06	2.7 ± 0.2
Levoglucosenone ^{b,c}	0.3 ± 0.2	0.5 ± 0.06	0.4 ± 0.06
Catechol ^b	0.25 ± 0.04	0.3 ± 0.03	0.7 ± 0.4
2(5H) Furanone ^b	0.20 ± 0.01	0.6 ± 0.05	0.5 ± 0.06
1,2-Cyclopentanedione ^a	0.20 ± 0.01	0.6 ± 0.05	0.6 ± 0.1
Furan ^{b,c,e}	0.65 ± 0.06	0.3 ± 0.03	0.1 ± 0.02
2-Methyl furan ^{b,c,e}	0.20 ± 0.04	0.3 ± 0.02	0.2 ± 0.01
CPHM ^{b,c}	0.2 ± 0.1	0.3 ± 0.03	0.2 ± 0.02
Total	86 ± 3	95 ± 3	86 ± 2

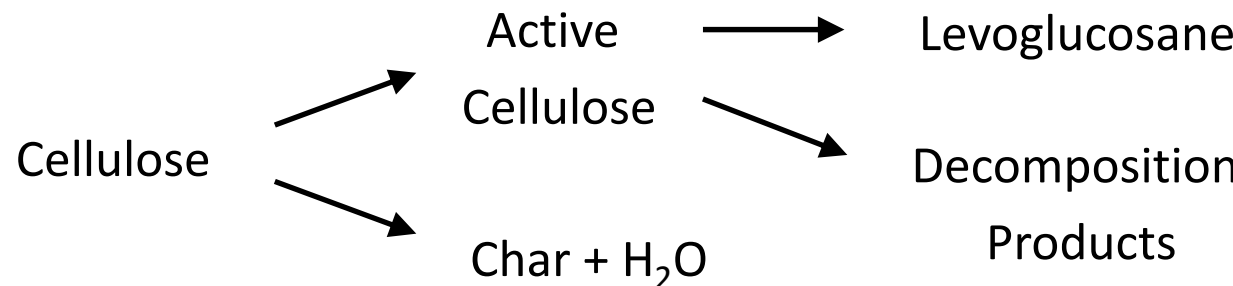
Average values are shown for thin-film pyrolysis at 500 C with 90% mean confidence intervals.

Pollutants from the combustion of biomass. (Py-GC-MS of Pine)



A. Williams, J.M. Jones, L. Ma, M. Pourkashanian 'Pollutants from the combustion of solid biomass fuels' Progress in Energy and Combustion Science 38 (2012) 113-137

Multistep Kinetic Model of Cellulose Pyrolysis



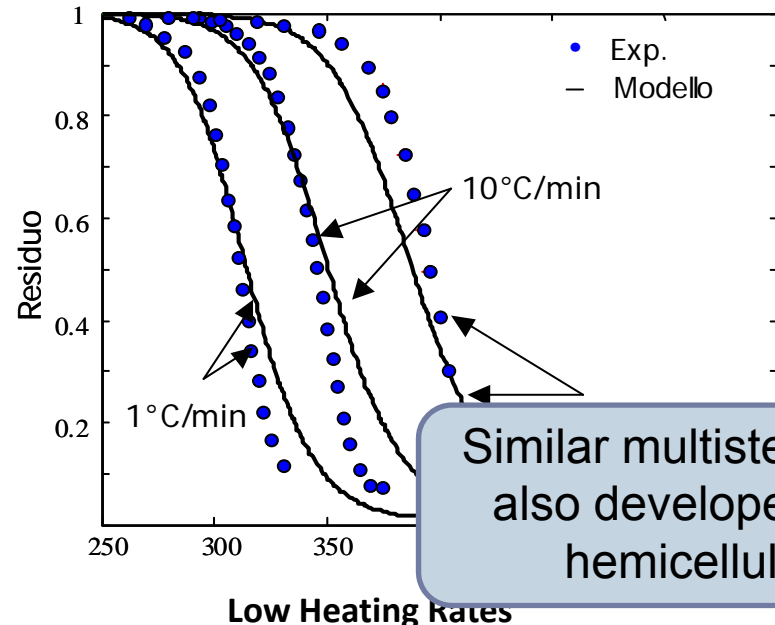
Reaction	Kinetic constant [s ⁻¹]	Reaction Heat [kj/kg]
Cellulose → Active Cellulose	$8 \times 10^{13} \exp(-45000/RT)$	0
Active Cellulose → Acetic Acid + 0.2 Glyoxal + 0.2 CH ₃ CHO + 0.25 HMFU + 0.2 C ₃ H ₆ O + 0.22 CO ₂ + 0.16 CO + 0.83 H ₂ O + 0.1 CH ₄ + 0.01 HCOOH + 0.01G{H ₂ } + 0.61 Char	$1 \times 10^9 \exp(-30000/RT)$	650
Active Cellulose → Levoglucosane	$4 \times T \exp(-10000/RT)$	490
CELL → 5 H ₂ O + 6 Char	$8 \times 10^7 \exp(-31000/RT)$	-1800

These reactions describe not only the residual char (Broido-Shafizadeh model), but also the detailed composition of released gas and tar species.

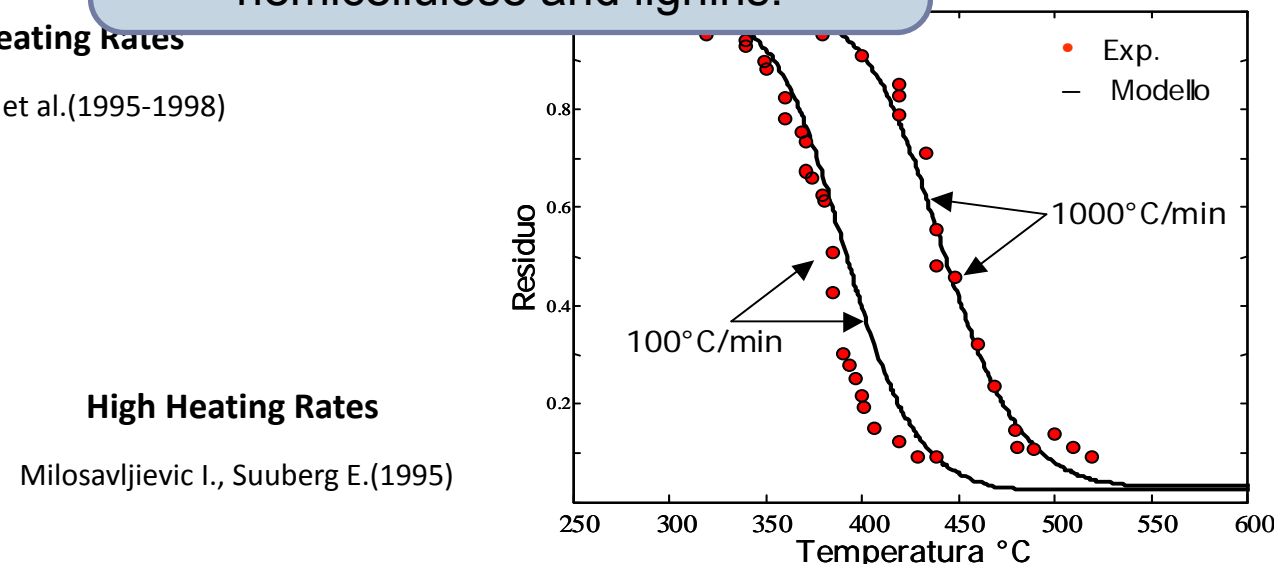
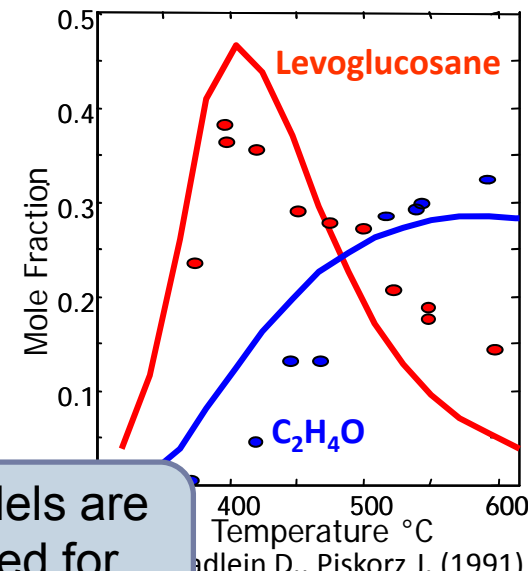
Ranzi, E., Cuoci, A., Faravelli, T., Frassoldati, A., Migliavacca, G., Pierucci, S., & Sommariva, S. (2008). Chemical kinetics of biomass pyrolysis. *Energy & Fuels*, 22(6), 4292-4300. *Energy & Fuels*, 2008, 4292-4300

Validation of Cellulose Pyrolysis Model

Comparisons with experimental TG data

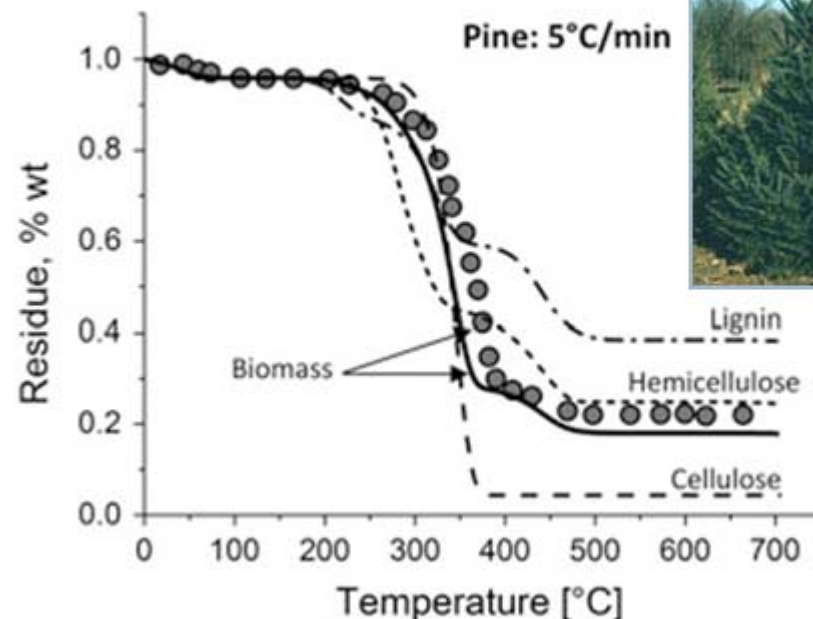
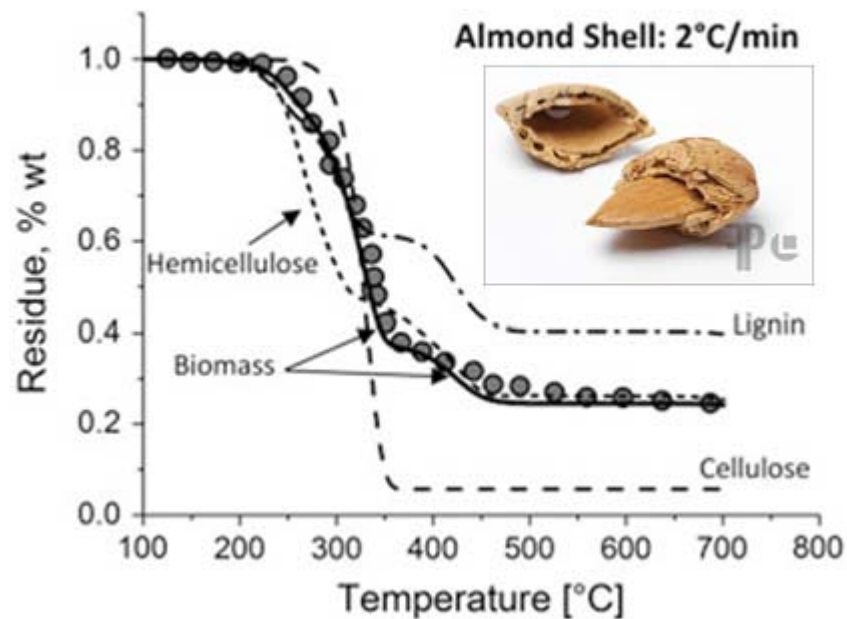


Similar multistep kinetic models are also developed and validated for hemicellulose and lignins.



Validation of Biomass Pyrolysis Model

Comparisons with experimental TG data



Biomass devolatilization is then the combination of the pyrolysis of cellulose, hemicellulose, and lignin

From Biomass to Coal

The same approach is used for:

- Coal Characterization
- Multistep Kinetic Model of Coal Devolatilization

Coal Characterization

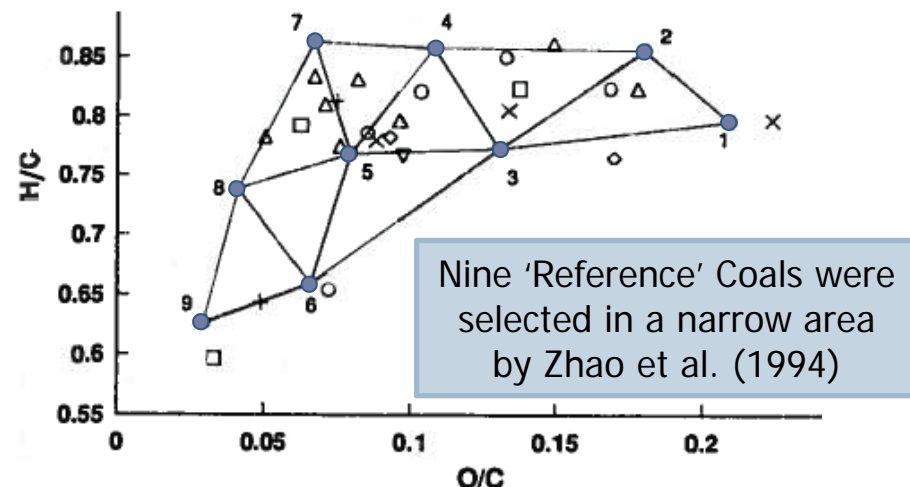
Three reference coals are selected:

COAL1 → anthracite

COAL2 → bituminous

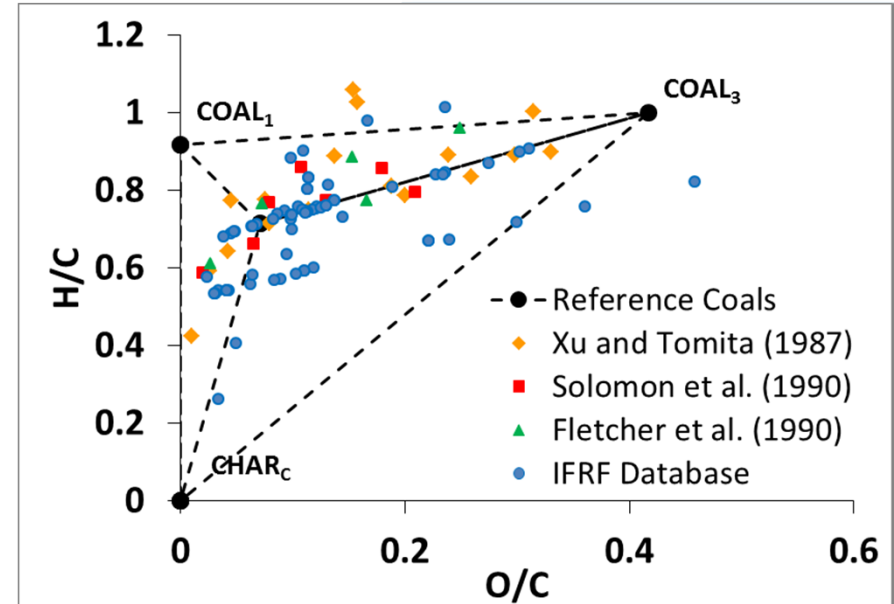
COAL3 → lignite

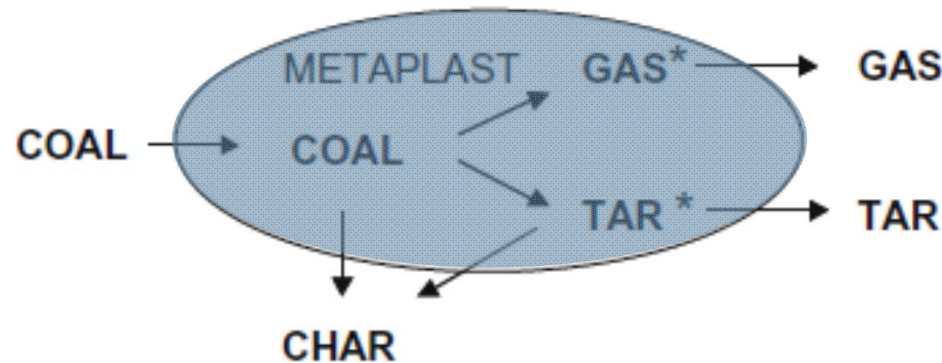
Again, Elemental Analysis and C/H/O balances allow to define actual coal as a mixture of three Reference Coals



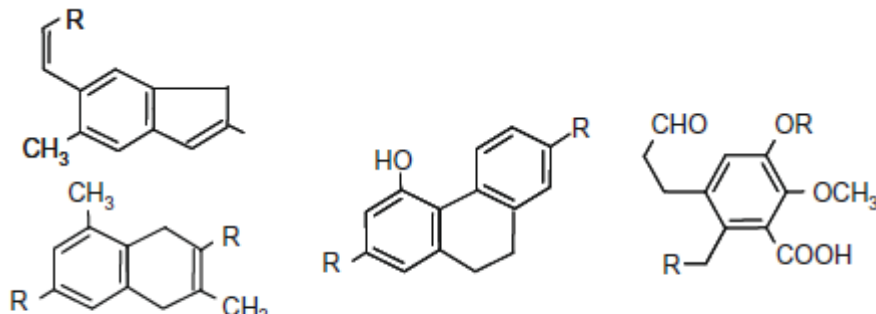
Zhao, Y., Serio, M. A., Bassilakis, R., & Solomon, P. R. (1994). A method of predicting coal devolatilization behavior based on the elemental composition. '25th Symposium on Combustion' 25(1): 553-560. Elsevier.

Sommariva, S., Maffei, T., Migliavacca, G., Faravelli, T., & Ranzi, E. (2010). A predictive multi-step kinetic model of coal devolatilization. Fuel, 89(2), 318-328.





Initially the coal forms a metaplastic phase, then, with different mechanisms at low and high temperatures, gas and tar species are released.



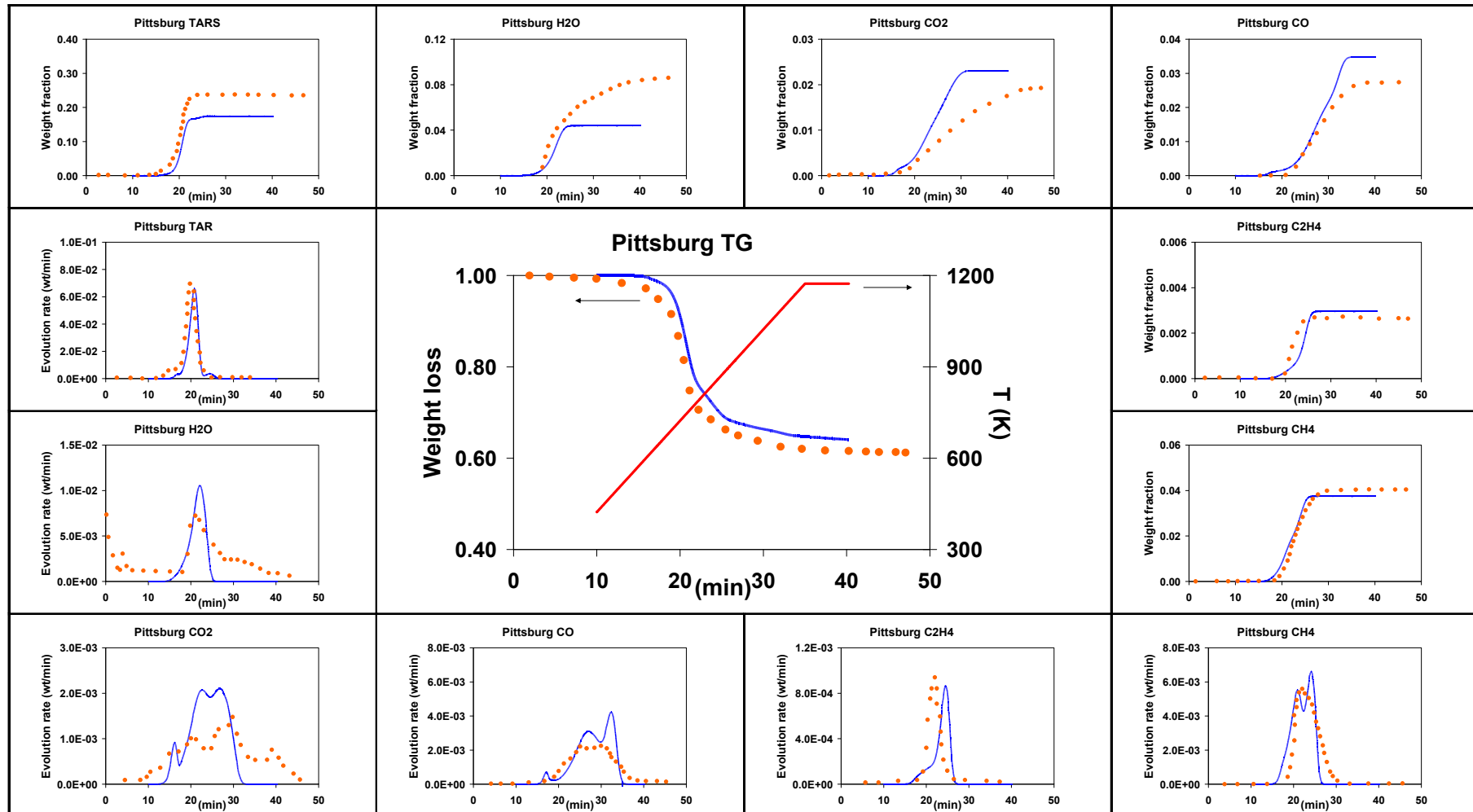
A multistep kinetic model was also developed and validated for the three reference coals.

Sommariva, S., Maffei, T., Migliavacca, G., Faravelli, T., & Ranzi, E. (2010). A predictive multi-step kinetic model of coal devolatilization. Fuel, 89(2), 318-328.

Extensive Validation of Coal Pyrolysis Model

TG Experiments of Solomon et al. (1990)

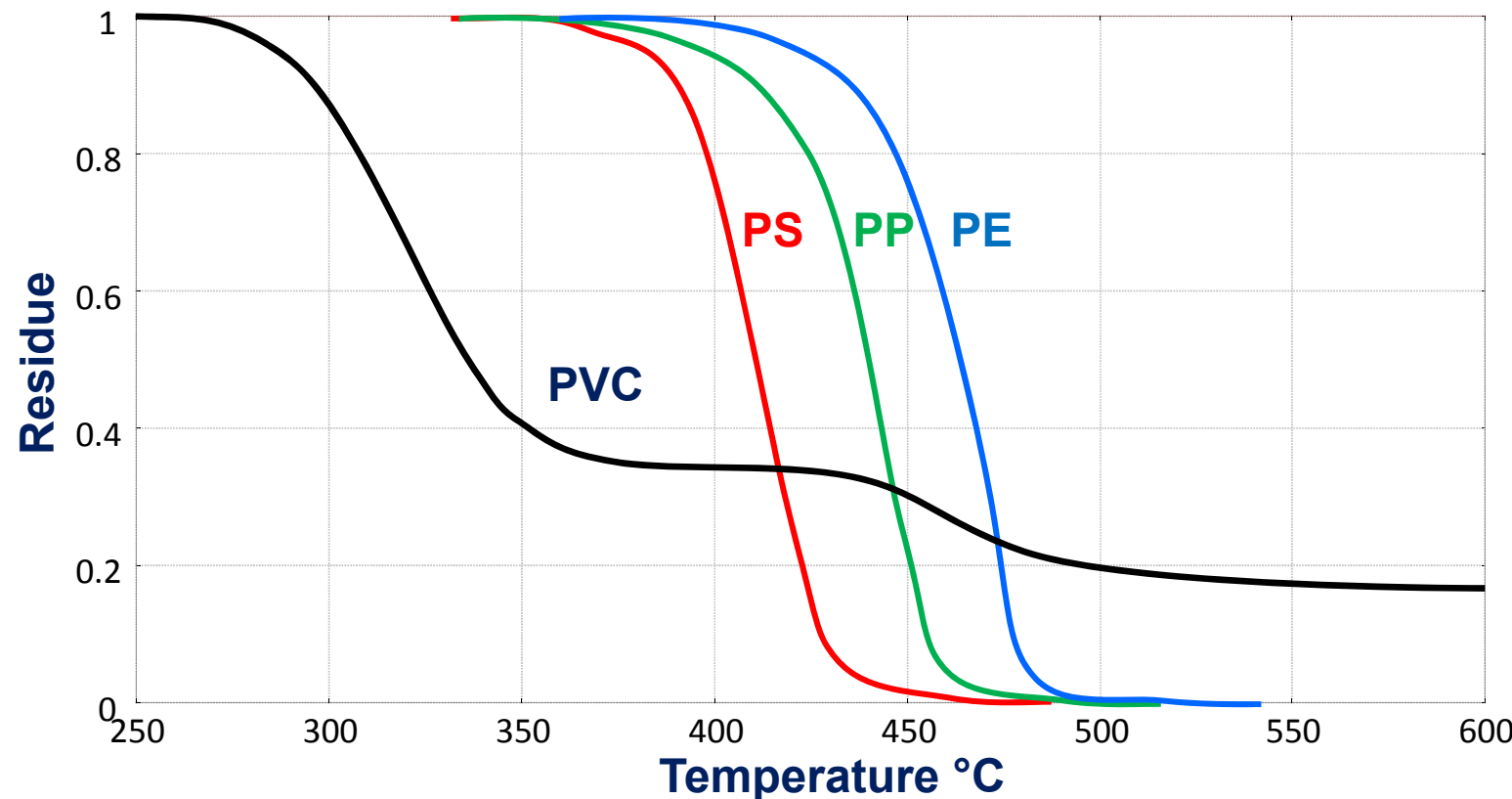
Solid residue, Tar , CO_x , H₂O, CH₄, C₂H₄ and their evolution rates



Sommariva, S., Maffei, T., Migliavacca, G., Faravelli, T., & Ranzi, E. (2010). A predictive multi-step kinetic model of coal devolatilization. Fuel, 89(2), 318-328.

Pyrolysis of Plastic Polymers

TG depolymerization of Poly-Styrene (PS), Poly-Propylene (PP), and Poly-Ethylene (PE) follows the Bond Dissociation Energies. Residual char is negligible.

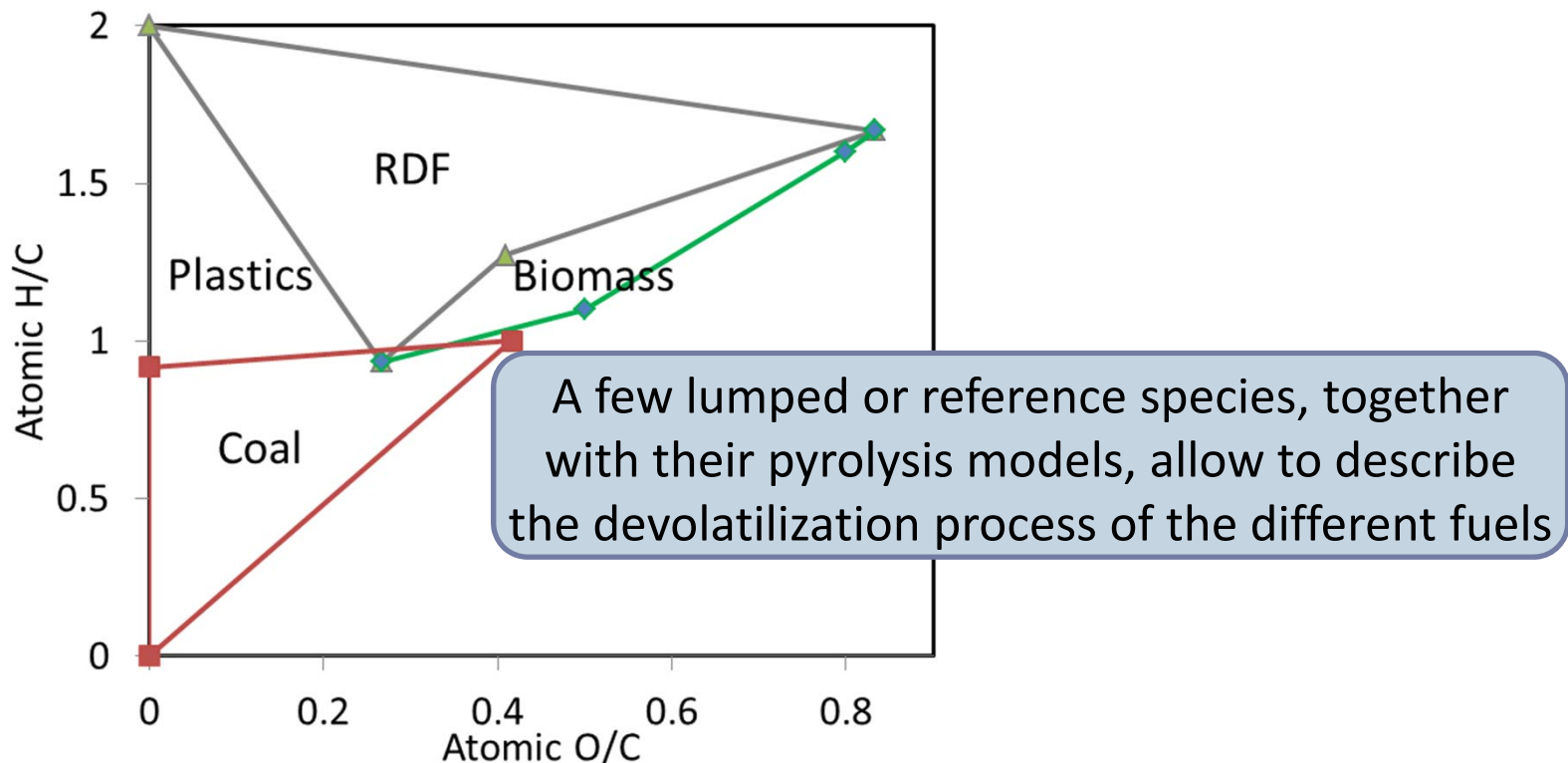


Dehydrochlorination of Poly-Vinyl-Chloride (PVC) is the fastest step.
The formation of $(-\text{CH}=\text{CH}-)_n$ is the reason for the successive residual char.

Ranzi, E., Dente, M., Faravelli, T., Bozzano, G., Fabini, S., Nava, R., ... & Tognotti, L. (1997). Kinetic modeling of polyethylene and polypropylene thermal degradation. Journal of Analytical and Applied Pyrolysis, 40, 305-319.

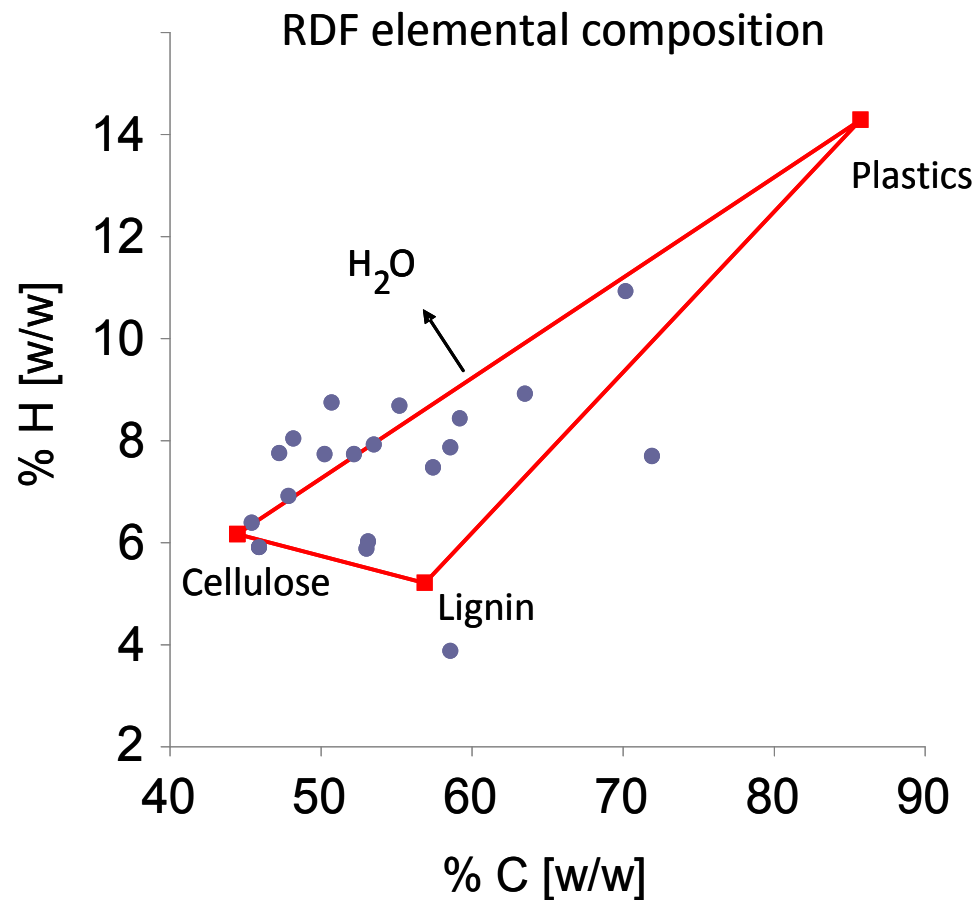
Solid Fuels and Reference (Lumped) Species

The overall kinetic model of **Solid Fuel Pyrolysis** is simply the combination of the multistep kinetic models of Biomass , Plastics, and Coals.



The peculiarity of this approach is that all these schemes consist of a limited number of devolatilization reactions, which are able to describe not only the solid residue, but also the detailed composition of released gas and tar species.

Elemental H/C/O Characterization of RDF



RDF (on daf basis) are simply characterized in terms of Plastics, Cellulose and Lignin on the basis of H/C/O balances and heating value.

Sommariva, S., Grana, R., Maffei, T., Pierucci, S., & Ranzi, E. (2011). A kinetic approach to the mathematical model of fixed bed gasifiers. *Computers & Chemical Engineering*, 35(5), 928-935.

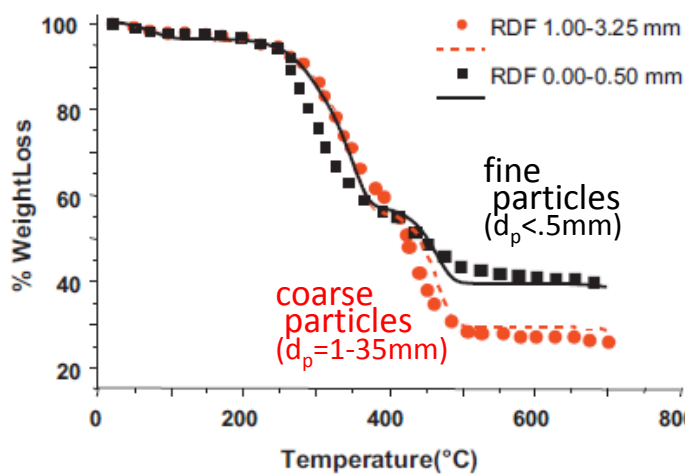


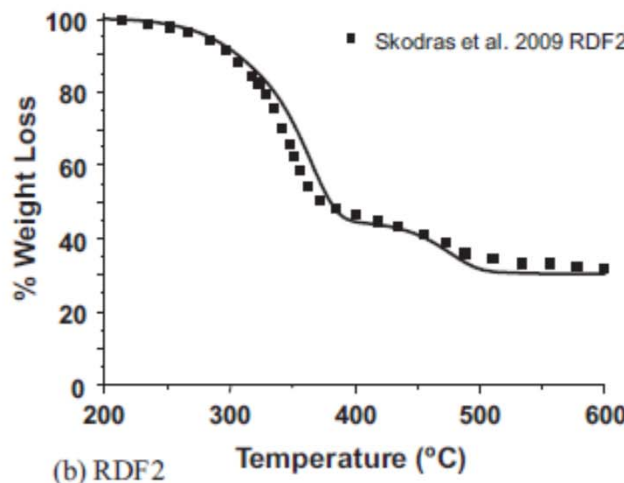
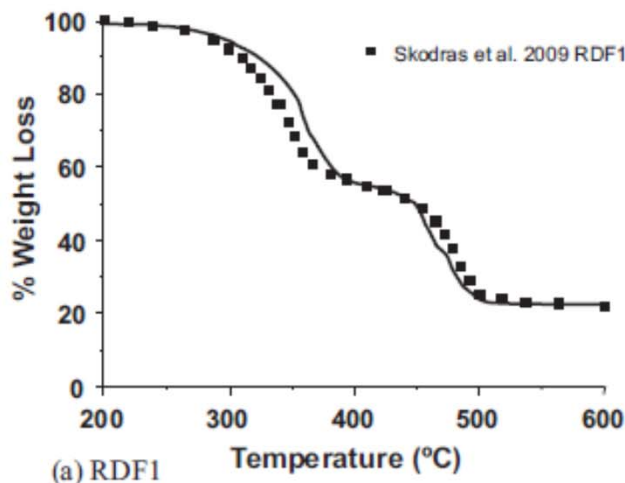
Fig. 3. Effect of RDF particle sizes on TGA at 10 K/min (Buah et al., 2007).

Plastic content is higher in coarse particles and it is responsible of the second devolatilization step at 400–500 °C.

Ash and inert materials are more abundant in fine particles.

(Buah et al., 2007)

This dependence of RDF composition on the particle size was also observed in terms of different heating value by Skodras et al. (2008).



Sommariva, S., Grana, R., Maffei, T., Pierucci, S., & Ranzi, E. (2011). A kinetic approach to the mathematical model of fixed bed gasifiers. *Computers & Chemical Engineering*, 35(5), 928-935.

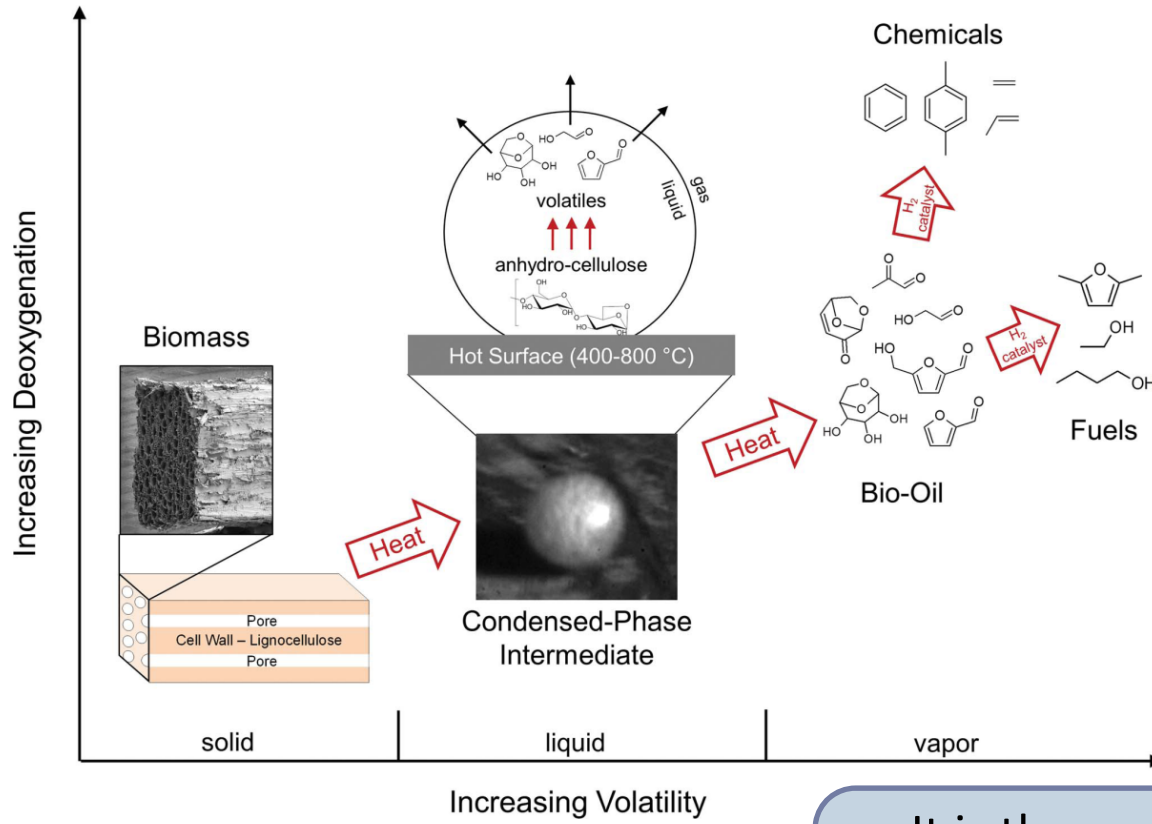
Multi-Phase Nature

of Solid Fuel Pyrolysis Process.

Importance of secondary gas-phase reactions

Multi-Component and Multi-Phase Nature

of Coal and Biomass Pyrolysis Process.



The initial thermal decomposition of coal and biomass produces a solid char residue. Further heating of the liquid intermediate produces

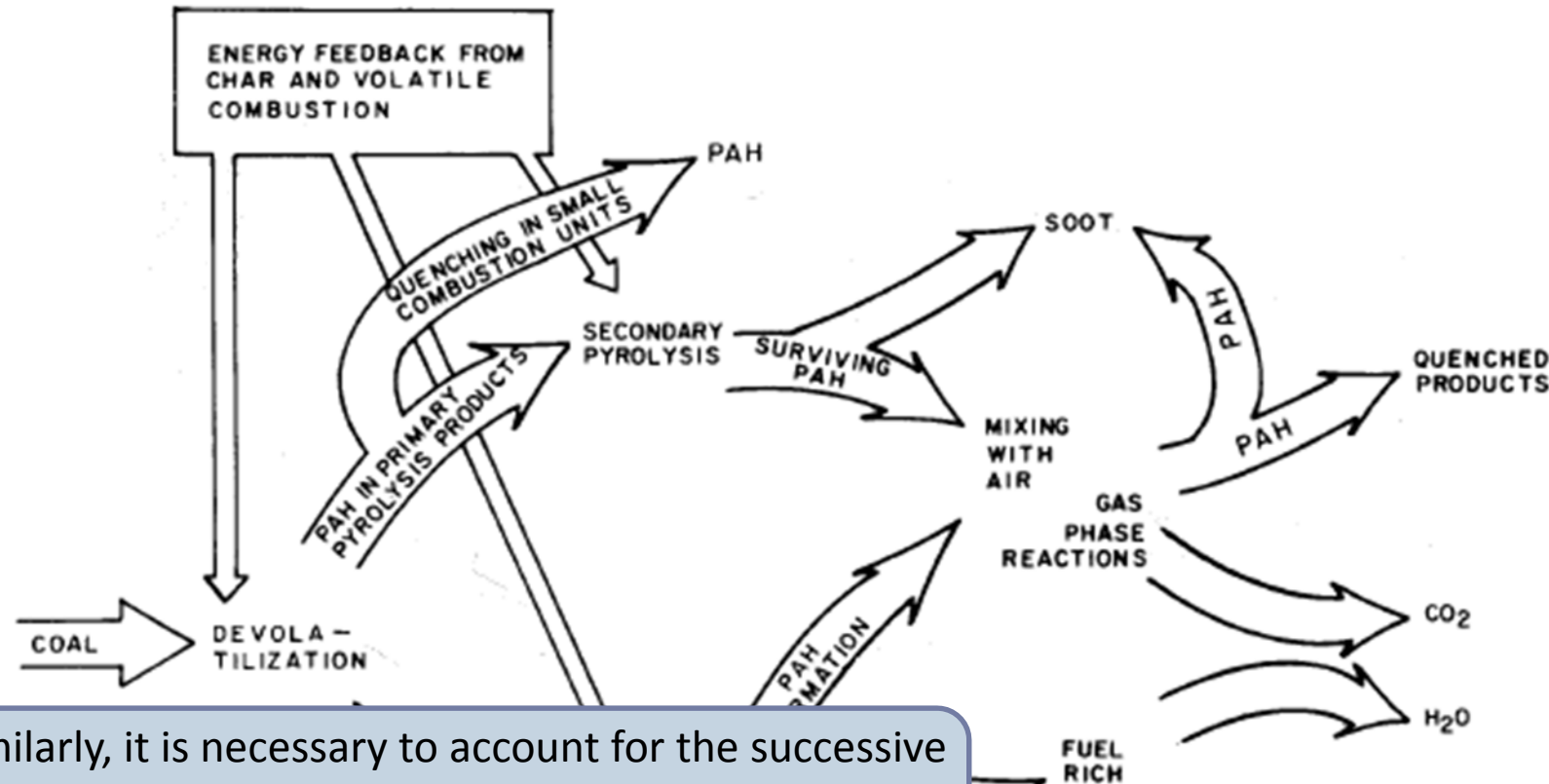
Thousands of solid, liquid, gas-phase reactions are involved in Coal and Biomass pyrolysis.

They deoxygenate and volatilize solid fuel to generate liquids and gases.

It is then necessary to account for
Gas-Phase Secondary Reactions
Heterogeneous Char reactions

M. S. Mettler, S. H. Mushrif, A. D. Paulsen, A. D. Javadekar, D. G. Vlachos and P. J. Dauenhauer 'Revealing pyrolysis chemistry for biofuels production: Conversion of cellulose to furans and small oxygenates' *Energy Environ. Sci.*, 2012, 5, 5414-5424

Secondary Gas Phase Reactions : PAH and Soot Formation in Coal Pyrolysis (Sarofim et al., 1987)



Similarly, it is necessary to account for the successive pyrolysis and oxidation reactions of all the volatiles (gas and tar) released by the solid fuels.

Mitra, A., Sarofim, A. F., & Bar-Ziv, E. (1987). The influence of coal type on the evolution of polycyclic aromatic hydrocarbons during coal devolatilization. *Aerosol science and technology*, 6(3), 261-271.

Size of Gas-Phase Kinetic Mechanisms

42

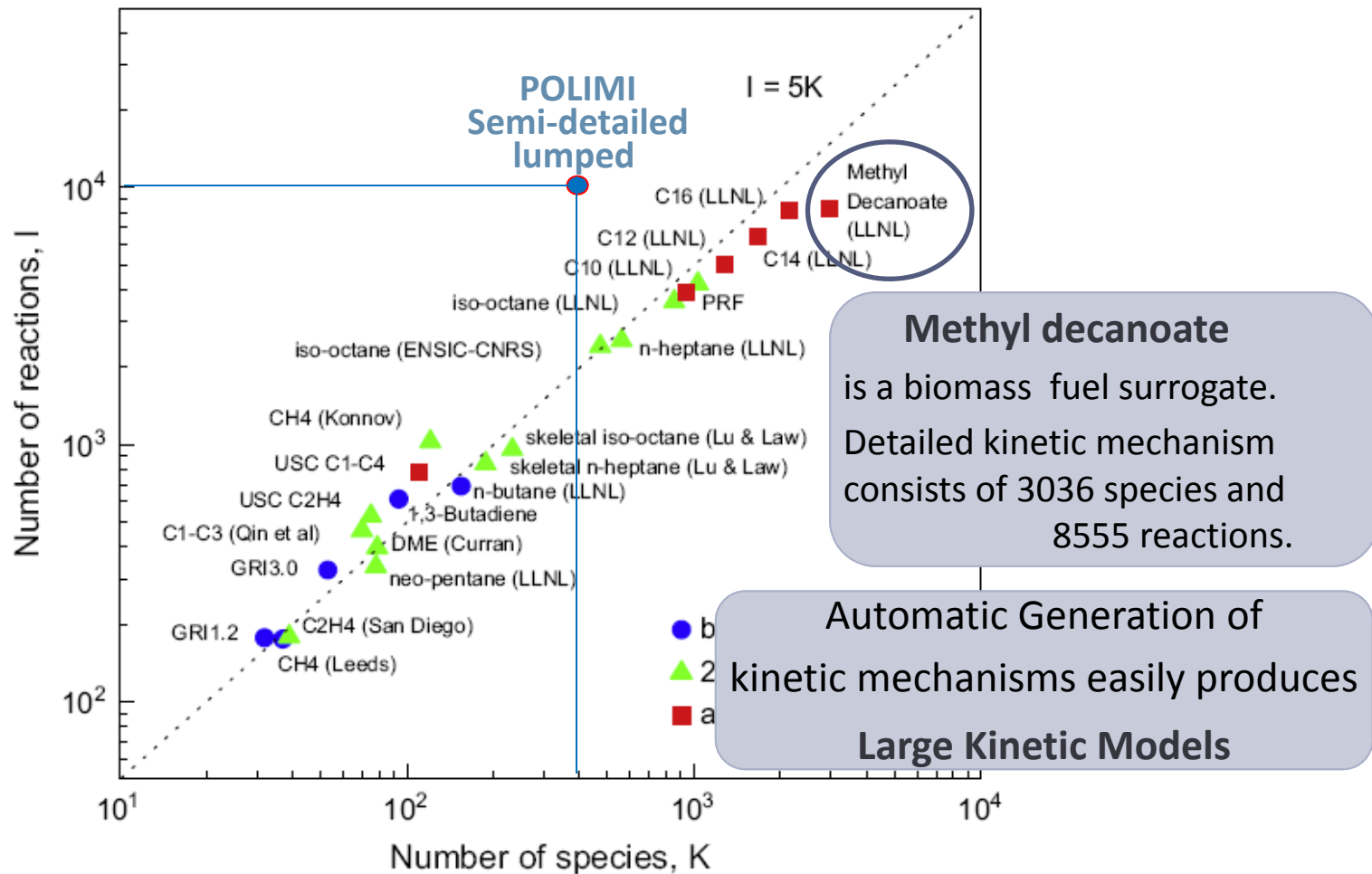


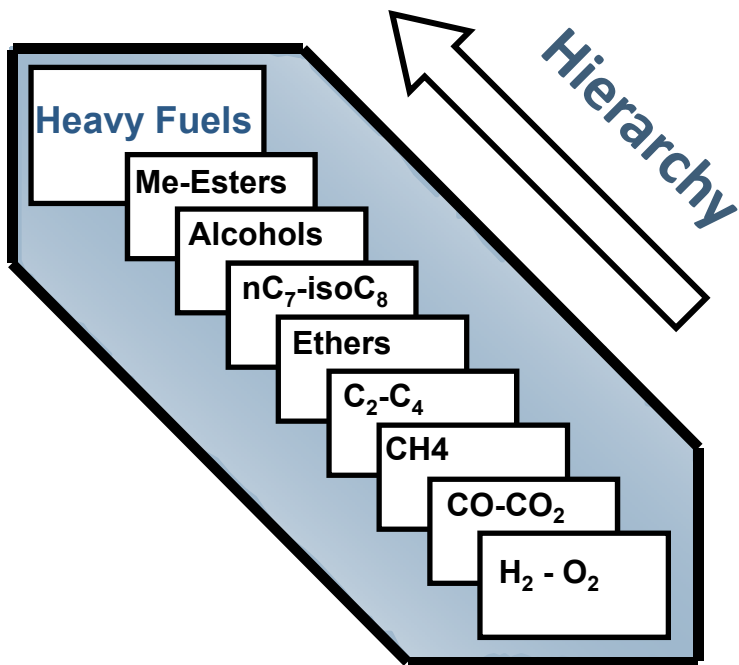
Fig. 10. Size of selected detailed and skeletal mechanisms for hydrocarbon fuels, together with the approximate years when the mechanisms were compiled.

T.F. Lu, C.K. Law 'Toward accommodating realistic fuel chemistry in large-scale computations'
Progress in Energy and Combustion Science 35 (2009) 192–215

Gas Phase Reactions

Detailed Kinetics of Pyrolysis and Combustion

(hundreds of species and thousands of reactions)



- GRI Kinetics for Gases
- PRF and additives for Gasolines
- Diesel and Jet Fuels
- Tar and Oxygenated Species

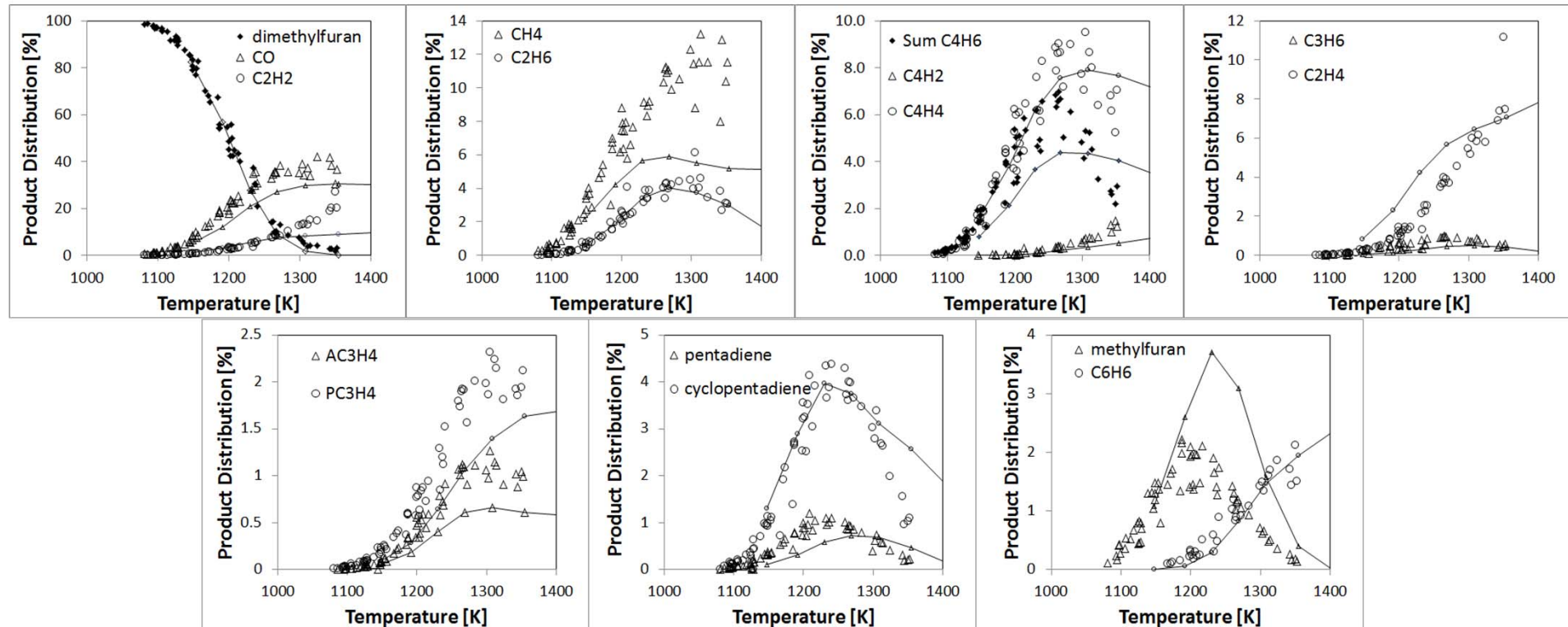
Due to the hierarchical and modular structure of detailed kinetic schemes, the extension to new oxygenated species only requires the addition of the primary propagation reactions.

Hierarchy and Modularity

are the main features of **Detailed Kinetic Schemes**

Secondary Gas-Phase Reactions: 2,5-dimethylfuran Pyrolysis (Lifshitz et al., 1998)

Comparisons of model predictions and experimental data



2,5-dimethylfuran pyrolysis in 99.5% Ar at 3 atm.

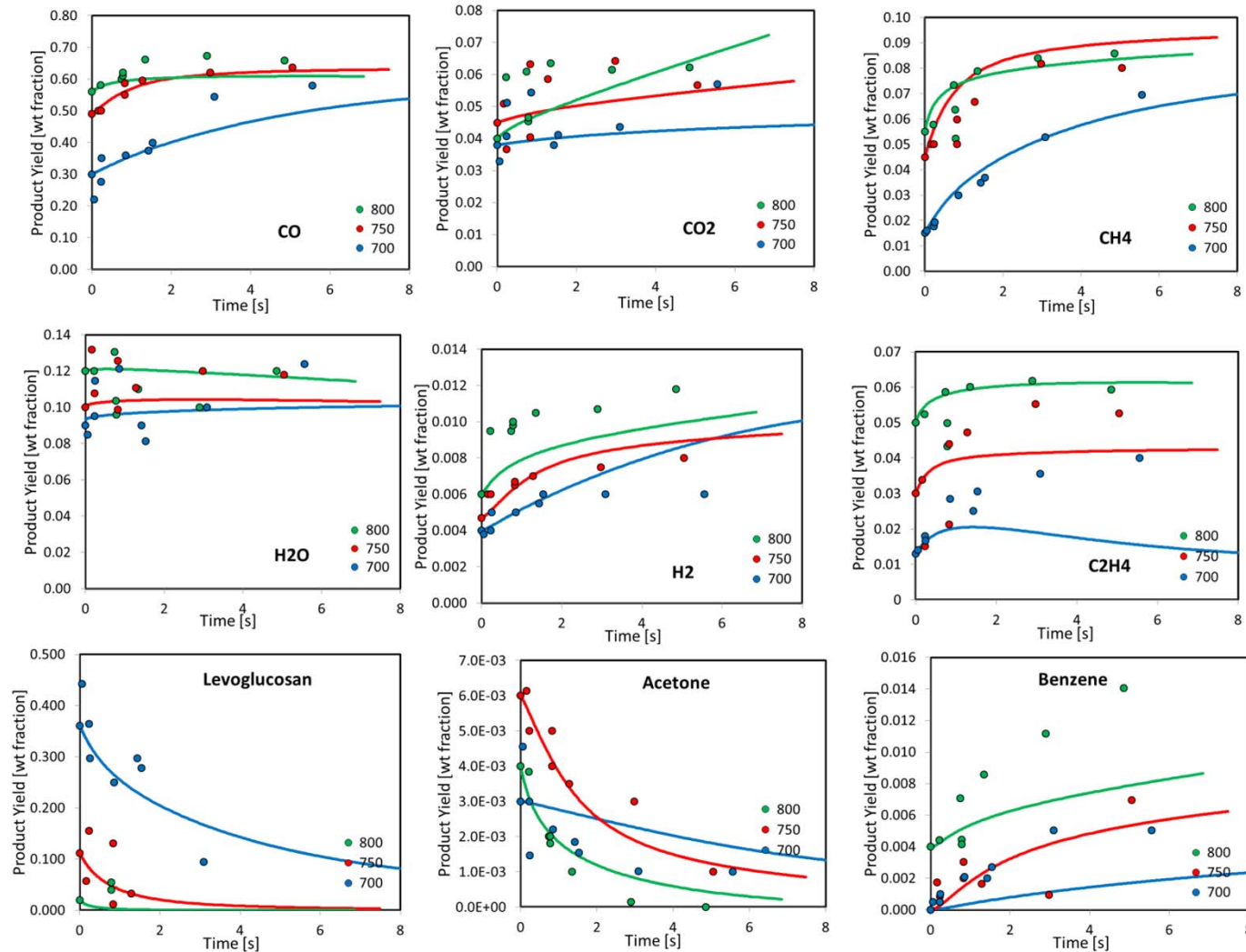
Lifshitz, A., Tamburu, C., Shashua, R., 'Thermal Decomposition of 2,5-Dimethylfuran. Experimental Results and Computer Modeling', J. Phys. Chem. A 102: 10655-10670 (1998)

Volatile released by cellulose pyrolysis

Species (wt.%)	Temperature (K)		
	973	1023	1073
H ₂	0.40	0.47	0.60
CO	30.0	49.0	56.0
CH ₄	1.50	4.50	5.50
CO ₂	3.80	4.50	4.00
C ₂ H ₄	1.30	3.00	5.00
C ₂ H ₆	0.30	0.75	1.00
H ₂ O	9.00	10.0	12.0
C ₃ H ₆	1.00	1.80	1.80
C ₃ H ₈	0.05	0.14	0.14
CH ₃ OH	2.00	3.00	4.00
CH ₃ CHO	6.00	5.80	3.00
Propenal	1.20	1.00	0.09
Furan	1.00	0.70	0.30
Acetone	0.30	0.60	0.40
CH ₃ COOH	1.50	0.80	2.20
C ₄ H ₈	0.75	0.90	1.00
C ₄ H ₁₀	0.30	0.28	0.19
Methylfiran	0.32	0.20	0.05
Butanal	0.50	0.16	0.11
Hydroxyacetone	1.80	0.50	0.07
C ₅ H ₈	0.30	0.25	0.02
C ₅ H ₁₀	0.45	0.25	0.08
Benzene	0.00	0.00	0.40
Toluene	0.05	0.15	0.10
Dimethylfiran	0.08	0.05	0.00
Levoglucosan (difference)	36.1	11.2	1.96
Total	100	100	100

Norinaga, K., Shoji, T., Kudo, S., & Hayashi, J. I. (2013). Detailed chemical kinetic modelling of vapour-phase cracking of multi-component molecular mixtures derived from the fast pyrolysis of cellulose. Fuel 103 (2013) 141–150.

Secondary Gas-Phase Reactions of Cellulose Pyrolysis Products at 700-800 °C



Norinaga, K., Shoji, T., Kudo, S., & Hayashi, J. I. (2013). Detailed chemical kinetic modelling of vapour-phase cracking of multi-component molecular mixtures derived from the fast pyrolysis of cellulose. Fuel 103 (2013) 141–150.



Heterogeneous Gas-Solid Reactions

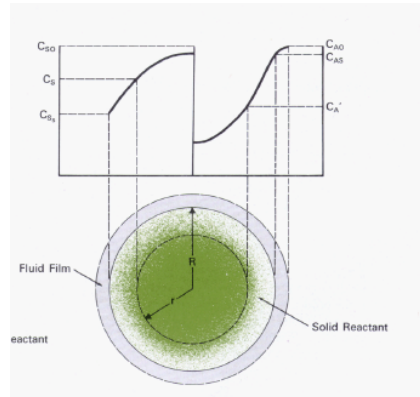
Multi-Phase Model at the Particle Scale



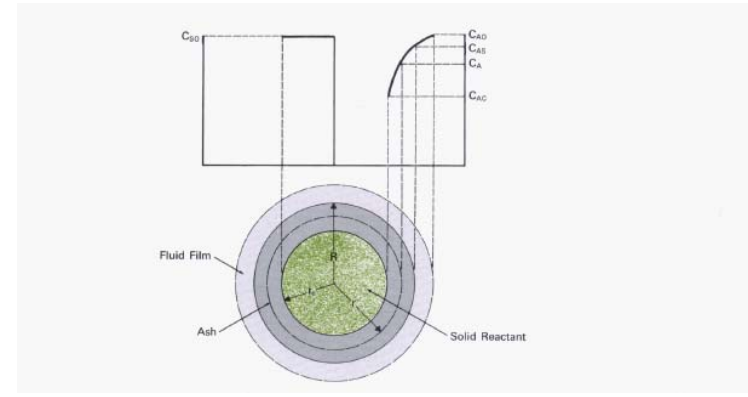
Heterogeneous Gas-Solid Reactions

Multi-Phase Model at the Particle Scale (Wen, 1968)

Particle Model consists of mass and energy balances for solid and gas phase



General Model (reacting volume)



Shrinking Model (unreacted core)

Two asymptotic regimes are usually defined:

a **kinetic controlled regime** for low temperatures and small particles
(Heat and Mass Transport are faster than Kinetics)

a **transport controlled regime** for high temperatures and big particles
(Transport rates become lower than the kinetic rates)

Wen, C. Y. (1968). Noncatalytic heterogeneous solid-fluid reaction models. *Industrial & Engineering Chemistry*, 60(9), 34-54.

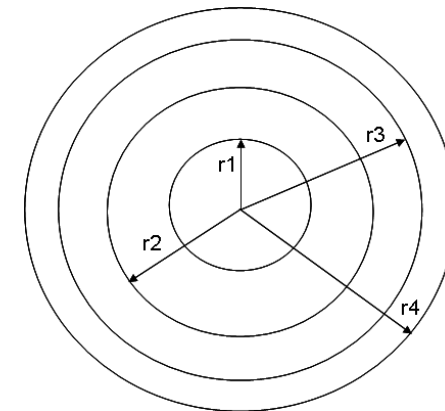
Particle Model

Particle Model consists of mass and energy balances

$R_{j,i}$ is the net formation rate of i^{th} species in the j^{th} sector

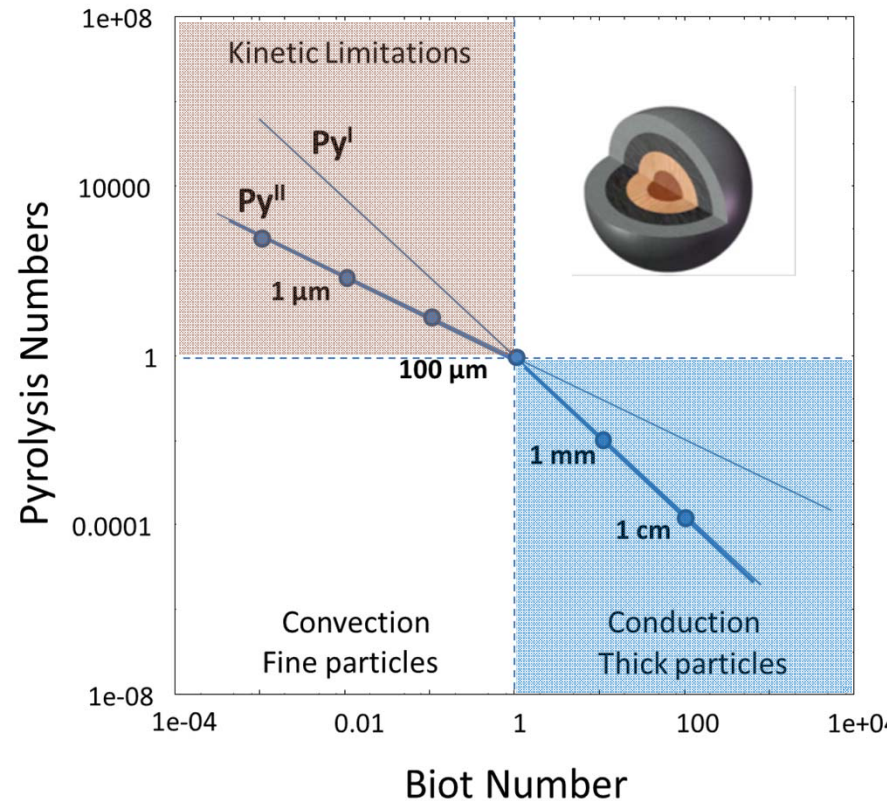
$$\left\{ \begin{array}{l} \frac{dm_{j,i}^S}{dt} = V_j \cdot R_{j,i} \\ \frac{dm_{j,i}}{dt} = [J_{j-1,i} \cdot S_{j-1} - J_{j,i} \cdot S_j] + V_j \cdot R_{j,i} \\ \frac{d \sum_{i=1}^{NCP} m_{j,i}^S c_{pj,i}^S T_j}{dt} = [JC_{j-1} \cdot S_{j-1} - JC_j \cdot S_j] + \left[S_{j-1} \cdot \sum_{i=1}^{NCP} J_{j-1,i} h_{j-1,i} - S_j \cdot \sum_{i=1}^{NCP} J_{j,i} h_{j,i} \right] + V_j \cdot HR_j \end{array} \right.$$

Conduction
Diffusion
Reaction



The density distribution is the sum of the densities of different species in each particle sector.
Similarly, the shrinking and porosity of each sector inside the particle is calculated.

Thermally Thick Particles: Biot and Pyrolysis Numbers



Py Numbers decrease
with increasing temperatures

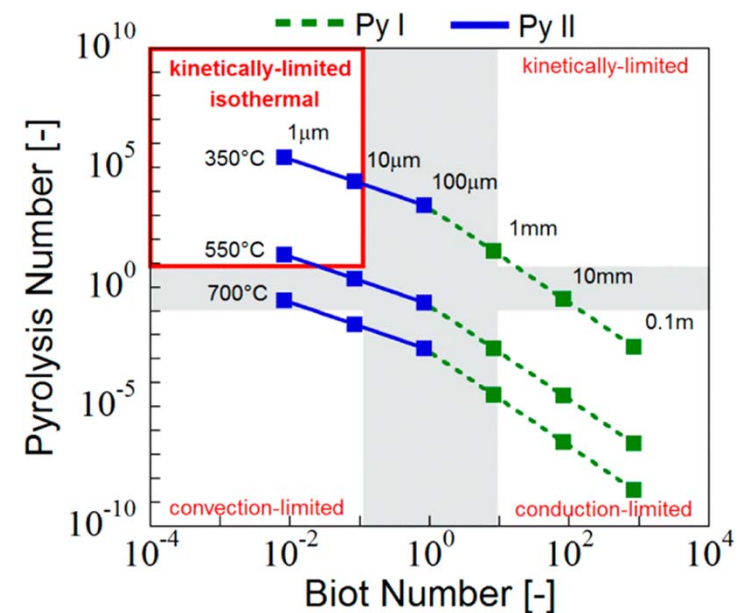
$$Bi = \frac{h \cdot d_p}{k}$$

Biot relates conduction and convection times.

$$Py^I = \frac{k}{\rho \cdot c_p \cdot d_p^2 \cdot k_{pyr}} = \frac{\alpha}{d_p^2 \cdot k_{pyr}}$$

$$Py^{II} = \frac{h}{\rho \cdot c_p \cdot d_p \cdot k_{pyr}}$$

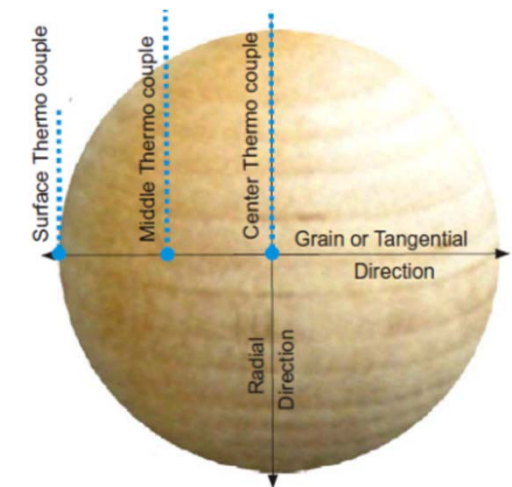
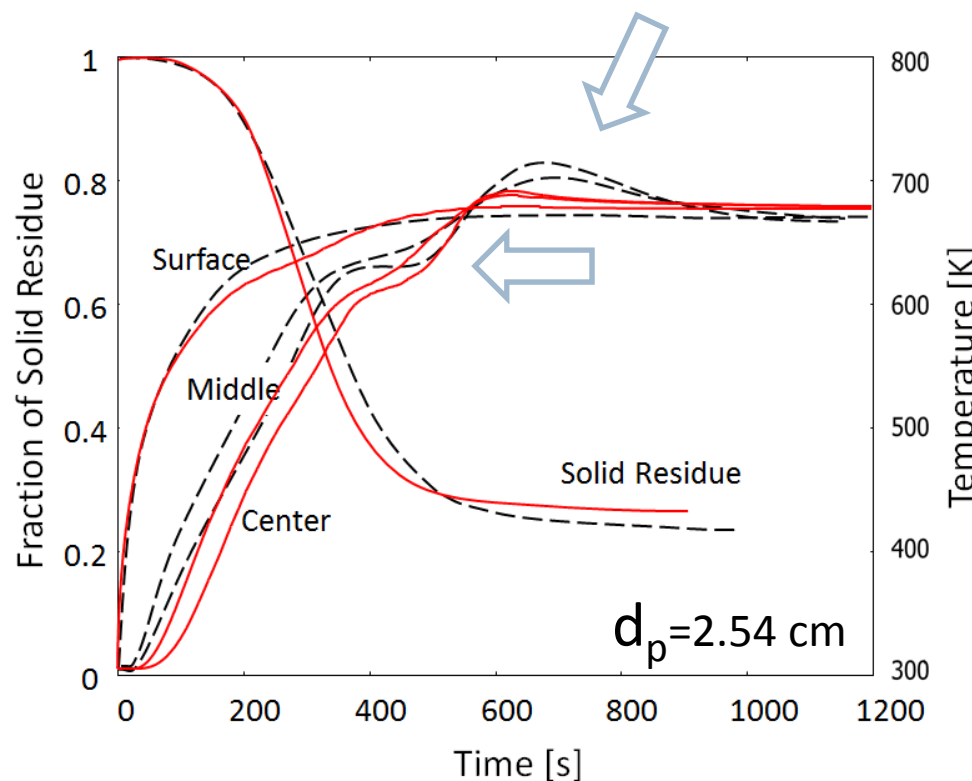
Pyrolysis Numbers relate thermal and kinetic times.



Paulsen et al. Energy Fuels 2013, 27, 2126–2134

Pyrolysis of Thermally Thick Biomass Particle

'Exotic' behavior of the center temperature profile



Wood sphere at 688 K.

The flat Temperature plateau at ~650 K is due to endothermic tar devolatilization.

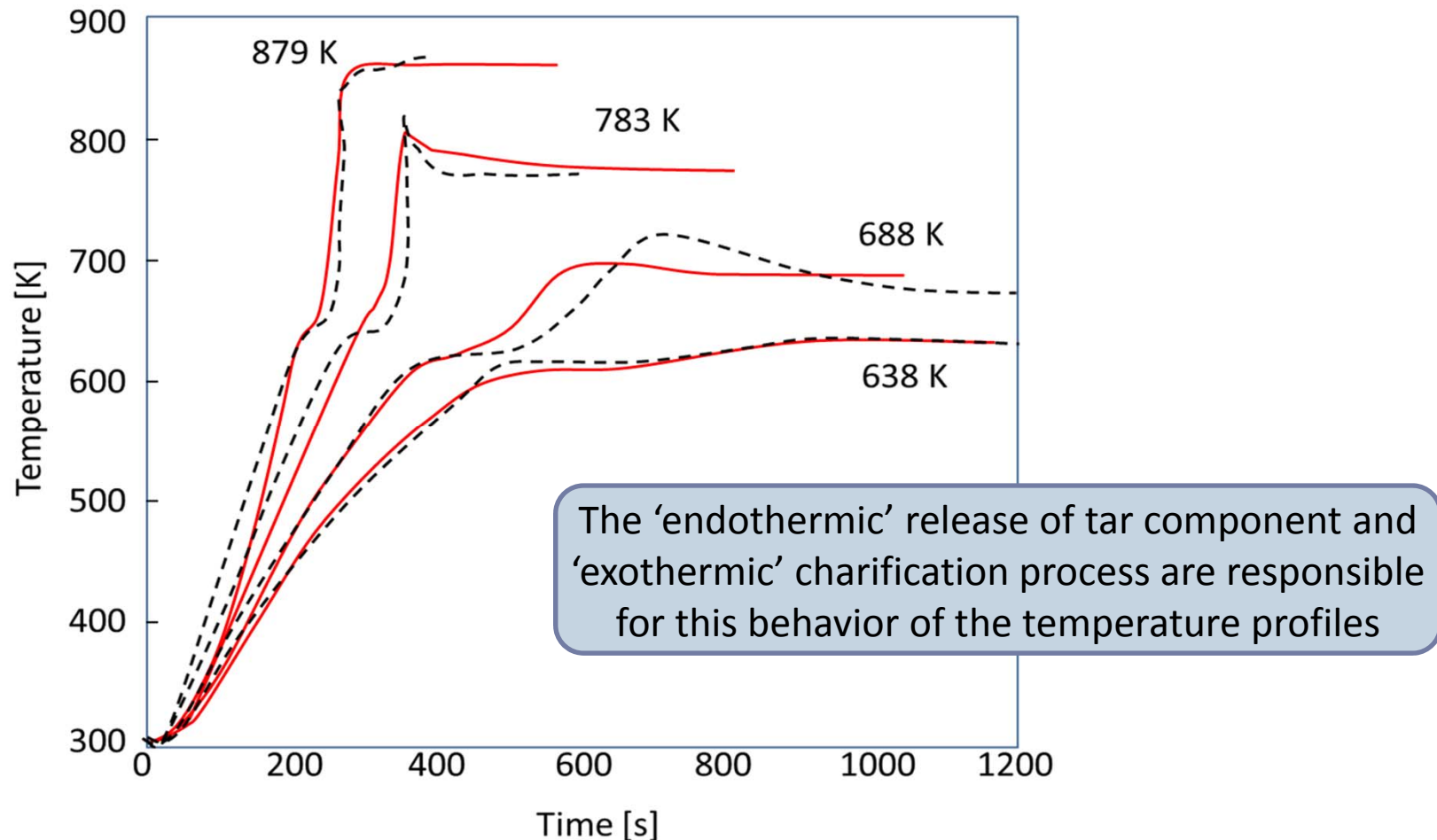
Experimental center temperature **overshoots** the external temperature,
due to the exothermic reactions of char formation

Comparisons of experimental and predicted (red lines) results.

Park, W. C., Atreya, A. and Baum, H. R. (2010) 'Experimental and theoretical investigation of heat and mass transfer processes during wood pyrolysis', Combustion and Flame, 157(3), 481-494.

Pyrolysis of Thick Biomass Particle

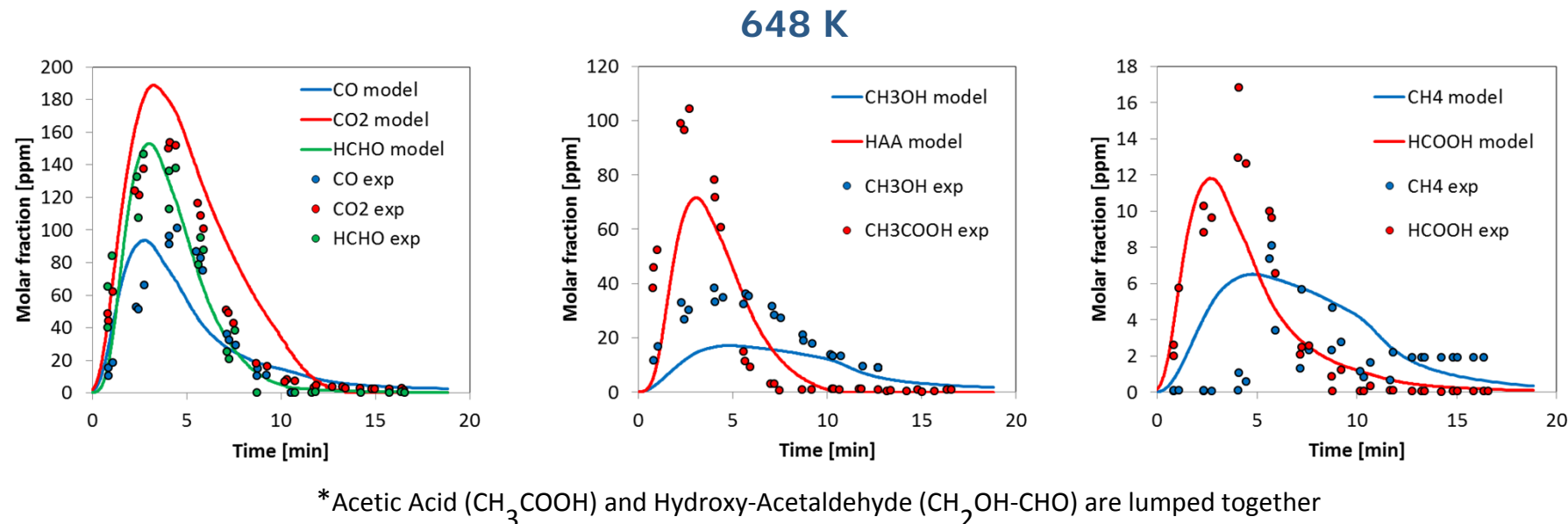
Comparisons of experimental and predicted (red lines) Center Temperature Profiles.



Park, W. C., Atreya, A. and Baum, H. R. (2010) 'Experimental and theoretical investigation of heat and mass transfer processes during wood pyrolysis', Combustion and Flame, 157(3), 481-494.



Pyrolysis of Thick Biomass Particle: time-resolved gas phase composition (Bennadji et al., 2013)

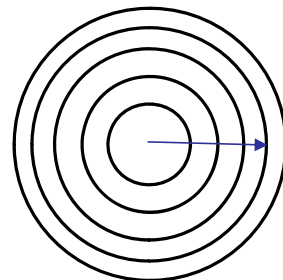


Secondary gas phase reactions are not important in these conditions.

Secondary Gas-Pase Reactions at the

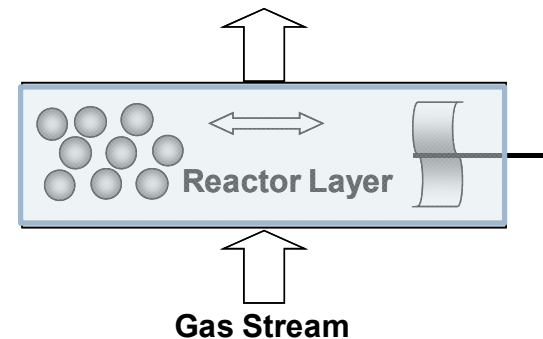
Elemental Reactor Scale

Secondary Gas-Phase Reactions
take place in the elemental reactor



Fuel Particle

Particle Model consists of
mass and heat balances



The dynamic model of the ideal Gas-Solid Reactor accounts for the exchanges and for kinetics both in the solid and the gas phase.

Elemental Reactor Model (Gas-phase)

The dynamic Mass and Energy Balances of the Perfectly Stirred Reactor accounts for

Gas-Solid exchanges

Devolatilization Kinetics

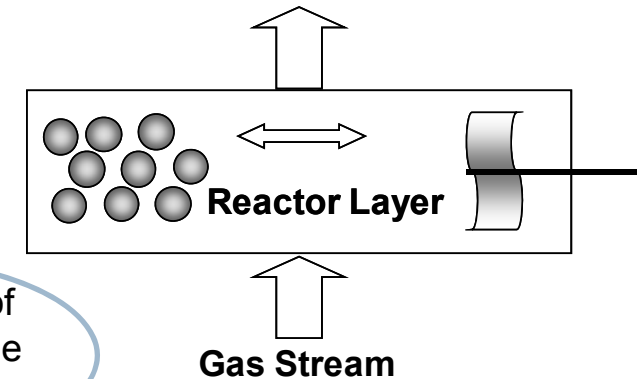
Heterogeneous Combustion/Gasification

Secondary Gas-Phase Reactions

$$\frac{dg_i}{dt} = [G_{IN,i} - G_{OUT,i}] + J_{N,i}\eta - V_R \cdot R_{g,i}$$

$$\frac{d \sum_{i=1}^{NCP} g_i C_{p_i} T_g}{dt} = \left[\sum_{i=1}^{NCP} G_{IN,i} \cdot h_{g_{IN,i}} - \sum_{i=1}^{NCP} G_{OUT,i} \cdot h_{g_{OUT,i}} \right] + \sum_{i=1}^{NCP} J_{N,i} h_{N,i} \eta + J_C \eta + J_{RAD} - HR_g$$

Convection



η is the number of fuel particles in the reactor volume (V_R)

Gas-Solid Exchange

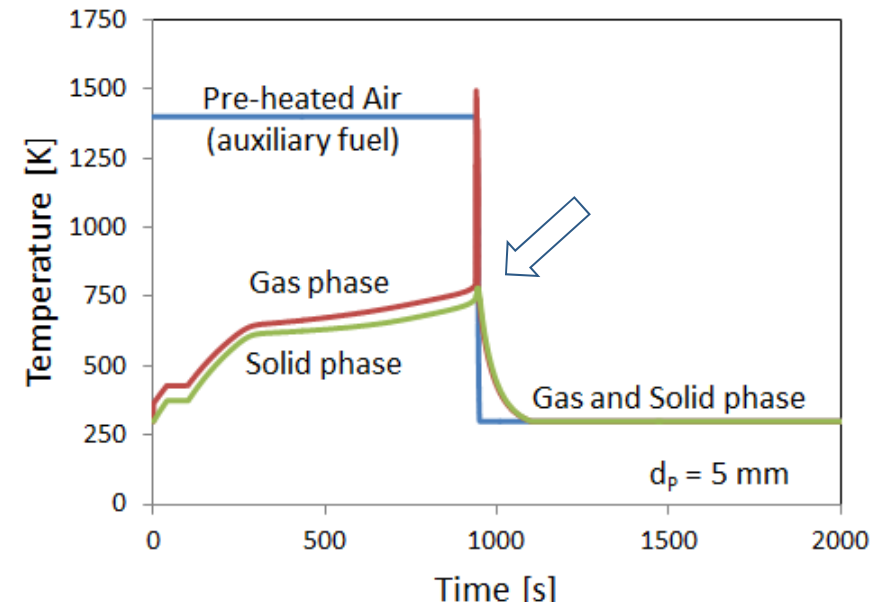
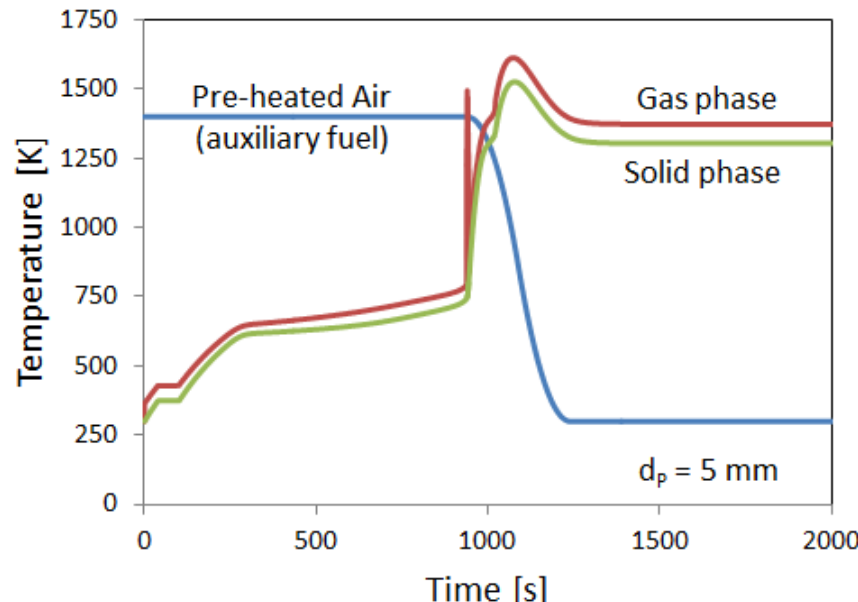
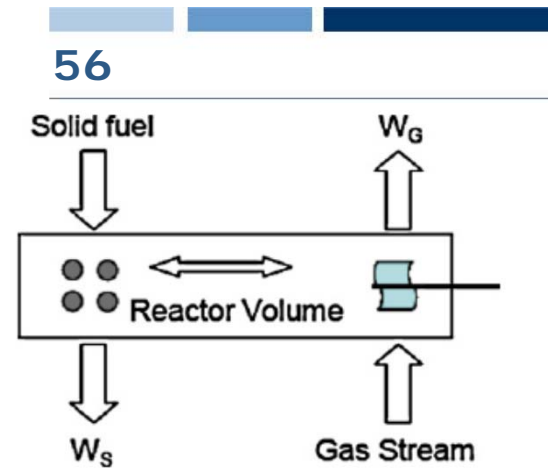
Reaction Heat

Gasification of Biomass Particles: Dynamic Analysis of the Ignition Process

A single reactor layer is fed with 5 mm Biomass Particles and Air at 300 K and a nominal $\Phi = 3$.

Selection of the start-up procedure:

Due to the thermal feed back, the system exhibits Hot and Cold steady solutions.

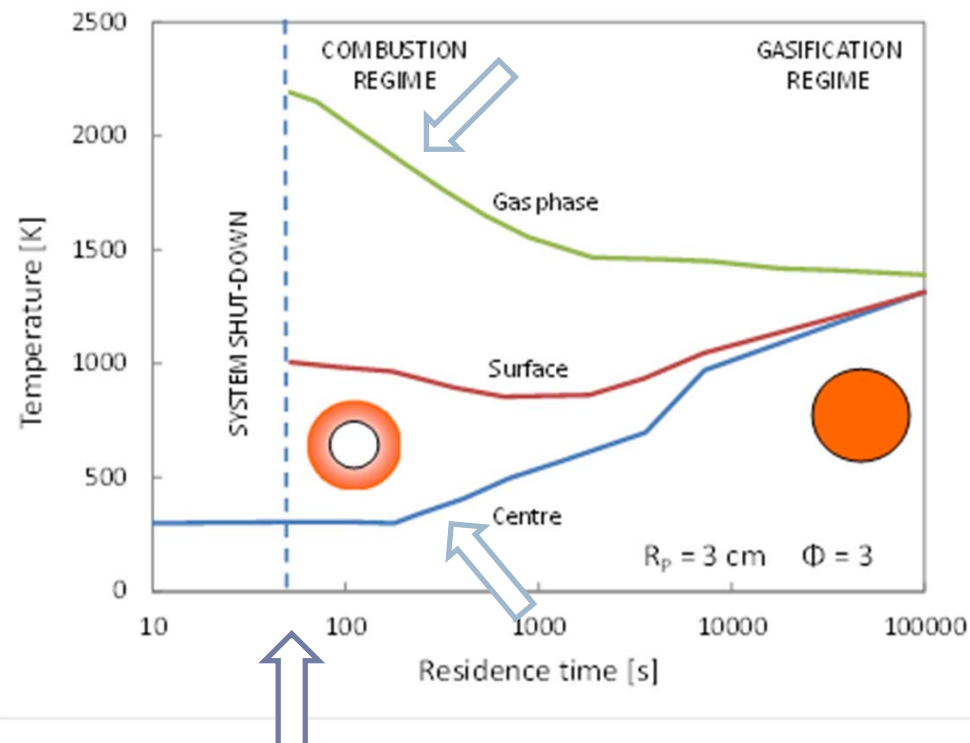


System evolution and steady-state conditions of gasification

Start up procedure needs to properly heat up the biomass particles to maintain the Hot solution.

Gasification Regime of Thick Particles

A single reactor layer is fed with thick Fuel particle
Air at 300 K and a nominal $\Phi = 3$.



Below a critical contact time there is a sudden shut down of the system.

	Gasification Regime	Combustion Regime
Biot Number	0.2	7
Gasification Efficiency*	~99%	~40%
Heating Value [kcal/kg]	~1100	-

*Defined as the ratio between gasified mass and inlet solid fuel mass

Gasification regime requires high contact times to homogeneously heat up the biomass particle.

Volatiles form CO and H₂.

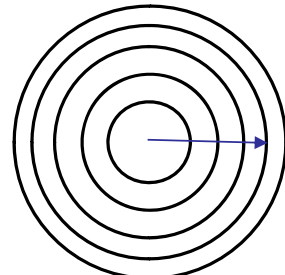
At low contact time of solid particles a combustion regime can prevail on gasification.

Gas phase temperature rises, while the center of the particle remains unreacted.

There is only a partial release of tar and volatiles, and the complete combustion to CO₂ and H₂O.

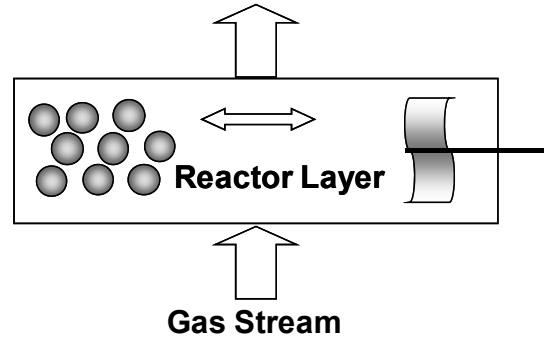
Multi-Phase Model at Particle and Reactor Scale

58

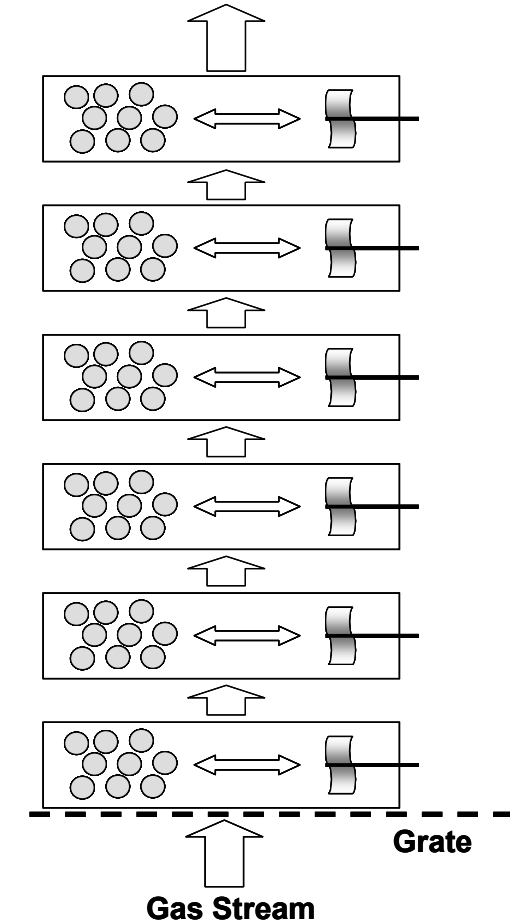


Fuel Particle

Particle Model consists of mass (solid and gases) and heat balances



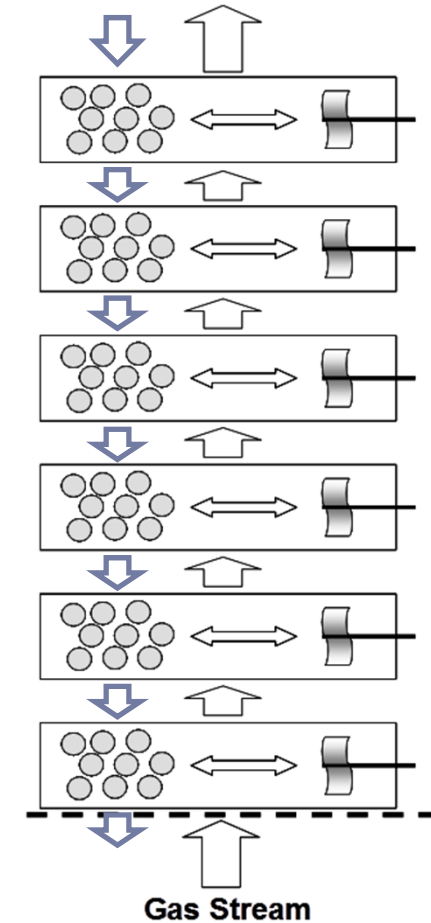
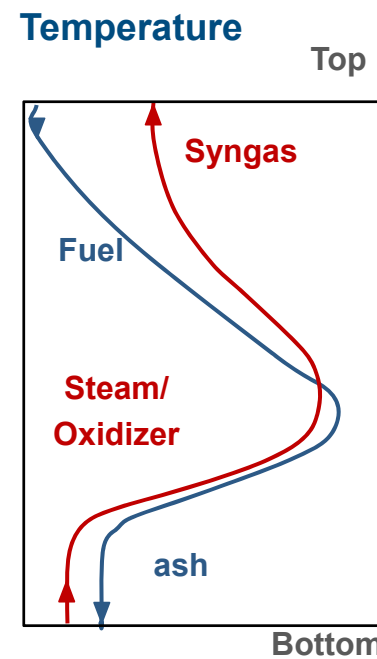
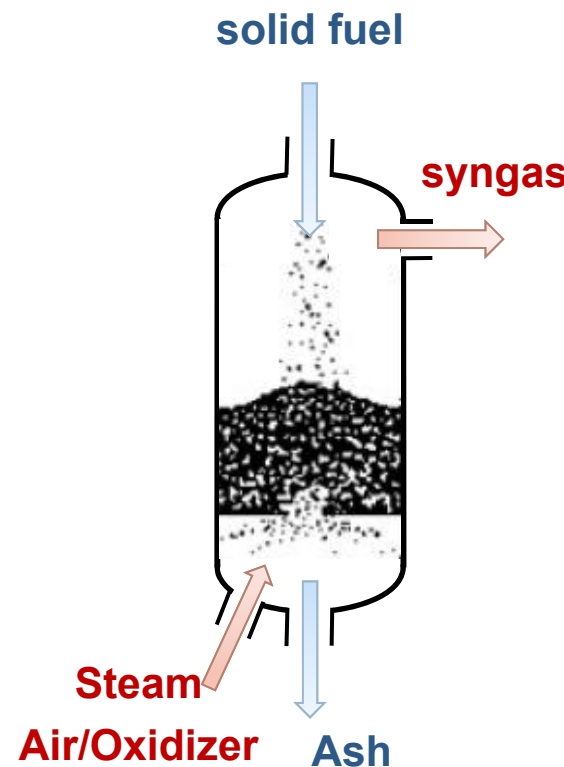
The dynamic model of the ideal Gas-Solid Reactor accounts for the exchanges and for kinetics both in the solid and the gas phase.



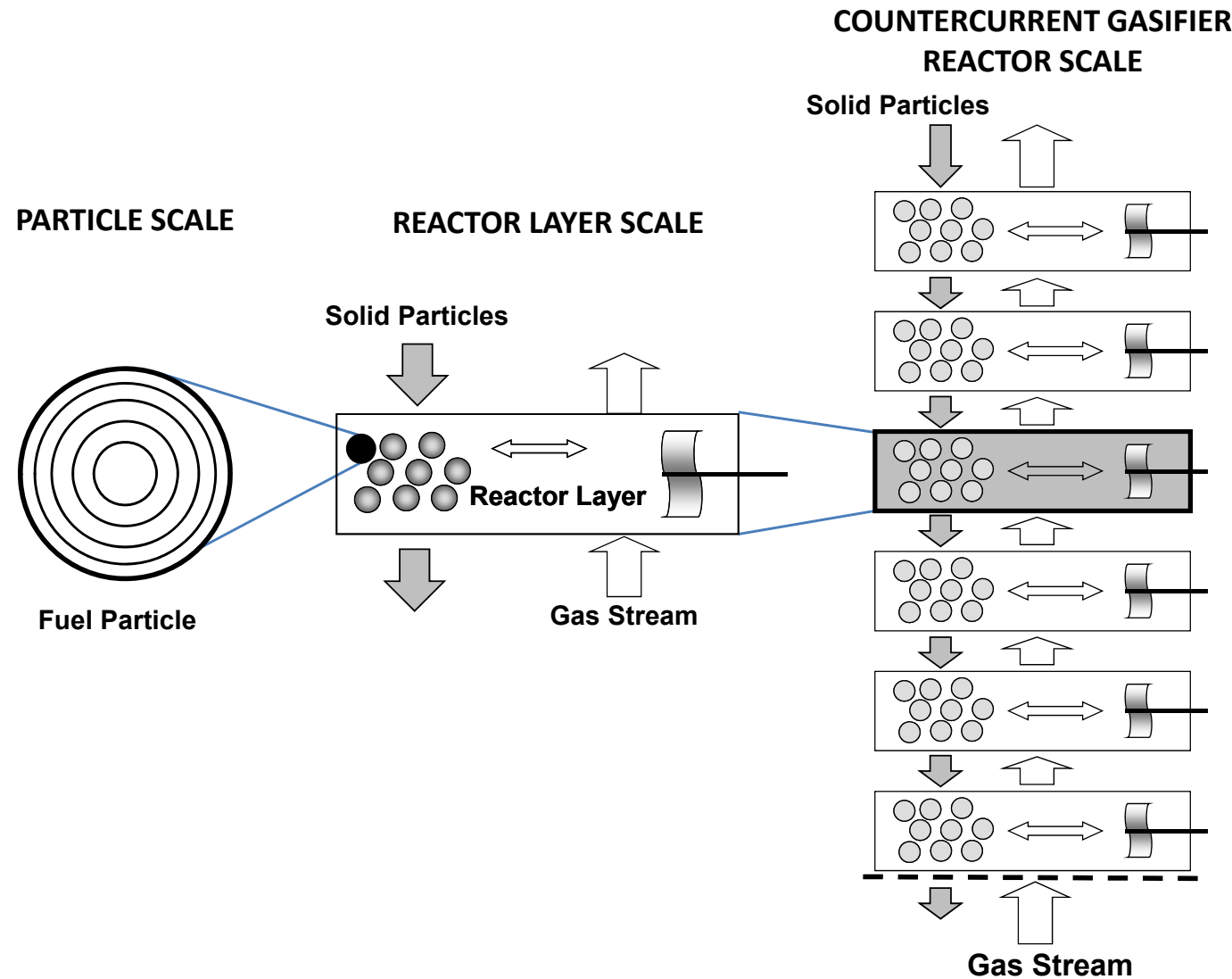
A fixed bed of solid particles is considered as a cascade of several Elemental Reactors

Gasifier is a Stack of Elemental Reactor Layers

(counter-current and co-current configuration)



Multi-Scale Nature of Solid Fuel Gasifier



Mathematical Model of the Counter-Current Gasifier

15-30 solid phase species,
100-200 gas-phase components,
5-10 reactor layers,
and 3-5 discretization sectors in the solid particle.

Several Thousands of Balance Equations

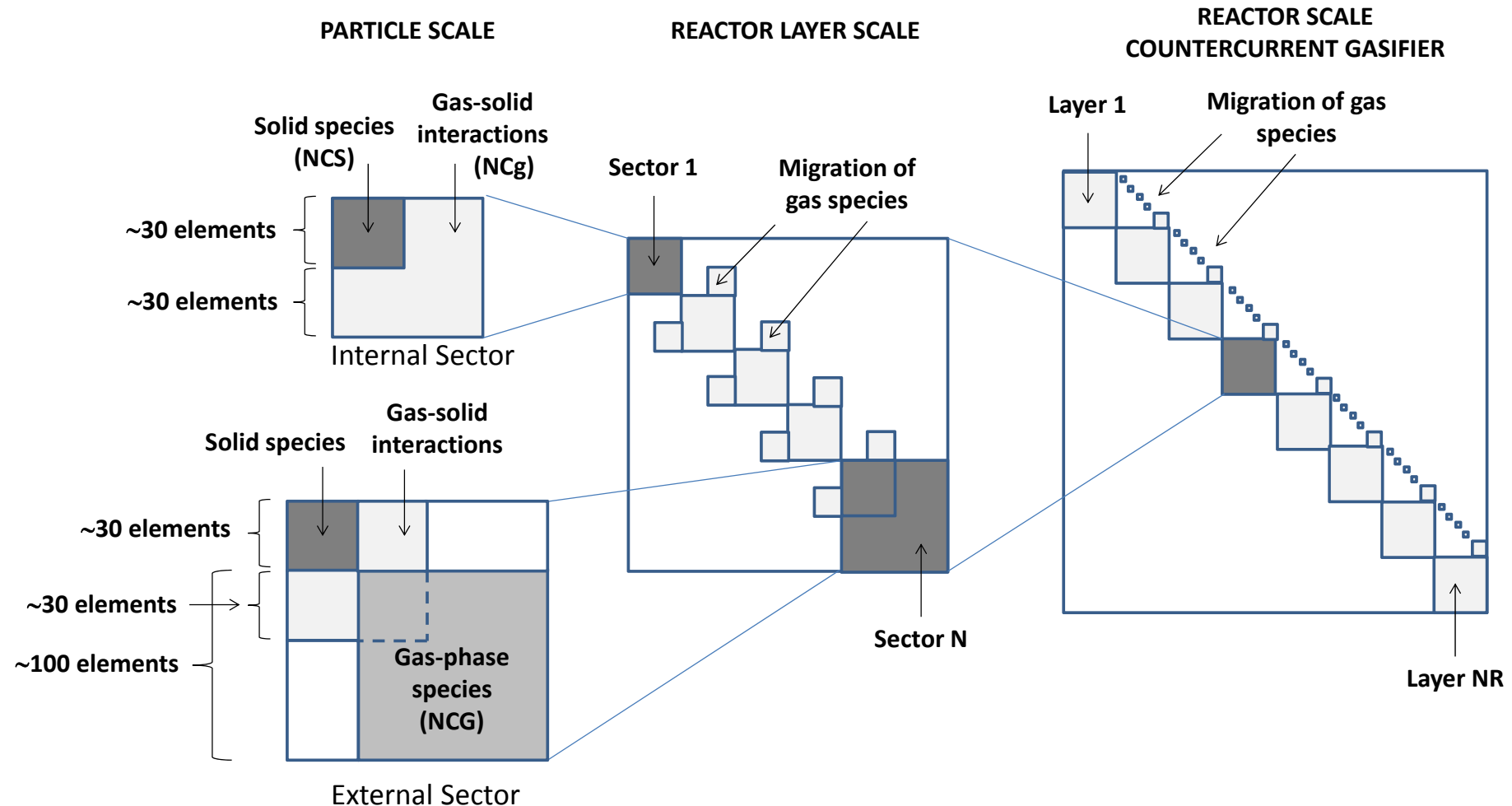
The resulting Stiff System of Differential Algebraic Equations (DAE)
is solved by using the **BZZMATH Library**.

The Jacobian matrix is structured in **Sparse Diagonal Blocks**.

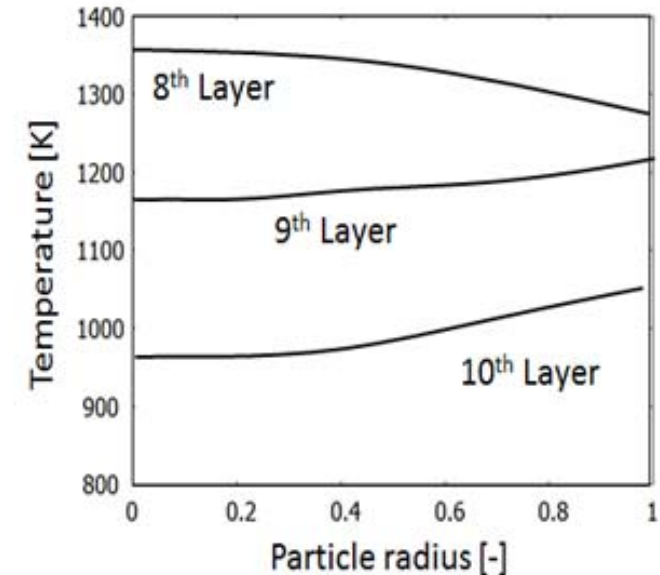
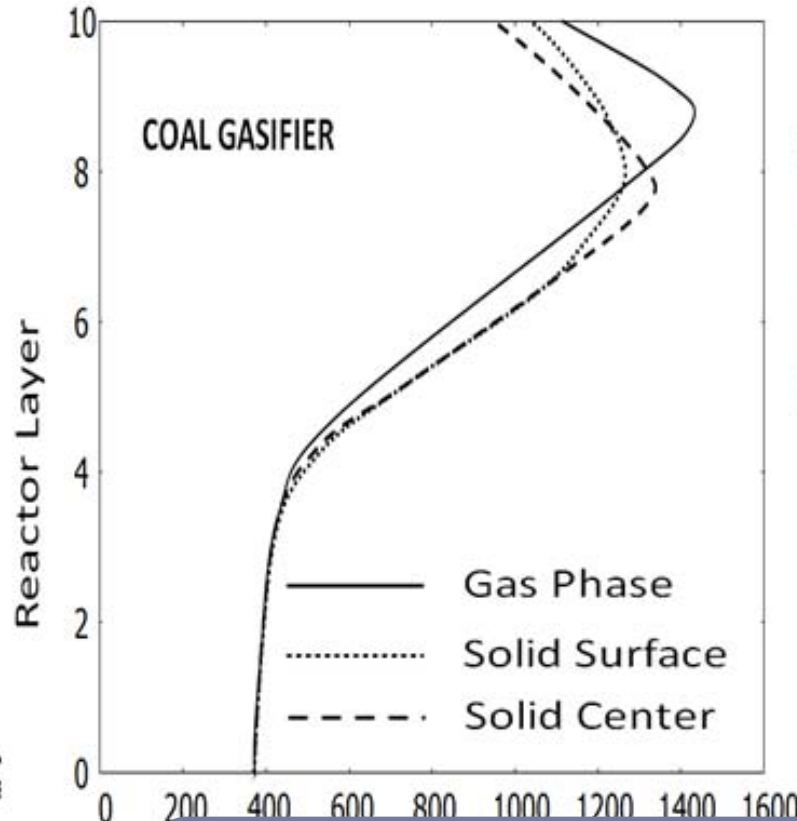
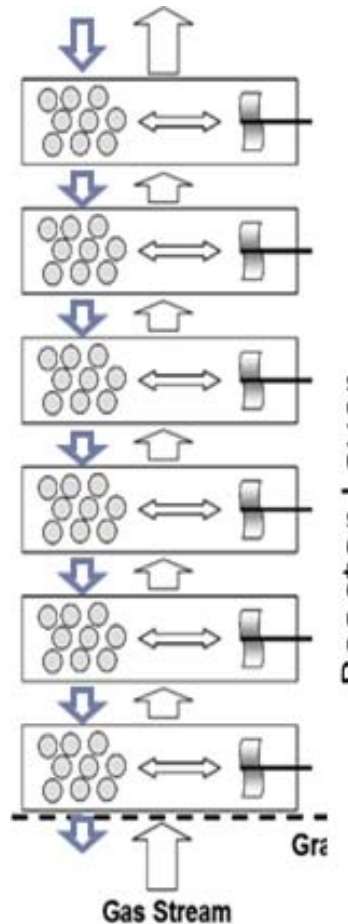
Buzzi-Ferraris, G. (1993). *Scientific C++; Building Numerical Libraries the Object-Oriented Way*. Addison-Wesley Longman Publishing Co., Inc..
Buzzi-Ferraris, G., & Manenti, F. (2010). Fundamentals and linear algebra for the chemical engineer: Solving numerical problems. Wiley-vch.

Solid Fuel Gasifier

Block Sparse Structure of the Jacobian



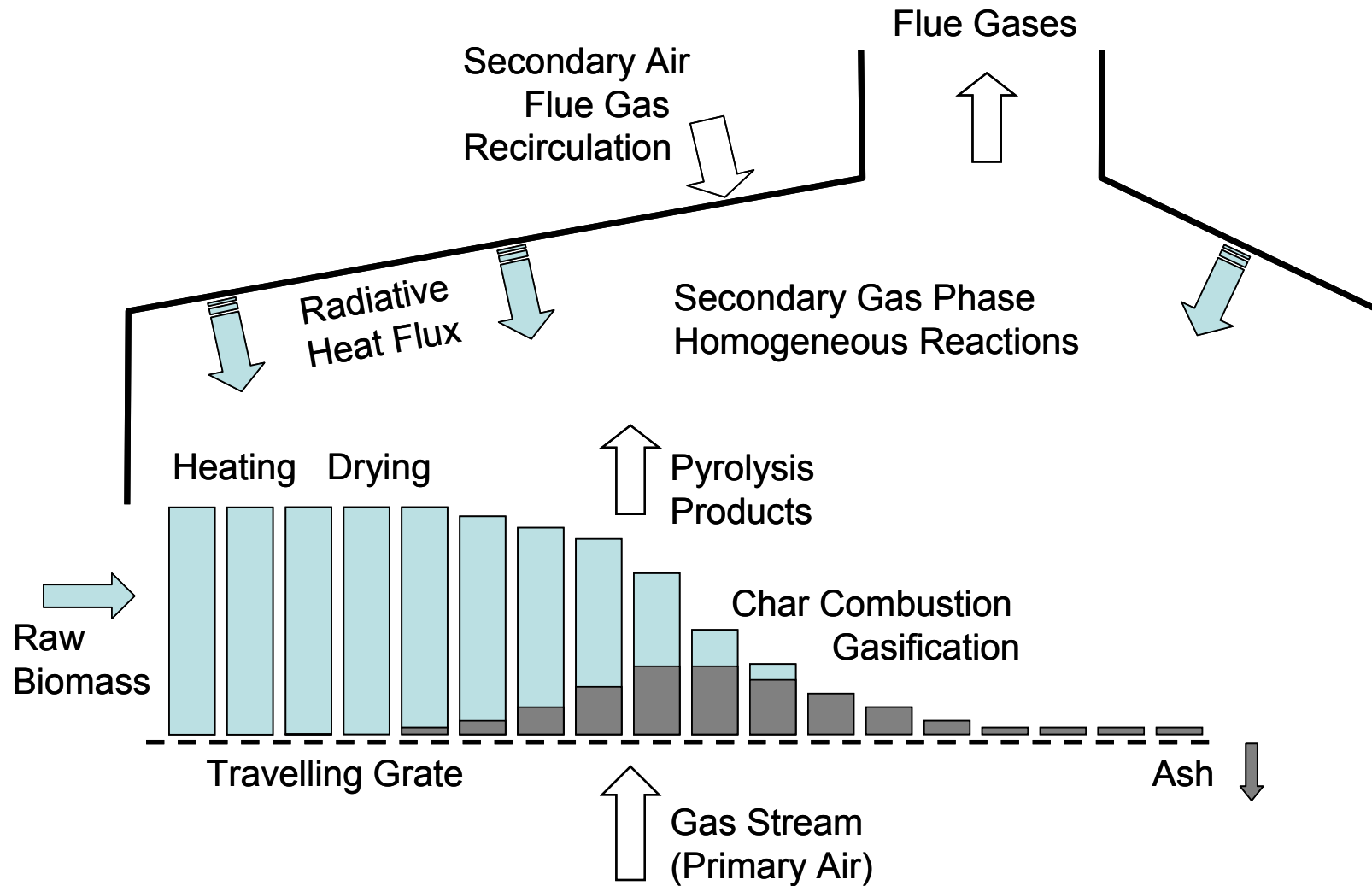
Counter-Current Coal Gasifier



Internal temperature profiles of the solid particles of the three top layers. Char combustion explains the center in the 8th layer.

Empirical correlations are required to account for the morphological changes of the coal particles and the fixed bed.
Shrinking and swelling, porosity and density, diffusivity....

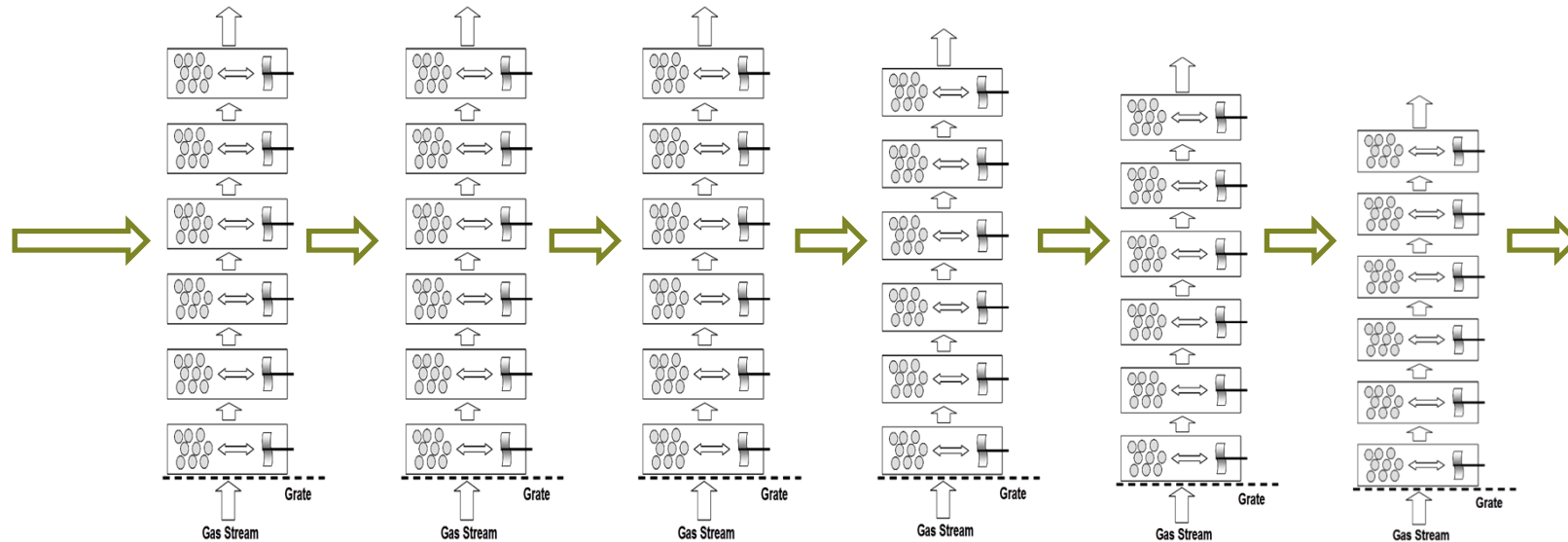
Simplified Structure of a Travelling Grate Combustor



Steady and Dynamic Problem

The biomass bed on the grate is assumed as several stacks of elemental reactor layers.

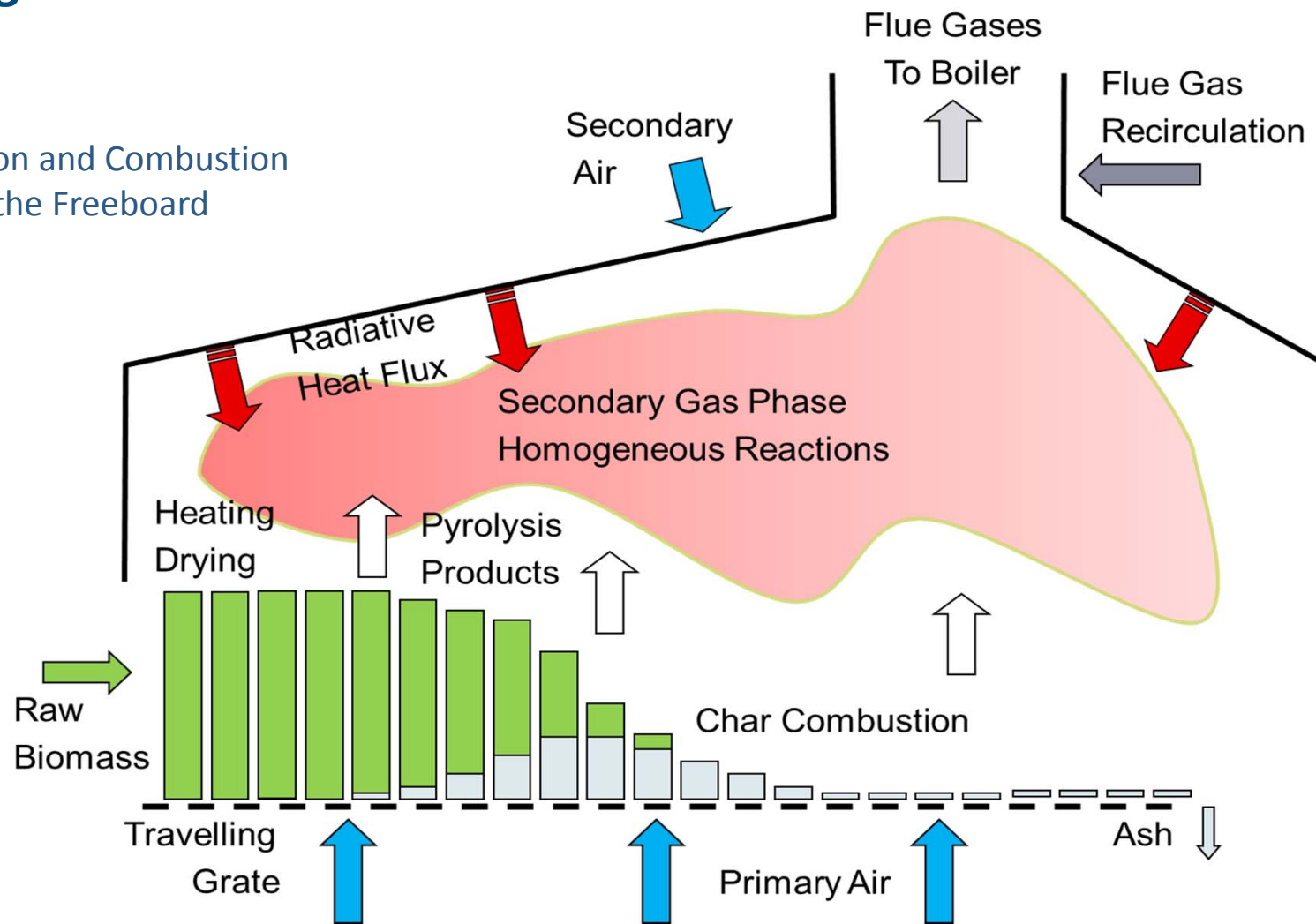
The grate movement determines the effective contact times of the biomass on the grate.



The steady problem is thus transformed
into a dynamic problem of a travelling 'Slice' of the fuel bed.

Travelling Grate Biomass Combustor

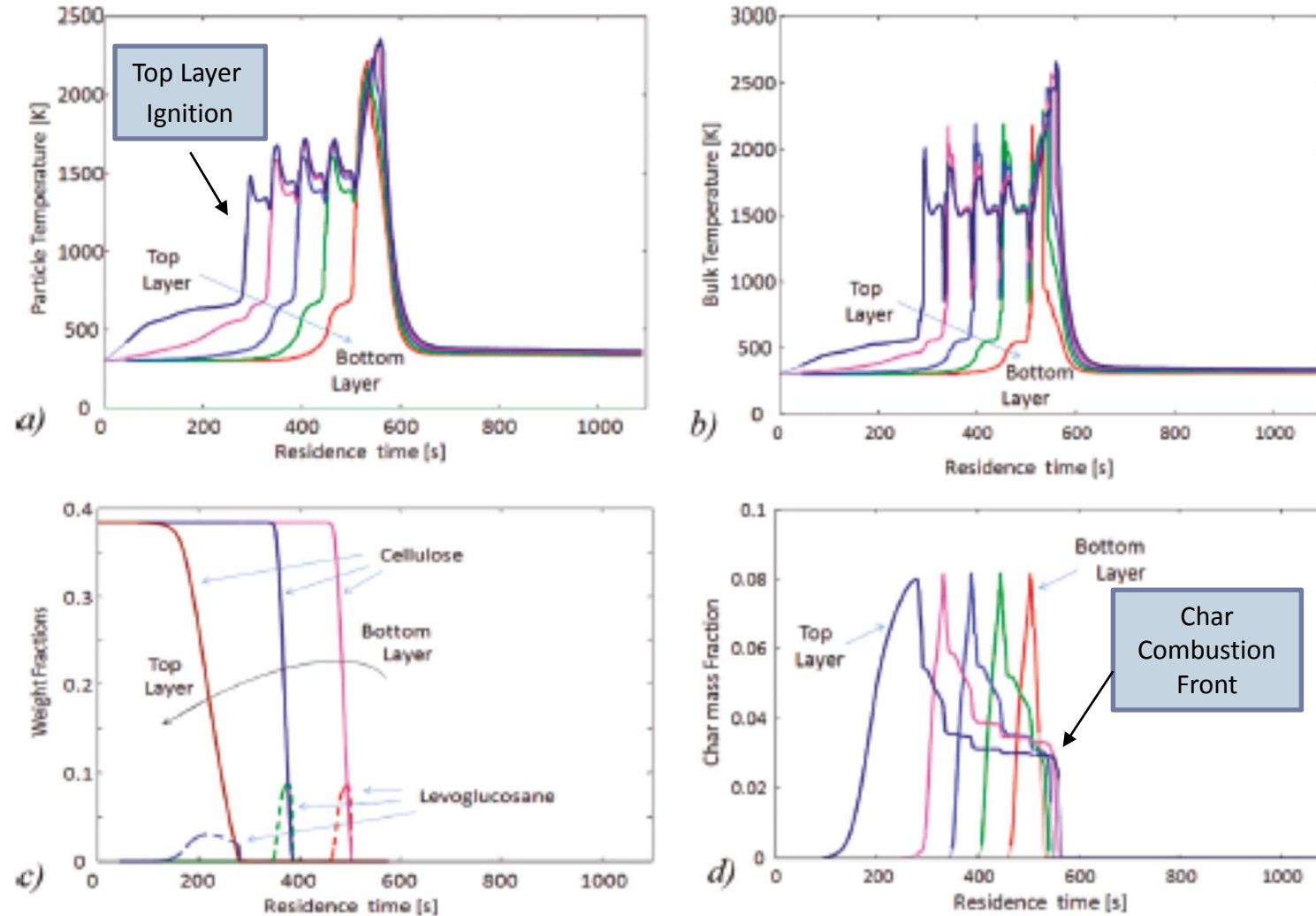
Decomposition and Combustion
Reactions in the Freeboard



Integral closure of mass and energy balances :

Pyrolysis products with primary and secondary air are involved in gas-phase reactions.
Flue gases heat up the radiating walls of the furnace.

inside the Travelling Grate Combustor.

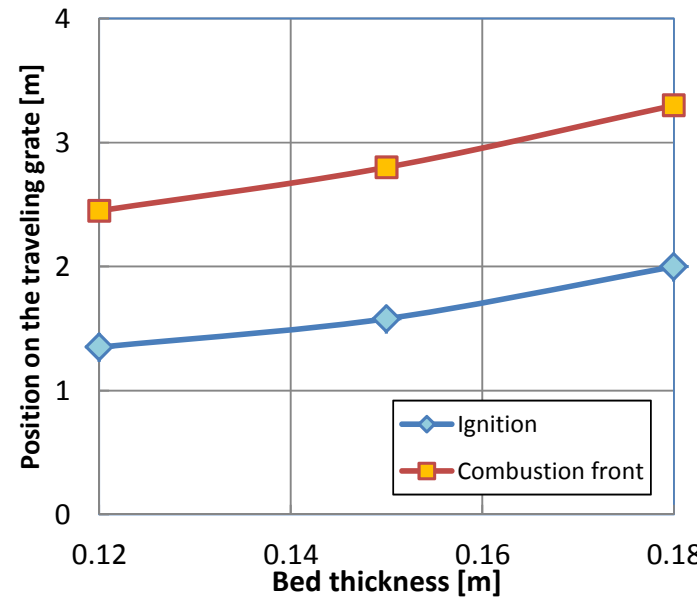
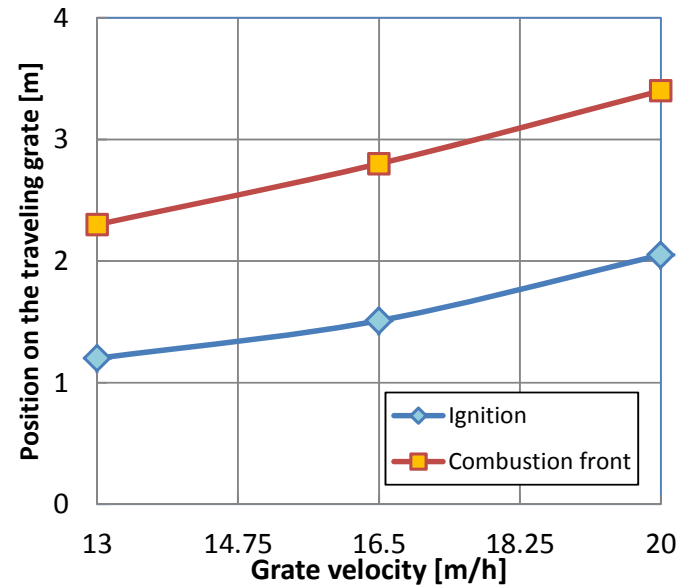


E. Ranzi, S. Pierucci, P. C. Aliprandi, S. Stringa (2011)

'Comprehensive and detailed kinetic model of a traveling grate combustor of biomass' Energy & Fuels 25:4195 - 4205

Detailed simulations allow to derive a Control Model⁶⁸ of the Travelling Grate Combustor.

Grate velocity and bed thickness
effect on ignition and combustion front.



Similarly, the effect of Biomass Composition, Fuel Size,
Radiating Temperature, Primary and Secondary Air Flowrate
is investigated.

E. Ranzi, S. Pierucci, P. C. Aliprandi, S. Stringa (2011)

'Comprehensive and detailed kinetic model of a traveling grate combustor of biomass' Energy & Fuels 25:4195 - 4205

Control Model of the Travelling Grate Combustor.

69

(12 MW biomass combustor operating in Belgium)

Cellulose (wt %)	38.4
HemiCell.	20.85
Lignine_C (wt %)	4.06
Lignine_H (wt %)	20.96
Lignine_O (wt %)	6.25
Ash (wt %)	1.5
Water (wt %)	8

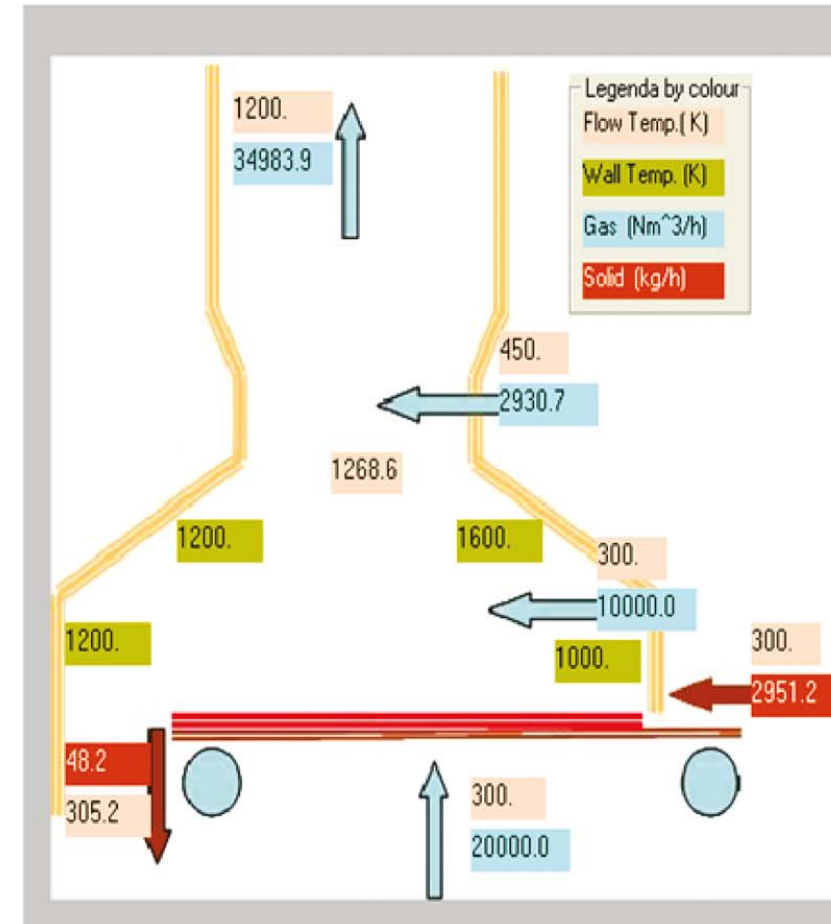
Particle diameter (m)	.008
Particle porosity %	30
Particle sectors	1

Bed height (m)	.15
Bed velocity (m/h)	16.5
Bed void fraction *100	50
Bed elements	3
Solid Feed Temperature (K)	300

Air Feed flowrate (Nm^3/h)	20000.
Air Feed temperature (K)	300
Relative air humidity %	20
Secondary Air flowrate (Nm^3/h)	10000.
Secondary Air temperature (K)	300.0
Recycle Flue gas temperature	450
Max inlet temperature to boiler	1200

Bed Density (kg/m^3) 428.92 Solid Feed Flowrate (kg/h) 2951.2

Chamber Volume (m^3) 22.9 Residence time (s) 1090.9



Summary of operating conditions, biomass characteristics, and model predictions.

E. Ranzi, S. Pierucci, P. C. Aliprandi, S. Stringa (2011)

'Comprehensive and detailed kinetic model of a traveling grate combustor of biomass' Energy & Fuels 25:4195 - 4205

Conclusion

- Solid fuel pyrolysis and combustion processes are intrinsically more difficult to describe than gas-phase processes on a fundamental mechanistic level and present major challenges to combustion scientists.
- For this reason, lumping procedures need to be applied at different levels.
- Once lumped models are available, it is always feasible and useful to increase the description level and to improve model predictions
- For several solid fuels, the simple knowledge of the C/H/O content is sufficient to understand their pyrolysis and combustion behavior.
For other fuels, this is not the case (plastics contain additives and flame retardants).
- The morphological changes during fuel conversion require to account for continuous modifications of physical and transport properties.

Thanks for the attention



CRECK Modeling Group at Politecnico di Milano

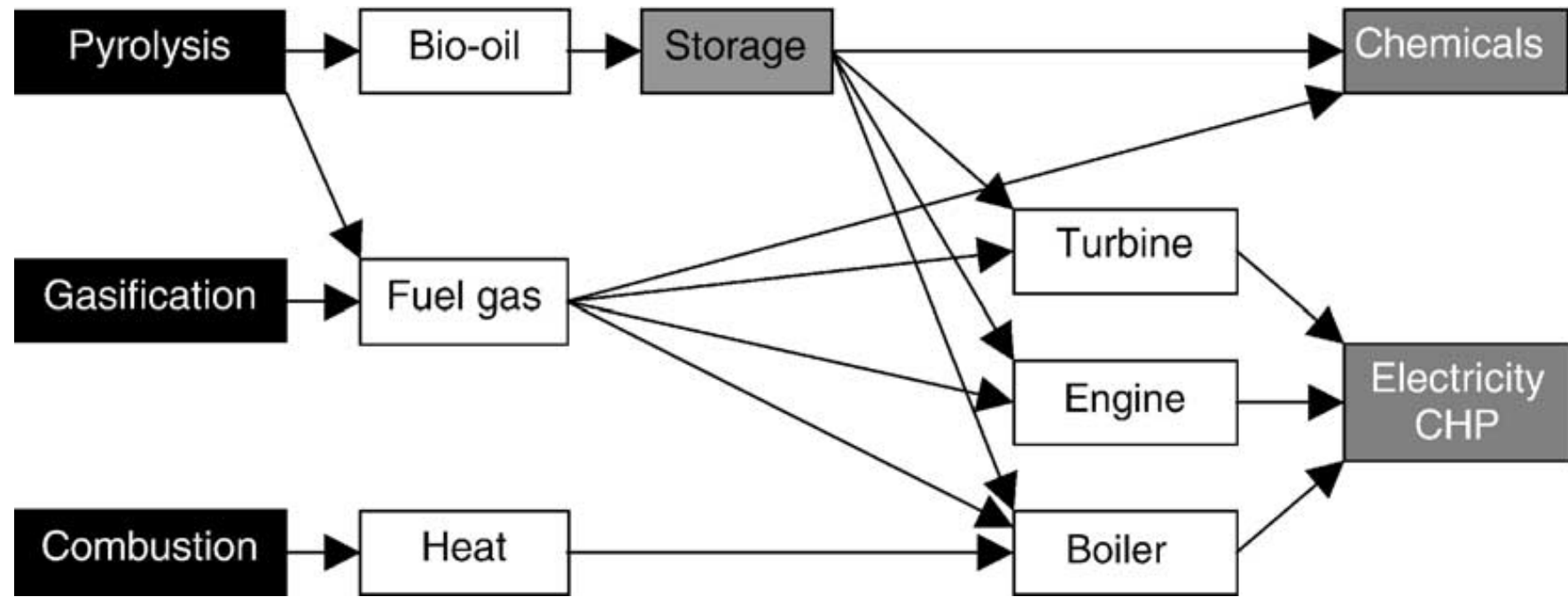
Thanks for the attention



The financial support of CNR/MSE 'Clean Coal Project' is gratefully acknowledged.



Products from thermal biomass conversion.



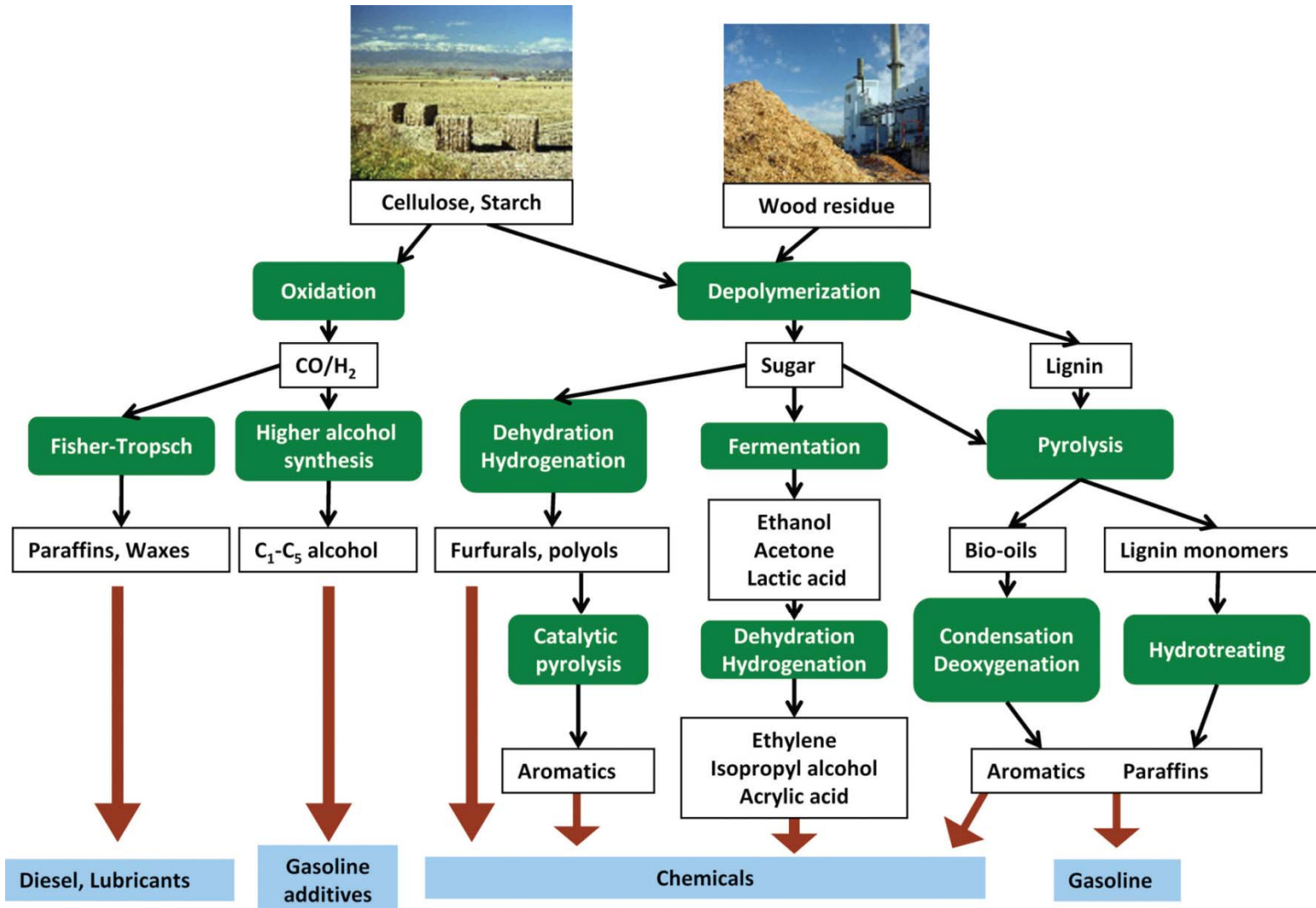
Gasification occurs in a number of sequential steps:

- drying to evaporate moisture,
- pyrolysis to give gas, vaporised tars or oils and a solid char residue,
- gasification or partial oxidation of the solid char, pyrolysis tars and pyrolysis gases.

Bridgwater, A. V. (2003). Renewable fuels and chemicals by thermal processing of biomass. Chemical Engineering Journal, 91(2), 87-102.

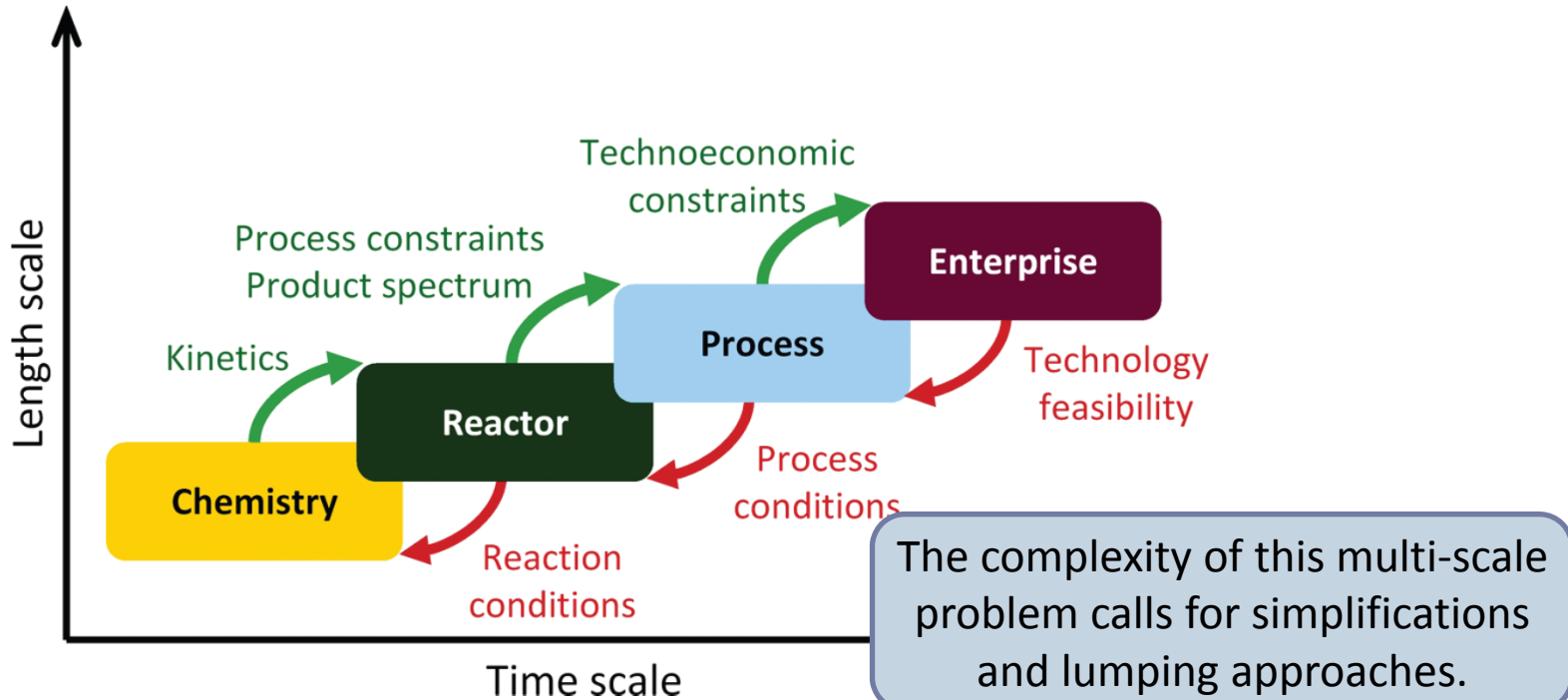
Engineering Biomass Conversion Processes

A schematic of a biorefinery.



Daoutidis, P., Marvin, W. A., Rangarajan, S. and Torres, A. I. (2013),
Engineering Biomass Conversion Processes: A Systems Perspective. AIChE J., 59: 3–18

Biomass Conversion is a Complex Multi-Scale Process.



Process engineering solutions for designing biorefineries will require addressing systems challenges at various levels:

- Elucidation of complex chemical systems
(mechanisms, kinetics, and thermochemistry).
- Design of novel reactors and reactor networks.
- Synthesis and optimization of novel flow sheets.
- Supply chain optimization at the enterprise level.

Daoutidis, P., Marvin, W. A., Rangarajan, S. and Torres, A. I. (2013), Engineering Biomass Conversion Processes: A Systems Perspective. *AIChE J.*, 59: 3–18